ERL-0325-TR

AR-004-237

AR-004-237

AD-A173 926

DEPARTMENT OF DEFENCE

DEFENCE SCIENCE AND TECHNOLOGY ORGANISATION

ELECTRONICS RESEARCH LABORATORY

DEFENCE RESEARCH CENTRE SALISBURY
SOUTH AUSTRALIA

TECHNICAL REPORT

ERL-0325-TR

THE EFFECT OF VARYING THE INTERNAL ANGLE OF A DIHEDRAL CORNER REFLECTOR

W.C. ANDERSON

Original contains color plates: All DTIC reproductions will be in black and white

Approved for Public Release

MAY 1985

COPY No. 10

DEPARTMENT OF DEFENCE

DEFENCE SCIENCE AND TECHNOLOGY ORGANISATION

ELECTRONICS RESEARCH LABORATORY

TECHNICAL REPORT

ERL-0325-TR

THE EFFECT OF VARYING THE INTERNAL ANGLE OF A DIHEDRAL CORNER REFLECTOR

W.C. Anderson

S U M M A R Y

Small deviations from orthogonality can reduce drastically the backscattering radar cross section of dihedral corner reflectors. In this paper this effect is studied using the method of physical optics with emphasis on the reductions of RCS achievable for modest departures from orthogonality.

POSTAL ADDRESS: Director, Electronics Research Laboratory,
Box 2151, GPO, Adelaide, South Australia, 5001.

TABLE OF CONTENTS

LIST OF TABLES

LIST OF FIGURES

9. RCS for 70° and 80° reflectors, $a = b = 5\lambda$, $c = 10\lambda$

10. RCS for 85° and 88° reflectors, $a = b = c = 100\lambda$

11. RCS pattern for the special case, reflector angle = 60°, compared with the orthogonal reflector

12. Reduction in RCS for $\delta = -2°$ and $-5°$, (vertical polarisation). $a = b = 20\lambda$

13. Reduction in RCS for $\delta = 2°$ and $5°$, (vertical polarisation). $a = b = 20\lambda$

14. RCS reduction as a function of δ at $\phi = \theta = 0°$ for $a = b = 5\lambda$

15. RCS reduction as a function of δ at $\phi = \theta = 0°$ for $a = b = 10\lambda$

16. RCS reduction as a function of δ at $\phi = \theta = 0°$ for $a = b = 20\lambda$

17. RCS reduction as a function of δ at $\phi = \theta = 0°$ for $a = b = 40\lambda$

18. RCS reduction as a function of plate size at $\phi = \theta = 0°$ for $\delta = -1°$

19. RCS reduction as a function of plate size at $\phi = \theta = 0°$ for $\delta = 1°$

20. RCS reduction as a function of plate size at $\phi = \theta = 0°$ for $\delta = -2°$

21. RCS reduction as a function of plate size at $\phi = \theta = 0°$ for $\delta = 2°$

22. RCS reduction as a function of plate size at $\phi = \theta = 0°$ for $\delta = -5°$

23. RCS reduction as a function of plate size at $\phi = \theta = 0°$ for $\delta = 5°$

24. RCS reduction as a function of plate size at $\phi = \theta = 0°$ for $\delta = -10°$

25. RCS reduction as a function of plate size at $\phi = \theta = 0°$ for $\delta = 10°$

26. RCS reduction as a function of plate size at $\phi = \theta = 0°$ for $\delta = -20°$

27. RCS reduction as a function of plate size at $\phi = \theta = 0°$ for $\delta = 20°$

28. RCS reduction as a function of plate size at $\phi = \theta = 0°$ for $\delta = -30°$

29. RCS reduction as a function of plate size at $\phi = \theta = 0°$ for $\delta = 30°$

30. Reduction in RCS for $\delta = -1°$, $-2°$ and $-5°$ (vertical polarisation). $a = b = 40\lambda$

31. Reduction in RCS for $\delta = 1°$, $2°$ and $5°$ (vertical polarisation). $a = b = 40\lambda$

32. Reduction in RCS for $\delta = -1°$, $-2°$ and $-5°$ (vertical polarisation). $a = b = 100\lambda$

33. Reduction in RCS for $\delta = 1°$, $2°$ and $5°$ (vertical polarisation). $a = b = 100\lambda$

34. RCS for an asymmetric reflector with reflector angle 90°

35. RCS for asymmetric reflectors with reflector angles 85° and 92°

1. INTRODUCTION

Orthogonal corner reflectors are often used to effect a large backscattering cross section over a substantial range of angles. The RCS of such reflectors are well known and well documented. In contrast, relatively little work appears to have been done on non-orthogonal reflectors despite the fact that it is inevitable that deviations from orthogonality will result in the process of construction of such reflectors, particularly large ones. It would be useful to know what degradation in performance one can expect for a given deviation from orthogonality. Alternatively one might be interested in knowing what angle of deviation from orthogonality is required to give a prescribed reduction in RCS.

This paper reports on an investigation of the effect of varying the internal angle of a dihedral corner reflector, using the method of physical optics. Singly, doubly and triply reflected contributions are considered so the results obtained here are valid for all dihedral reflectors with reflector angles greater than 60°. This is an extension of Knott's results(ref.1) which are valid only for obtuse and orthogonal reflectors as he failed to take triply reflected rays into account. Moreover, Knott's results deal only with the case of zero elevation angle whereas the results here allow for non-zero elevation angles.

Three dihedral reflectors with included angles 85°, 90° and 95° were fabricated and measurements were performed in the ERL anechoic chamber for experimental validation of the theoretical results. Very good agreement was obtained.

The results indicate that marked reductions in RCS are possible for quite modest deviations from orthogonality for large reflectors. Interestingly for symmetric reflectors very deep nulls can appear along the axis of symmetry, an interference effect which is a function of the plate size and the deviation angle. This suggests that, contrary to common practice, the axis of symmetry might not be a good choice for 'sighting' a dihedral reflector.

2. THEORY

2.1 The physical optics approach

The physical optics method(ref.2,3) approximates the electromagnetic field on the scatterer by the geometric optics field with scattering taking place at each point of the illuminated surface as though from an infinite tangent plane at that point. The physical optics surface current density for the conducting body is therefore

$$\vec{J}_{po} = \begin{cases} 2\hat{n} \times \vec{H}^i & \text{illuminated region} \\ 0 & \text{shadow region} \end{cases} \qquad (1)$$

where $\hat{n}$ is the outward unit vector normal to the surface and $\vec{H}^i$ is the incident field on the surface. This approximation to the surface current density is only valid for scatterers whose dimension is not too small in relation to the wavelength, λ, of the incident field.

The magnetic field integral equation for scattering from a perfectly conducting body whose surface current is known, together with the approximation (1), yields for the scattered field $\vec{H}$ at any point in space

$$\vec{H} = \frac{1}{4\pi} \int_{S'} \vec{J}_{po} \times \nabla \frac{e^{ikR}}{R} \, dS' \qquad (2)$$

where $k = 2\pi/\lambda$, and R is the distance between the field point and the integration point on the illuminated surface S' of the scatterer.

When the field point, located by radius vector $\vec{r}$ from the origin, is at a large distance from the scatterer, equation (2) is reduced to the far field approximation

$$\vec{H} = \frac{ik}{4\pi} \frac{e^{ikr}}{r} \int_{S'} 2(\hat{n} \times \vec{H}^i) \times \hat{r} \, e^{-ik\hat{r}.\vec{r}'} \, dS' \qquad (3)$$

where $\hat{r} = \frac{\vec{r}}{r}$, $\vec{r}'$ is the radius vector from the origin to the integration point on the scatterer and $\int_{S'}$ denotes the integral over the illuminated surface. A time factor $e^{-i\omega t}$ is assumed and suppressed throughout.

2.2 Applications to the dihedral corner reflector

The geometry of the dihedral corner reflector with reflector angle 2γ is shown in figure 1.

The reflector supports multiple reflections to an order which depends on the reflector angle 2γ. Only singly and doubly reflected rays contribute to the scattered field for $2\gamma \geq 90°$ and only singly, doubly and triply reflected rays contribute to the scattered field for $90° > 2\gamma \geq 60°$. As 2γ decreases, higher and higher order reflections have to be taken into account. In this investigation attention is confined to reflectors with $2\gamma \geq 60°$.

Consider a plane electromagnetic wave incident on the reflector in the direction $\hat{k} = (-\cos\phi \cos\theta, -\sin\phi \cos\theta, -\sin\theta)$. Suppressing the time factor, the incident magnetic field with magnitude H_o and direction represented by the unit vector $\hat{\ell}$ is

$$\vec{H}^I = \hat{\ell} \, H_o \, e^{i\vec{k}.\vec{r}'} \qquad (4)$$

where $\hat{\ell} = (\sin\phi, -\cos\phi, 0)$ for a vertically polarised incident field and $\hat{\ell} = (-\cos\phi \sin\theta, -\sin\phi \sin\theta, \cos\theta)$ for a horizontally polarised incident field. Incident directions are confined to $-\gamma \leq \phi \leq \gamma$ and $0° \leq \theta \leq 90°$.

Backscattered single bounce returns are then obtained from equation (3) with $\vec{H}^i = \vec{H}^I$ and $\hat{r} = -\hat{k}$. Thus the single bounce backscattered magnetic field $\vec{H}^S$ is

$$\vec{H}^S = \frac{ik}{4\pi} \frac{e^{ikr}}{r} \, 2 \, H_o \, (\hat{n} \times \hat{\ell}) \times (-\hat{k}) \int_{S'} e^{2ik(\hat{k}.\vec{r}')} \, dS' \qquad (5)$$

where $\hat{n} = \hat{n}_1 = (\sin\gamma, \cos\gamma, 0)$ for single bounce scattering from face 1 to give $\vec{H}_1^S$ and $\hat{n} = \hat{n}_2 = (\sin\gamma, -\cos\gamma, 0)$ for single bounce scattering from face 2 to give $\vec{H}_2^S$.

The magnetic field incident on a face with normal $\hat{n}$ after reflection from a face with normal $\hat{n}_r$ is

$$\vec{H}_D^i = [\hat{\ell} - 2(\hat{\ell}.\hat{n}_r)\hat{n}_r]\, H_o\, e^{ik[\hat{k}-2(\hat{k}.\hat{n}_r)\hat{n}_r].\vec{r}'} \tag{6}$$

Thus the double bounce backscattered magnetic field $\vec{H}^D$ is

$$\vec{H}^D = \frac{ik}{4\pi}\frac{e^{ikr}}{r}\, 2\, H_o\, [\hat{n} \times (\hat{\ell} - 2(\hat{\ell}.\hat{n}_r)\hat{n}_r)] \times (-\hat{k}) \int_{S'} e^{2ik[\hat{k}-(\hat{k}.\hat{n}_r)\hat{n}_r].\vec{r}'}\, dS' \tag{7}$$

There are two double bounce contributions $\vec{H}_{12}^D$ and $\vec{H}_{21}^D$, the former arising from reflection off face 1 to face 2 and then back in the backscattering direction while the latter reflects first from face 2. $\hat{n} = \hat{n}_1$, $\hat{n}_r = \hat{n}_2$ for $\vec{H}_{12}^D$ and $\hat{n} = \hat{n}_2$, $\hat{n}_r = \hat{n}_1$ for $\vec{H}_{21}^D$.

In the case of triply reflected rays, the magnetic field incident on a face with normal $\hat{n}$ after reflection first from a face with normal $\hat{n}_r$ and then from a face with normal $\hat{n}_R$ is

$$\vec{H}_T^i = [\vec{\ell}_r - 2\vec{\ell}_r.\hat{n}_R]\, H_o\, e^{ik[\vec{k}_r-2(\vec{k}_r.\hat{n}_R)\hat{n}_R].\vec{r}'} \tag{8}$$

where

$$\vec{\ell}_r = [\hat{\ell} - 2(\hat{\ell}.\hat{n}_r)\hat{n}_r]$$

and

$$\vec{k}_r = [\hat{k} - 2(\hat{k}.\hat{n}_r)\hat{n}_r]$$

The triple bounce backscattered magnetic field is obtained from equation (3) with equation (8) as the incident field

$$\vec{H}^T = \frac{ik}{4\pi}\frac{e^{ikr}}{r}\, 2\, H_o\, [\hat{n} \times (\vec{\ell}_r - 2\vec{\ell}_r.\hat{n}_R)]$$

$$\times (-\hat{k}) \int_{S'} e^{2ik[\hat{k}-(\hat{k}.\hat{n}_r)\hat{n}_r-(\vec{k}_r.\hat{n}_R)\hat{n}_R].\vec{r}'}\, dS' \tag{9}$$

Two triple bounce contributions are possible for $\gamma < 45°$. $\vec{H}^T_{121}$ results from reflections off face 1 to face 2, back to face 1 and then back in the backscattering direction with $\hat{n} = \hat{n}_1$, $\hat{n}_r = \hat{n}_2$ and $\hat{n}_R = \hat{n}_1$. $\vec{H}^T_{212}$ results from reflections off face 2 to face 1, back to face 2 and thence back in the backscatter direction with $\hat{n} = \hat{n}_2$, $\hat{n}_r = \hat{n}_1$ and $\hat{n}_R = \hat{n}_2$.

The contributions from the three mechanisms can be written concisely as

$$\vec{H}^\nu = \frac{ik}{2\pi} \frac{e^{ikr}}{r} H_o P^\nu \vec{Q}^\nu, \quad \nu = S, D, T \tag{10}$$

where

$$P^S = \int_{S'} e^{2ik(\hat{k}.\vec{r'})} dS'$$

$$P^D = \int_{S'} e^{2ik[\hat{k}-(\hat{k}.\hat{n}_r)\hat{n}_r].\vec{r'}} dS'$$

$$P^T = \int_{S'} e^{2ik[\hat{k}-(\hat{k}.\hat{n}_r)\hat{n}_r-(\vec{k}_r.\hat{n}_R)\hat{n}_R].\vec{r'}} dS'$$

$$\vec{Q}^S = (\hat{n} \times \hat{\ell}) \times (-\hat{k})$$

$$\vec{Q}^D = [\hat{n} \times (\hat{\ell} - 2(\hat{\ell}.\hat{n}_r)\hat{n}_r)] \times (-\hat{k})$$

$$\vec{Q}^T = [\hat{n} \times (\vec{\ell}_r - 2\vec{\ell}_r.\hat{n}_R)] \times (-\hat{k})$$

Only $\vec{Q}^\nu$ is polarisation dependent.

The illuminated areas for each of these mechanisms are worked out using ray tracing and the integrals are then evaluated over these illuminated areas. Discontinuity can arise in the solution for horizontal polarisation when full illumination of a plate by a multiply reflected ray drops abruptly to zero as the reflected ray moves through the tangent to that plate with a small change in incident angle. In the case of vertical polarisation this is compensated for by $\vec{Q}^\nu$ so that no discontinuity appears. The results for equation (10) are tabulated in Tables 1, 2, 3 and 4.

The total backscattered magnetic field $\vec{H}_{tot}$ is then

$$\vec{H}_{tot} = \vec{H}^S_1 + \vec{H}^S_2 + \vec{H}^D_{12} + \vec{H}^D_{21} + \vec{H}^T_{121} + \vec{H}^T_{212} \tag{11}$$

and the radar cross section is given by

$$\sigma = \lim_{r\to\infty} \frac{4\pi r^2 \left|\vec{H}_{tot}\right|^2}{H_o^2} \qquad (12)$$

3. THEORETICAL RESULTS

A computer program has been written to evaluate the RCS patterns for varying plate sizes and reflector angles down to 60°. The RCS of the reflectors are computed in units of λ^2; RCS reduction (dB) values are the reduction in RCS of the non-orthogonal reflector from that of the orthogonal reflector at the corresponding aspect angle. For the case $\theta = 0°$ the reduction (in decibels) is independent of the reflector length c.

Figure 2 shows the azimuth RCS pattern of an orthogonal reflector with $a = b = 5\lambda$ and $c = 10\lambda$ for $\theta = 0°$ and $\theta = 5°$. It can be seen that the dihedral reflector has a very broad double bounce contribution over ϕ with the single bounce contributions appearing as ripples. Specular single bounce returns from the individual faces appear as peaks at $\phi = \pm 45°$. There is a very dramatic drop in RCS as θ departs from 0° as evidenced in the $\theta = 5°$ pattern and shown explicitly in figure 3 which gives the elevation RCS pattern for $\phi = 0°$. Figure 4 shows the RCS patterns for two dihedral reflectors with the same plate sizes as before but with reflector angles of 80° and 100°. The double bounce contributions are dramatically reduced but the single bounce specular returns at $\phi = \pm 40°$ for the 100° reflector stay the same, as expected.

Figure 5 shows the reduction in RCS for acute angled reflectors with angles of deviation from orthogonality $\delta = -2°$, $-5°$, $-10°$ and $-20°$ while figure 6 shows the reduction in RCS for obtuse angled reflectors with $\delta = 2°$, 5°, 10° and 20°. All the preceding results are for vertical polarisation of the incident field. Figures 7 and 8 show the reduction in RCS for horizontal polarisation.

In obtuse reflectors the dominant contribution to the backscattered field over most of ϕ comes from doubly reflected rays, the single bounce contribution being significantly lower except in the specular directions ie in directions orthogonal to the individual plates. These individual flashes of the plates, observed at $\phi = \pm(90 - \gamma)°$ for the obtuse reflectors are not reduced by deviations from orthogonality. The average level of reduction in RCS achieved over a large ϕ coverage increases with increasing deviation angle (figures 6 and 8). In acute reflectors, the dominant contribution is still from doubly reflected rays for small angles of deviation. Triple bounce contributions become increasingly important with increasing magnitude in deviation angles; in fact these contributions are non-zero for $\phi = -\gamma$ to $-(\gamma + 2\delta)$ and $\phi = \gamma$ to $\gamma + 2\delta$. When $\delta < -18°$, the coverage of triple bounce contributions is from $\phi = -\gamma$ to γ. The triple bounce contributions can then dominate, instead of double bounce contributions. Thus, in figures 5 and 7, the increased significance of triple bounce contributions leads to a lower RCS reduction being achieved for $\delta = -20°$ than for $\delta = -10°$ which has non-zero triple bounce contributions only for $|\phi| > 20°$ compared to $|\phi| \leq 35°$ for $\delta = -20°$.

When $\theta = 0°$, $\phi = \pm(3\gamma - 90)°$ are the specular directions for the two triply reflected rays. Depending on their magnitudes compared to those of the doubly reflected rays and the relative phases of all the rays, the triple bounce contribution can reveal its presence as ripples in the RCS pattern (near $\phi = \pm 30°$ for $2\gamma = 80°$, figure 9 and near $\phi = \pm 42°$ for $2\gamma = 88°$, figure 10), slight peaks (at $\phi = \pm 15°$ for $2\gamma = 70°$, figure 9) or flashes as at $\phi = \pm 37.5°$ for $2\gamma = 85°$ in figure 10. $\gamma = 30°$ is the special case when $\phi = 0°$ is the specular direction for both triply reflected rays which add coherently for the 60° symmetric reflector to give a very large return centred at $\phi = 0°$ (figure 11).

The reduction in RCS achieved is dependent on the plate size. Figures 5, 6, 7 and 8 corresponding to the case $a = b = 5\lambda$ show that a 2° deviation from orthogonality produces a reduction in RCS of 1 dB over most of ϕ. Figures 12 and 13 show that when $a = b = 20\lambda$ a 2° deviation is sufficient to give very marked reduction, up to 30 dB near $\phi = 0°$. Interestingly, figures 12 and 13 reveal that while the overall RCS reduction is higher for $|\delta| = 5°$ than for $|\delta| = 2°$, the RCS reduction along the line of symmetry, $\phi = 0°$, is unexpectedly higher for $|\delta| = 2°$ than for $|\delta| = 5°$, particularly for the obtuse reflectors (figure 13). This is a significant result in that users of symmetric dihedral reflectors frequently 'sight' the reflector along the axis of symmetry as it is the direction in which a maximum return is expected for an orthogonal reflector. However, figures 12 and 13 indicate that a small error in the construction of the reflector can reduce this return drastically. In view of this, attention is focussed on the backscattered return along the axis of symmetry. The level of this return is a function of δ and the plate size.

Figures 14 to 17 show the reduction in RCS in the direction $\phi = \theta = 0°$ as a function of δ for a given plate size. These figures show a symmetry about the orthogonal reflector ($\delta = 0°$) for small δ when double bounce contributions dominate for both acute and obtuse reflectors. The increasing importance of triple bounce contributions becomes evident in the lower RCS reductions achieved as $\delta \to -30°$.

Figures 18 to 29 show the reduction in RCS in the direction $\phi = \theta = 0°$ for symmetric reflectors ($a = b$) as a function of a for a given δ. These figures show the typical interference lobe structures; thus for a given δ there are numerous plate sizes, in arithmetic progression, for which nulls are expected in the backscattered RCS of the reflector at $\phi = \theta = 0°$. The peaks in figures 18 to 29 correspond to these nulls. Figures 20 to 23 show that the $a = b = 20\lambda$ reflectors are closer to these nulls for $\delta = \pm 2°$ than for $\delta = \pm 5°$. This explains the much higher reduction in RCS obtained for $\delta = \pm 2°$ than for $\delta = \pm 5°$ in figures 12 and 13. The minima in figures 18 to 27 and 29 increase in magnitude as plate size increases over a large range in plate size except for the special case of $\delta = 30°$ (figure 28). In this special case, $\phi = 0°$ is the specular direction for triply reflected rays which add coherently to give a large return that is about 3 dB below the peak return for the corresponding orthogonal reflector over a large range of plate sizes.

Knott(ref.1) has derived an approximate expression for predicting the reduction, X, in the scattered field strength when $\theta = 0°$ for dihedral reflectors with small deviations from orthogonality and plate sizes large relative to wavelength, these conditions being necessary for his assumption that double bounce contributions are the dominant contributions. The double bounce contribution for the non-orthogonal reflector, D_N, with small deviation angle δ is (equation (14), reference 1)

$$D_N \approx \frac{c(1 - e^{2ikb \sin\delta \cos(\phi+\pi/4)})}{\lambda \sin\delta} \qquad (13)$$

He then obtained X by dividing the maximum value of equation (13), $|D_N|_{max}$, by the maximum double bounce contribution of the orthogonal reflector, $|D_o|_{max}$ where

$$|D_N|_{max} \approx \frac{2c}{\lambda \sin\delta} \qquad (14(a))$$

and

$$|D_o|_{max} = \frac{2kbc \cos(\tan^{-1} b/a)}{\lambda} \qquad (14(b))$$

Thus, the reduction in the backscattered field strength is

$$X \approx \frac{1}{kb \sin\delta \cos(\tan^{-1} b/a)} \qquad (15)$$

and the reduction in backscattered radar cross section is X^2.

It will be shown here that X as given by equation (15) here and in Knott(ref.1) gives a very rough estimate of the reduction actually achieved. Equation (15), applied to the reflectors in figure 13, gives a reduction of 9.8 dB for $\delta = 2°$ and 17.8 dB for $\delta = 5°$. While the 17.8 dB reduction predicted for $\delta = 5°$ is a good description of the reduction level achieved over most of ϕ, the 9.8 dB reduction predicted for $\delta = 2°$ falls very short of that achieved for a large region around $\phi = 0°$. This results from the fact that this reflector has a very deep null there which arises from cancellation between the two doubly reflected rays and thus equation (14(a)) is an overestimation of the scattered field in that region. If, instead of equation (14), equation (13) is used to calculate X at $\phi = 0°$, a reduction of 37.7 dB is obtained and that agrees with figure 13. Thus equation (15) has to be used with care.

Figures 30, 31, 32 and 33 show the reduction in RCS from reflectors with $a = b = 40\lambda$ and $a = b = 100\lambda$ respectively for $|\delta| = 1°, 2°, 5°$. Here it is seen that even a 1° deviation from orthogonality yields very substantial reductions in RCS.

Figures 34, 35, 36 and 37 illustrate the asymmetry in the RCS patterns for dihedral reflectors with unequal plates. It is clear that large reductions in RCS are not conditional on the equal size plate geometry.

4. EXPERIMENTAL MEASUREMENTS

4.1 The anechoic chamber

The experimental observations carried out to check the theoretical predictions were performed in the ERL anechoic chamber. This facility has a normal source-target separation of 12 m, a frequency range extending from 2.5 GHz to 40 GHz, and analogue recording of measurements(ref.4).

4.2 The dihedral reflectors

Three dihedral reflectors with reflector angles 85°, 90° and 95°, a = b = 10 cm and c = 20 cm, were fabricated of aluminium of thickness 6 mm. Two plates of dimensions 10 cm by 20 cm were held together at the required angle with polypropylene supports at the back. The long edges of the reflectors were chamfered back to approximate a thin edge.

Three frequencies were employed, viz 7.5, 10 and 15 GHz corresponding to a/λ of 2.5, 3.3 and 5.0. Measurements of backscattered RCS were made over the full azimuthal range but only results for $-\gamma \leq \phi \leq \gamma$ were analysed. The analogue X-Y plotter output was sampled at 1° intervals.

5. COMPARISON OF EXPERIMENTAL AND THEORETICAL RESULTS

The $\theta = 0°$, vertical and horizontal polarisation RCS patterns in figures 38 to 55 include the experimental data for reflectors with $\delta = -5°, 0°, 5°$ and plate sizes of $a/\lambda = 2.5, 3.3, 5.0$. Agreement between theory and experiment is good - within ±2 dB for $|\phi| \leq 30°$ in all cases except for figures 43 and 49 where it is within ±3 dB. For $|\phi| \geq 30°$, theory predicts much deeper nulls for the 85° reflectors; apart from that agreement is still reasonable.

From these experimental data, the reduction in RCS has been calculated and is plotted against the predicted values in figures 56 to 63 for $\delta = \pm 5°$, $a/\lambda = 2.5, 3.3, 5.0$, vertical polarisation and $\delta = \pm 5°$, $a/\lambda = 5.0$, horizontal polarisation. These measured values confirm that the reduction in RCS achievable is dependent on the sizes of the reflectors relative to the incident wavelength.

Figure 64 verifies the RCS pattern for the 95° reflector with $a/\lambda = 2.5$ viewed at $\theta = 5°$ for vertical polarisation.

Figures 22 and 23 predict that the RCS patterns of the 85° and 95° reflectors made for experimental validation have nulls at $\phi = \theta = 0°$ for $a = b = 9\lambda$ and $a = b = 8.5\lambda$, ie at 26.9 GHz and 25.5 GHz respectively for vertical polarisation. Unfortunately, attempts to collect reliable data at these frequencies failed because the available sources in the ERL chamber are not sufficiently stable for the necessary nulling in the chamber to be accomplished for frequencies over 21 GHz. In order to verify some of the predicted nulls discussed in Section 3, new reflectors would have to be made of a scale suited for measurement below 21 GHz. This is a task that may well be undertaken in the future.

Knott(ref.1) has an experimental validation of a reflector with $\delta = 7.5°$ and $a = b = 5.6\lambda$ at $\theta = 0°$. Figure 65 shows that a fairly deep null can be expected at $\phi = \theta = 0°$ for this reflector and this is indeed shown to be the case in reference 1, figure 5, with reasonable agreement with experiment.

6. CONCLUSIONS

This investigation has demonstrated the success of physical optics in predicting the backscattering radar cross section of dihedral corner reflectors with arbitrary included angle. Experimental measurements performed in the ERL anechoic chamber for reflectors with included angles of 85°, 90° and 95° are in excellent accord with theory over a wide range of incident angles. Further, this agreement has been verified to hold for plates from 5λ width down to 2.5λ in width. The theory can be expected to yield even better results as plate sizes increase.

The reduction in RCS achievable for a given deviation from orthogonality is dependent on the size of the reflector, in terms of wavelength of the incident radiation. For plate sizes in excess of a few wavelengths, very significant reductions in backscattered RCS can result from quite modest deviations from orthogonality. As many practical dihedral scatterers are at least ten wavelengths wide, their RCS is extremely sensitive to such deviations. In addition non-orthogonality introduces deep interference nulls that are a function of plate size and the deviation angle into the RCS patterns of these reflectors. It has been shown here that a small deviation angle in a reflector can meet the conditions for an interference null along the axis of symmetry. This somewhat unexpected result should be borne in mind when employing such reflectors.

7. ACKNOWLEDGEMENT

The anechoic chamber measurements incorporated in this paper were obtained by Mr J. Crombie under the direction of Mr A. Tickner of Radar Division. Mr L. Nicholls of Weapon Systems Division, WSRL, made useful suggestions on practical applications of the results.

REFERENCES

No.	Author	Title
1	Knott, E.F.	"RCS Reduction of Dihedral Corners". IEEE Trans Antennas Propagat, Vol. AP-25, pp 406-409, 1977
2	Ruck, G.T., Barrick, D.E., Stuart, W.D. and Krichbaum, C.K.	"Radar Cross Section Handbook Volume 1". Plenum Press, New York, 1970
3	Crispin, J.W. and Siegel, K.M.	"Methods of Radar Cross-Section Analysis". Academic Press, New York, 1968
4	Tickner, A.T. and Sinnott, D.H.	"The Electronics Research Laboratory Anechoic Chamber and its Evaluation". Seminar on Electromagnetic Antenna and Scattering Measurements, Part II, CSIRO Division of Applied Physics, National Measurements Laboratory, November 1982

TABLE 1. EXPRESSIONS FOR THE CONTRIBUTIONS TO THE BACKSCATTERED FIELD

Backscattered Magnetic Field	$\bar{Q}^{\nu}$		P^{ν}	
	Vertical Polarisation	Horizontal Polarisation		
$\vec{H}_1^s$	$\cos\theta \sin(\gamma+\phi)$. $(\sin\phi, -\cos\phi, 0)$	$\cos\theta \sin(\gamma+\phi)$. $(-\sin\theta\cos\phi, -\sin\theta\sin\phi, \cos\theta)$	$\exp\{-ik[c\sin\theta + a\cos\theta\cos(\gamma+\phi)]\}$. ac. $\frac{\sin(kc\sin\theta)}{kc\sin\theta} \cdot \frac{\sin[ka\cos\theta\cos(\gamma+\phi)]}{ka\cos\theta\cos(\gamma+\phi)}$	$-\gamma \le \phi \le \gamma$; $0 \le \theta \le \frac{\pi}{2}$
$\vec{H}_2^s$	$\cos\theta \sin(\gamma-\phi)$. $(\sin\phi, -\cos\phi, 0)$	$\cos\theta \sin(\gamma-\phi)$. $(-\sin\theta\cos\phi, -\sin\theta\sin\phi, \cos\theta)$	$\exp\{-ik[c\sin\theta + b\cos\theta\cos(\gamma-\phi)]\}$. bc. $\frac{\sin(kc\sin\theta)}{kc\sin\theta} \cdot \frac{\sin[kb\cos\theta\cos(\gamma-\phi)]}{kb\cos\theta\cos(\gamma-\phi)}$	$-\gamma \le \phi \le \gamma$; $0 \le \theta \le \frac{\pi}{2}$
$\vec{H}_{12}^D$	$\cos\theta \sin(3\gamma+\phi)$. $(-\sin\phi, \cos\phi, 0)$	$\cos\theta$. $\{-\sin\theta[\sin\gamma\sin\phi\cos(3\gamma+\phi)]$, $\sin\theta[\cos\gamma\cos\phi\cos(3\gamma+\phi)]$, $\cos\theta\sin(\gamma-\phi)\}$	$\exp[-ikb'\cos\theta\cos2\gamma\cos(\gamma+\phi)] \cdot \frac{b'}{2ik\sin\theta} \cdot \left\{\frac{\sin[kb'\cos\theta\cos2\gamma\cos(\gamma+\phi)]}{kb'\cos\theta\cos2\gamma\cos(\gamma+\phi)} - \exp\left[-2ikc\sin\theta + \frac{ikb'\sin\theta\tan\theta\sin2\gamma}{\sin(\gamma+\phi)}\right] \cdot \sin\left[kb'\cos\theta\cos2\gamma\cos(\gamma+\phi) - \frac{kb'\sin\theta\tan\theta\sin2\gamma}{\sin(\gamma+\phi)}\right] \cdot \left[kb'\cos\theta\cos2\gamma\cos(\gamma+\phi) - \frac{kb'\sin\theta\tan\theta\sin2\gamma}{\sin(\gamma+\phi)}\right]^{-1}\right\}$	$-\gamma < \phi < \pi-3\gamma$; $0 < \theta < \frac{\pi}{2}$
			$\exp[-ikb'\cos2\gamma\cos(\gamma+\phi)]$. bc. $\frac{\sin[kb'\cos2\gamma\cos(\gamma+\phi)]}{kb'\cos2\gamma\cos(\gamma+\phi)}$	$-\gamma < \phi < \pi-3\gamma$; $\theta = 0$
			0	otherwise

TABLE I (CONTD.).

$\bar{\bar{H}}^{D}_{21}$	$\cos\theta \sin(3\gamma-\phi)$. $(-\sin\phi, \cos\phi, 0)$	$\cos\theta$. $\lvert -\sin\theta\lvert \sin\gamma+\sin\phi \cos(3\gamma-\phi)\rvert$, $\sin\theta\lvert \cos\phi \cos(3\gamma-\phi)-\cos\gamma\rvert$, $\cos\theta \sin(\gamma+\phi)\rvert$	$\exp\lvert -ika'\cos\theta \cos 2\gamma \cos(\gamma-\phi)\rvert \cdot \frac{a'}{2ik \sin\theta} \cdot$ $\left\{ \frac{\sin\lvert ka'\cos\theta \cos 2\gamma \cos(\gamma-\phi)\rvert}{ka'\cos\theta \cos 2\gamma \cos(\gamma-\phi)} \right.$ $\exp\left[-2ikc\sin\theta + \frac{ika'\sin\theta \tan\theta \sin 2\gamma}{\sin(\gamma-\phi)} \right]$. $\sin\left[ka'\cos\theta \cos 2\gamma \cos(\gamma-\phi) - \frac{ka'\sin\theta \tan\theta \sin 2\gamma}{\sin(\gamma-\phi)} \right]$. $\left. \left[ka'\cos\theta \cos 2\gamma \cos(\gamma-\phi) - \frac{ka'\sin\theta \tan\theta \sin 2\gamma}{\sin(\gamma-\phi)} \right]^{-1} \right\}$	$3\gamma-\pi < \phi < \gamma$; $0 < \theta < \frac{\pi}{2}$
			$\exp\lvert -ika' \cos 2\gamma \cos(\gamma-\phi)\rvert . a'c.$ $\frac{\sin\lvert ka' \cos 2\gamma \cos(\gamma-\phi)\rvert}{ka' \cos 2\gamma \cos(\gamma-\phi)}$	$3\gamma-\pi < \phi < \gamma$; $\theta = 0$
			0	otherwise
$\bar{\bar{H}}^{T}_{21}$	$\cos\theta \sin(5\gamma+\phi)$. $(\sin\phi, -\cos\phi, 0)$	$\cos\theta$. $\lvert \sin\theta\lvert \sin\phi \cos(5\gamma+\phi)-\sin\gamma\rvert$, $-\sin\theta\lvert \cos\phi \cos(5\gamma+\phi)+\cos\gamma\rvert$, $\cos\theta \sin(\gamma+\phi)\rvert$	$\exp\left[-ika'' \cos\theta \cos 2\gamma \cos(3\gamma+\phi) \cdot \frac{a''}{2ik \sin\theta} \right] \cdot$ $\left\{ \frac{\sin\lvert ka'' \cos\theta \cos 2\gamma \cos(3\gamma+\phi)\rvert}{ka'' \cos\theta \cos 2\gamma \cos(3\gamma+\phi)} \right.$ $\exp\left[-2ikc\sin\theta + \frac{ika'' \sin\theta \tan\theta \sin 4\gamma}{\sin(\gamma+\phi)} \right]$. $\sin\left[ka'' \cos\theta \cos 2\gamma \cos(3\gamma+\phi) - \frac{ka'' \sin\theta \tan\theta \sin 4\gamma}{\sin(\gamma+\phi)} \right]$. $\left. \left[ka'' \cos\theta \cos 2\gamma \cos(3\gamma+\phi) - \frac{ka'' \sin\theta \tan\theta \sin 4\gamma}{\sin(\gamma+\phi)} \right]^{-1} \right\}$	$\gamma < \frac{\pi}{4}$; $-\gamma < \phi < \pi-5\gamma$; $0 < \theta < \frac{\pi}{2}$

TABLE 1(CONTD.).

$\vec{\Pi}^{\Gamma}_{1,1}$	$\cos\theta\ \sin(5\gamma+\phi)\cdot$ $(\sin\phi,-\cos\phi,0)$	$\cos\theta\cdot$ $\{\sin\theta\lvert\sin\phi\ \cos(5\gamma+\phi)-\sin\gamma\rvert,$ $-\sin\theta\lvert\cos\phi\ \cos(5\gamma+\phi)+\cos\gamma\rvert,$ $\cos\theta\ \sin(\gamma+\phi)\}$	$\exp\lvert -ika''\ \cos2\gamma\ \cos(3\gamma+\phi)\rvert . a''c.$ $\frac{\sin\lvert ka''\ \cos2\gamma\ \cos(3\gamma+\phi)\rvert}{ka''\ \cos2\gamma\ \cos(3\gamma+\phi)}$	$\gamma < \frac{\pi}{4}$; $-\gamma < \phi < \pi-5\gamma$; $\theta=0$
			0	otherwise
$\vec{\Pi}^{\Gamma}_{2,2}$	$\cos\theta\ \sin(5\gamma-\phi)\cdot$ $(\sin\phi,-\cos\phi,0)$	$\cos\theta\cdot$ $\{\sin\theta\lvert\sin\phi\ \cos(5\gamma-\phi)-\sin\gamma\rvert,$ $-\sin\theta\lvert\cos\phi\ \cos(5\gamma-\phi)-\cos\gamma\rvert,$ $\cos\theta\ \sin(\gamma-\phi)\rvert$	$\exp\lvert -ikb''\ \cos\theta\ \cos2\gamma\ \cos(3\gamma-\phi)\rvert \cdot \frac{b''}{2ik\ \sin\theta} \cdot$ $\left\{\frac{\sin\lvert kb''\ \cos\theta\ \cos2\gamma\ \cos(3\gamma-\phi)\rvert}{kb''\ \cos\theta\ \cos2\gamma\ \cos(3\gamma-\phi)}\right.$ $\exp\left[-2ikc\sin\theta + \frac{ikb''\ \sin\theta\ \tan\theta\ \sin4\gamma}{\sin(\gamma-\phi)}\right] \cdot$ $\sin\left[kb''\ \cos\theta\ \cos2\gamma\ \cos(3\gamma-\phi) - \frac{kb''\ \sin\theta\ \tan\theta\ \sin4\gamma}{\sin(\gamma-\phi)}\right] \cdot$ $\left.\left[kb''\ \cos\theta\ \cos2\gamma\ \cos(3\gamma-\phi) - \frac{kb''\ \sin\theta\ \tan\theta\ \sin4\gamma}{\sin(\gamma-\phi)}\right]^{-1}\right\}$	$\gamma < \frac{\pi}{4}$; $5\gamma-\pi < \phi < \gamma$; $0 < \theta < \frac{\pi}{2}$
			$\exp\lvert -ikb''\ \cos2\gamma\ \cos(3\gamma-\phi)\rvert . b''c.$ $\frac{\sin\lvert kb''\ \cos2\gamma\ \cos(3\gamma-\phi)\rvert}{kb''\ \cos2\gamma\ \cos(3\gamma-\phi)}$	$\gamma < \frac{\pi}{4}$; $5\gamma-\pi < \phi < \gamma$; $\theta=0$
			0	otherwise

TABLE 2. DEFINITIONS FOR a' AND b' AND THEIR ASSOCIATED DOMAINS OF VALIDITY

Variable	Definition	Domains of Validity
a'	a	$\phi \leq \tan^{-1}\left(\frac{b\sin\gamma - a\sin 3\gamma}{b\cos\gamma - a\cos 3\gamma}\right)$; $c - \frac{a\tan\theta\ \sin 2\gamma}{\sin(\gamma-\phi)} \geq 0$
	$\frac{c\sin(\gamma-\phi)}{\tan\theta\ \sin 2\gamma}$	$\phi \leq \tan^{-1}\left(\frac{b\sin\gamma - a\sin 3\gamma}{b\cos\gamma - a\cos 3\gamma}\right)$; $c - \frac{a\tan\theta\ \sin 2\gamma}{\sin(\gamma-\phi)} < 0$
		$\phi > \tan^{-1}\left(\frac{b\sin\gamma - a\sin 3\gamma}{b\cos\gamma - a\cos 3\gamma}\right)$; $c - \frac{b\tan\theta\ \sin 2\gamma}{\sin(3\gamma-\phi)} < 0$
	$\frac{b\sin(\gamma-\phi)}{\sin(3\gamma-\phi)}$	$\phi > \tan^{-1}\left(\frac{b\sin\gamma - a\sin 3\gamma}{b\cos\gamma - a\cos 3\gamma}\right)$; $c - \frac{b\tan\theta\ \sin 2\gamma}{\sin(3\gamma-\phi)} \geq 0$
b'	$\frac{a\sin(\gamma+\phi)}{\sin(3\gamma+\phi)}$	$\phi \leq \tan^{-1}\left(\frac{b\sin 3\gamma - a\sin\gamma}{a\cos\gamma - b\cos 3\gamma}\right)$; $c - \frac{a\tan\theta\ \sin 2\gamma}{\sin(3\gamma+\phi)} \geq 0$
	$\frac{c\sin(\gamma+\phi)}{\tan\theta\ \sin 2\gamma}$	$\phi \leq \tan^{-1}\left(\frac{b\sin 3\gamma - a\sin\gamma}{a\cos\gamma - b\cos 3\gamma}\right)$; $c - \frac{a\tan\theta\ \sin 2\gamma}{\sin(3\gamma+\phi)} < 0$
		$\phi > \tan^{-1}\left(\frac{b\sin 3\gamma - a\sin\gamma}{a\cos\gamma - b\cos 3\gamma}\right)$; $c - \frac{b\tan\theta\ \sin 2\gamma}{\sin(\gamma+\phi)} < 0$
	b	$\phi > \tan^{-1}\left(\frac{b\sin 3\gamma - a\sin\gamma}{a\cos\gamma - b\cos 3\gamma}\right)$; $c - \frac{b\tan\theta\ \sin 2\gamma}{\sin(\gamma+\phi)} \geq 0$

TABLE 3. DEFINITIONS FOR a" AND THEIR ASSOCIATED DOMAINS OF VALIDITY

Variable	Definition	Domains of Validity
a"	$\frac{a\sin(\gamma+\phi)}{\sin(5\gamma+\phi)}$	$\tan^{-1}\left(\frac{b\sin3\gamma - a\sin\gamma}{a\cos\gamma - b\cos3\gamma}\right) \geq \pi-5\gamma;\ \phi \leq \frac{\pi}{2} - 3\gamma;\ c - \frac{a\tan\theta\ \sin4\gamma}{\sin(5\gamma+\phi)} \geq 0;$
		$\tan^{-1}\left(\frac{b\sin3\gamma - a\sin\gamma}{a\cos\gamma - b\cos3\gamma}\right) < \pi-5\gamma;\ \phi \leq \tan^{-1}\left(\frac{b\sin3\gamma - a\sin\gamma}{a\cos\gamma - b\cos3\gamma}\right);\ \phi \leq \frac{\pi}{2} - 3\gamma;\ c - \frac{a\tan\theta\ \sin4\gamma}{\sin(5\gamma+\phi)} \geq 0$
	$\frac{b\sin(3\gamma+\phi)}{\sin(5\gamma+\phi)}$	$\tan^{-1}\left(\frac{b\sin3\gamma - a\sin\gamma}{a\cos\gamma - b\cos3\gamma}\right) < \pi-5\gamma;\ \phi > \tan^{-1}\left(\frac{b\sin3\gamma - a\sin\gamma}{a\cos\gamma - b\cos3\gamma}\right);\ \phi \leq \tan^{-1}\left(\frac{a\sin5\gamma - b\sin3\gamma}{b\cos3\gamma - a\cos5\gamma}\right);\ c - \frac{b\tan\theta\ \sin4\gamma\ \sin(3\gamma+\phi)}{\sin(\gamma+\phi)\ \sin(5\gamma+\phi)} \geq 0$
	$\frac{c\sin(\gamma+\phi)}{\tan\theta\ \sin4\gamma}$	$\tan^{-1}\left(\frac{b\sin3\gamma - a\sin\gamma}{a\cos\gamma - b\cos3\gamma}\right) \geq \pi-5\gamma;\ \phi \leq \frac{\pi}{2} - 3\gamma;\ c - \frac{a\tan\theta\ \sin4\gamma}{\sin(5\gamma+\phi)} < 0;$
		$\tan^{-1}\left(\frac{b\sin3\gamma - a\sin\gamma}{a\cos\gamma - b\cos3\gamma}\right) \geq \pi-5\gamma;\ \phi > \frac{\pi}{2} - 3\gamma;\ c - \frac{a\tan\theta\ \sin4\gamma}{\sin(\gamma+\phi)} < 0;$
		$\tan^{-1}\left(\frac{b\sin3\gamma - a\sin\gamma}{a\cos\gamma - b\cos3\gamma}\right) < \pi-5\gamma;\ \phi \leq \tan^{-1}\left(\frac{b\sin3\gamma - a\sin\gamma}{a\cos\gamma - b\cos3\gamma}\right);\ \phi \leq \frac{\pi}{2} - 3\gamma;\ c - \frac{a\tan\theta\ \sin4\gamma}{\sin(5\gamma+\phi)} < 0$
		$\tan^{-1}\left(\frac{b\sin3\gamma - a\sin\gamma}{a\cos\gamma - b\cos3\gamma}\right) < \pi-5\gamma;\ \phi \leq \tan^{-1}\left(\frac{b\sin3\gamma - a\sin\gamma}{a\cos\gamma - b\cos3\gamma}\right);\ \phi > \frac{\pi}{2} - 3\gamma;\ c - \frac{a\tan\theta\ \sin4\gamma}{\sin(\gamma+\phi)} < 0$
		$\tan^{-1}\left(\frac{b\sin3\gamma - a\sin\gamma}{a\cos\gamma - b\cos3\gamma}\right) < \pi-5\gamma;\ \phi > \tan^{-1}\left(\frac{b\sin3\gamma - a\sin\gamma}{a\cos\gamma - b\cos3\gamma}\right);\ \phi \leq \tan^{-1}\left(\frac{a\sin5\gamma - b\sin3\gamma}{b\cos3\gamma - a\cos5\gamma}\right);\ c - \frac{b\tan\theta\ \sin4\gamma\ \sin(3\gamma+\phi)}{\sin(\gamma+\phi)\ \sin(5\gamma+\phi)} < 0$
		$\tan^{-1}\left(\frac{b\sin3\gamma - a\sin\gamma}{a\cos\gamma - b\cos3\gamma}\right) < \pi-5\gamma;\ \phi > \tan^{-1}\left(\frac{b\sin3\gamma - a\sin\gamma}{a\cos\gamma - b\cos3\gamma}\right);\ \phi > \tan^{-1}\left(\frac{a\sin5\gamma - b\sin3\gamma}{b\cos3\gamma - a\cos5\gamma}\right);\ c - \frac{a\tan\theta\ \sin4\gamma}{\sin(\gamma+\phi)} < 0$
	a	$\tan^{-1}\left(\frac{b\sin3\gamma - a\sin\gamma}{a\cos\gamma - b\cos3\gamma}\right) \geq \pi-5\gamma;\ \phi > \frac{\pi}{2} - 3\gamma;\ c - \frac{a\tan\theta\ \sin4\gamma}{\sin(\gamma+\phi)} \geq 0$
		$\tan^{-1}\left(\frac{b\sin3\gamma - a\sin\gamma}{a\cos\gamma - b\cos3\gamma}\right) < \pi-5\gamma;\ \phi \leq \tan^{-1}\left(\frac{b\sin3\gamma - a\sin\gamma}{a\cos\gamma - b\cos3\gamma}\right);\ \phi > \frac{\pi}{2} - 3\gamma;\ c - \frac{a\tan\theta\ \sin4\gamma}{\sin(\gamma+\phi)} \geq 0$
		$\tan^{-1}\left(\frac{b\sin3\gamma - a\sin\gamma}{a\cos\gamma - b\cos3\gamma}\right) < \pi-5\gamma;\ \phi > \tan^{-1}\left(\frac{b\sin3\gamma - a\sin\gamma}{a\cos\gamma - b\cos3\gamma}\right);\ \phi > \tan^{-1}\left(\frac{a\sin5\gamma - b\sin3\gamma}{b\cos3\gamma - a\cos5\gamma}\right);\ c - \frac{a\tan\theta\ \sin4\gamma}{\sin(\gamma+\phi)} \geq 0$

TABLE 4. DEFINITIONS FOR b'' AND THEIR ASSOCIATED DOMAINS OF VALIDITY

Variable	Definition	Domains of Validity
b''	$\frac{a\sin(3\gamma-\phi)}{\sin(5\gamma-\phi)}$	$\tan^{-1}\left(\frac{b\sin\gamma - a\sin3\gamma}{b\cos\gamma - a\cos3\gamma}\right) \geq 5\gamma-\pi;\ \phi \leq \tan^{-1}\left(\frac{b\sin\gamma - a\sin3\gamma}{b\cos\gamma - a\cos3\gamma}\right);\phi \leq \tan^{-1}\left(\frac{b\sin5\gamma - a\sin3\gamma}{b\cos5\gamma - a\cos3\gamma}\right);\quad c - \frac{a\tan\theta\ \sin4\gamma\ \sin(3\gamma-\phi)}{\sin(\gamma-\phi)\ \sin(5\gamma-\phi)} \geq 0$
	$\frac{b\sin(\gamma-\phi)}{\sin(5\gamma-\phi)}$	$\tan^{-1}\left(\frac{b\sin\gamma - a\sin3\gamma}{b\cos\gamma - a\cos3\gamma}\right) \geq 5\gamma-\pi;\ \phi > \tan^{-1}\left(\frac{b\sin\gamma - a\sin3\gamma}{b\cos\gamma - a\cos3\gamma}\right);\phi \geq 3\gamma - \frac{\pi}{2};\ c - \frac{b\tan\theta\ \sin4\gamma}{\sin(5\gamma-\phi)} \geq 0$
		$\tan^{-1}\left(\frac{b\sin\gamma - a\sin3\gamma}{b\cos\gamma - a\cos3\gamma}\right) < 5\gamma-\pi;\ \phi \geq 3\gamma - \frac{\pi}{2};\ c - \frac{b\tan\theta\ \sin4\gamma}{\sin(5\gamma-\phi)} \geq 0$
	$c\sin(\gamma-\phi)$ $\tan\theta\ \sin4\gamma$	$\tan^{-1}\left(\frac{b\sin\gamma - a\sin3\gamma}{b\cos\gamma - a\cos3\gamma}\right) \geq 5\gamma-\pi;\ \phi \leq \tan^{-1}\left(\frac{b\sin\gamma - a\sin3\gamma}{b\cos\gamma - a\cos3\gamma}\right);\phi \leq \tan^{-1}\left(\frac{b\sin5\gamma - a\sin3\gamma}{b\cos5\gamma - a\cos3\gamma}\right);\quad c - \frac{a\tan\theta\ \sin4\gamma\ \sin(3\gamma-\phi)}{\sin(\gamma-\phi)\ \sin(5\gamma-\phi)} < 0$
		$\tan^{-1}\left(\frac{b\sin\gamma - a\sin3\gamma}{b\cos\gamma - a\cos3\gamma}\right) \geq 5\gamma-\pi;\ \phi \leq \tan^{-1}\left(\frac{b\sin\gamma - a\sin3\gamma}{b\cos\gamma - a\cos3\gamma}\right);\phi > \tan^{-1}\left(\frac{b\sin5\gamma - a\sin3\gamma}{b\cos5\gamma - a\cos3\gamma}\right);\quad c - \frac{b\tan\theta\ \sin4\gamma}{\sin(\gamma-\phi)} < 0$
		$\tan^{-1}\left(\frac{b\sin\gamma - a\sin3\gamma}{b\cos\gamma - a\cos3\gamma}\right) \geq 5\gamma-\pi;\ \phi > \tan^{-1}\left(\frac{b\sin\gamma - a\sin3\gamma}{b\cos\gamma - a\cos3\gamma}\right);\phi \geq 3\gamma - \frac{\pi}{2};\ c - \frac{b\tan\theta\ \sin4\gamma}{\sin(5\gamma-\phi)} < 0$
		$\tan^{-1}\left(\frac{b\sin\gamma - a\sin3\gamma}{b\cos\gamma - a\cos3\gamma}\right) \geq 5\gamma-\pi;\ \phi > \tan^{-1}\left(\frac{b\sin\gamma - a\sin3\gamma}{b\cos\gamma - a\cos3\gamma}\right);\phi < 3\gamma - \frac{\pi}{2};\ c - \frac{b\tan\theta\ \sin4\gamma}{\sin(\gamma-\phi)} < 0$
		$\tan^{-1}\left(\frac{b\sin\gamma - a\sin3\gamma}{b\cos\gamma - a\cos3\gamma}\right) < 5\gamma-\pi;\ \phi \geq 3\gamma - \frac{\pi}{2};\ c - \frac{b\tan\theta\ \sin4\gamma}{\sin(5\gamma-\phi)} < 0$
		$\tan^{-1}\left(\frac{b\sin\gamma - a\sin3\gamma}{b\cos\gamma - a\cos3\gamma}\right) < 5\gamma-\pi;\ \phi < 3\gamma - \frac{\pi}{2};\ c - \frac{b\tan\theta\ \sin4\gamma}{\sin(\gamma-\phi)} < 0$
	b	$\tan^{-1}\left(\frac{b\sin\gamma - a\sin3\gamma}{b\cos\gamma - a\cos3\gamma}\right) \geq 5\gamma-\pi;\ \phi \leq \tan^{-1}\left(\frac{b\sin\gamma - a\sin3\gamma}{b\cos\gamma - a\cos3\gamma}\right);\phi > \tan^{-1}\left(\frac{b\sin5\gamma - a\sin3\gamma}{b\cos5\gamma - a\cos3\gamma}\right);\quad c - \frac{b\tan\theta\ \sin4\gamma}{\sin(\gamma-\phi)} \geq 0$
		$\tan^{-1}\left(\frac{b\sin\gamma - a\sin3\gamma}{b\cos\gamma - a\cos3\gamma}\right) \geq 5\gamma-\pi;\ \phi > \tan^{-1}\left(\frac{b\sin\gamma - a\sin3\gamma}{b\cos\gamma - a\cos3\gamma}\right);\phi < 3\gamma - \frac{\pi}{2};\ c - \frac{b\tan\theta\ \sin4\gamma}{\sin(\gamma-\phi)} \geq 0$
		$\tan^{-1}\left(\frac{b\sin\gamma - a\sin3\gamma}{b\cos\gamma - a\cos3\gamma}\right) < 5\gamma-\pi;\ \phi < 3\gamma - \frac{\pi}{2};\ c - \frac{b\tan\theta\ \sin4\gamma}{\sin(\gamma-\phi)} \geq 0$

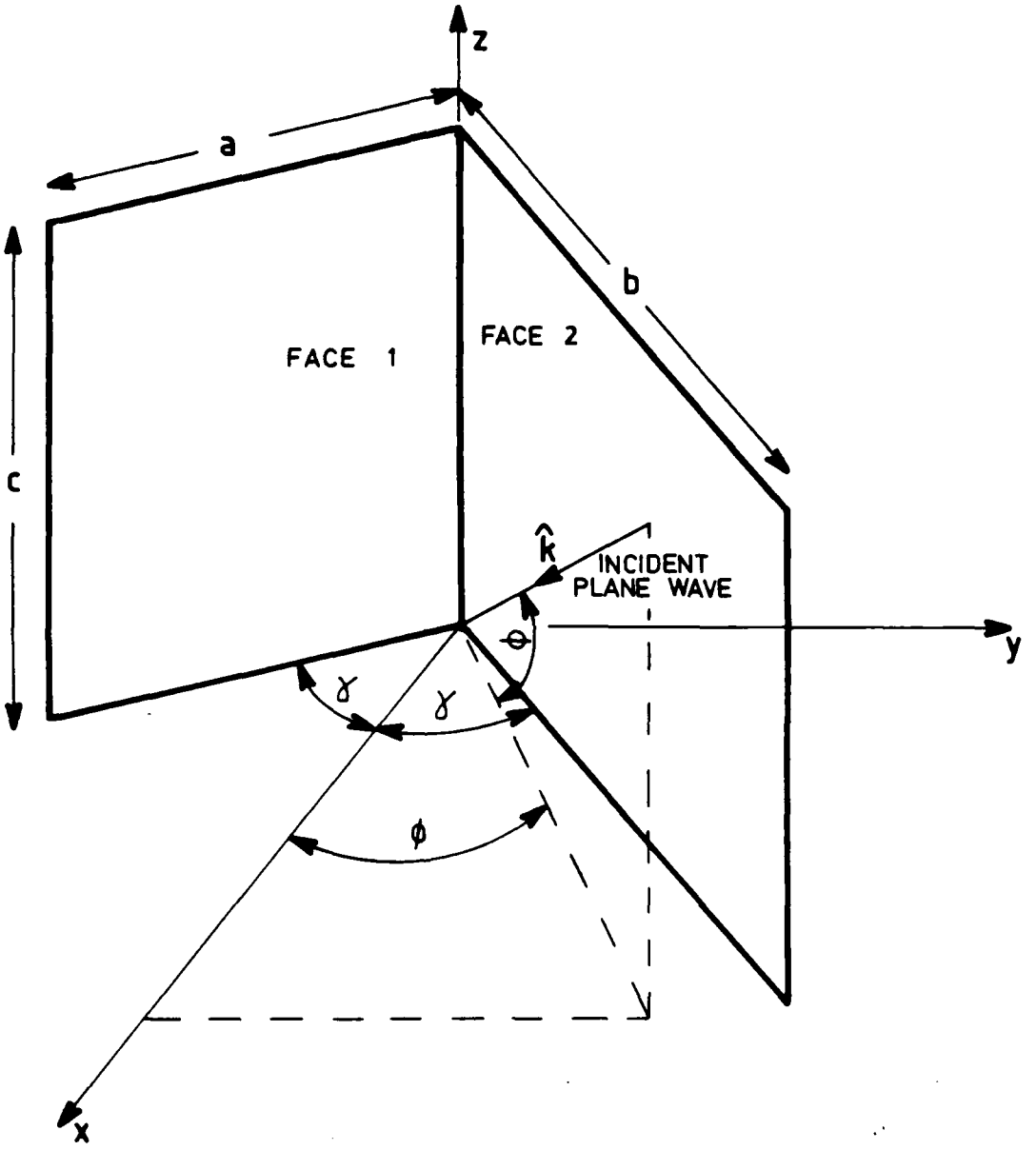

Figure 1. Dihedral corner reflector

ERL-0325-TR
Figure 2

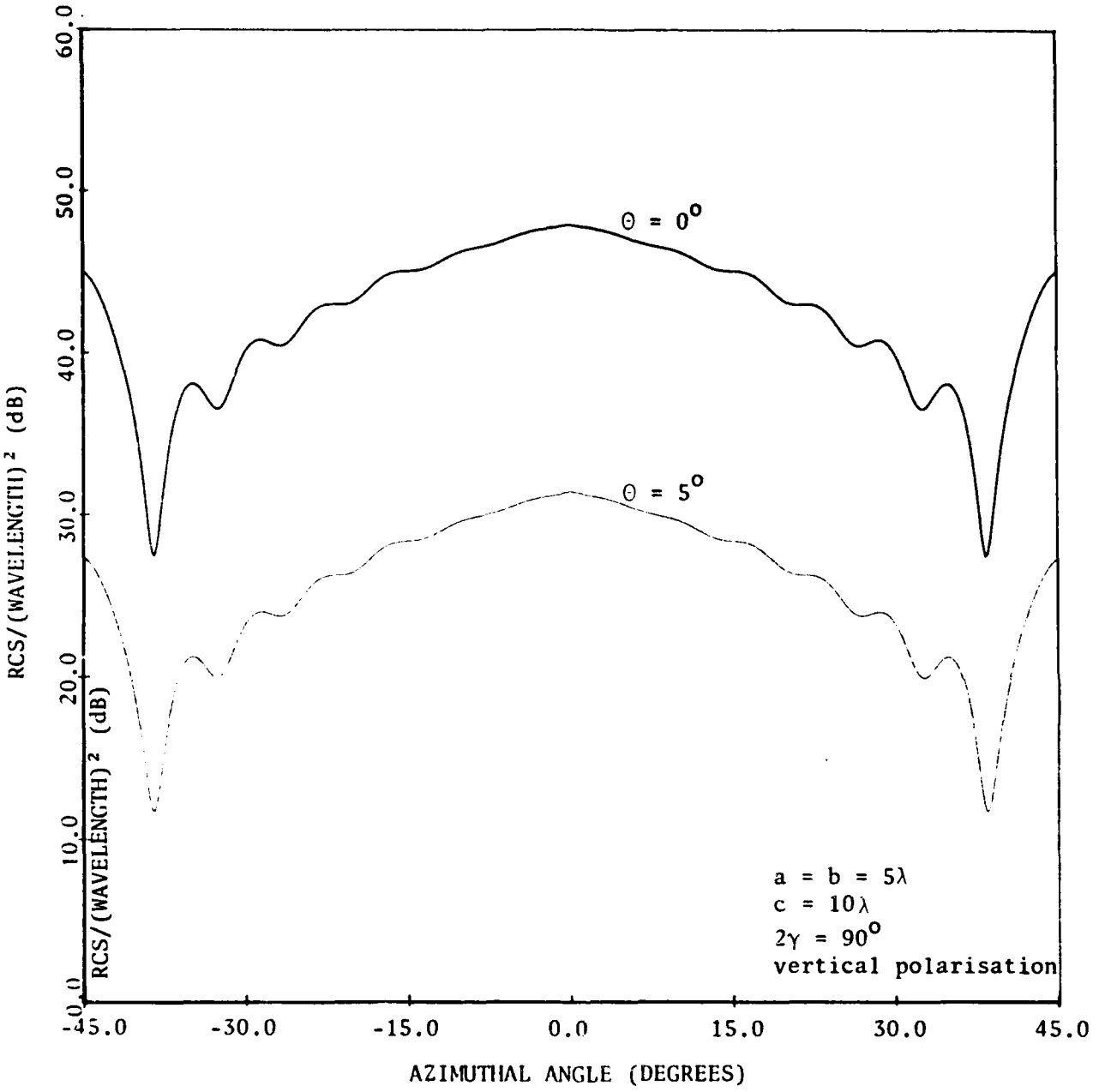

Figure 2. Comparison of RCS for $\Theta = 0^{\circ}$ and $\Theta = 5^{\circ}$

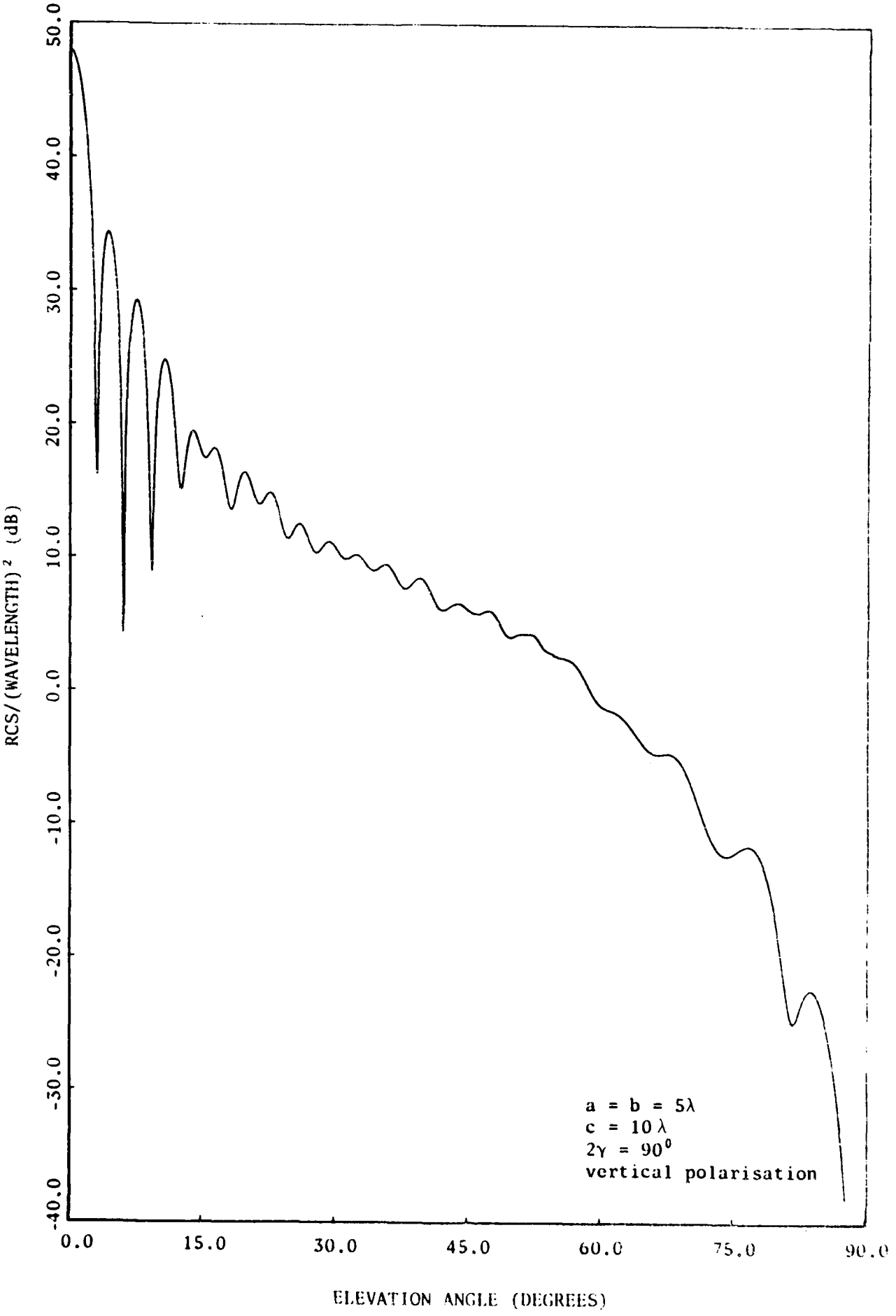

Figure 3. Elevation RCS for $\phi = 0^{\circ}$

ERL-0325-TR
Figure 4

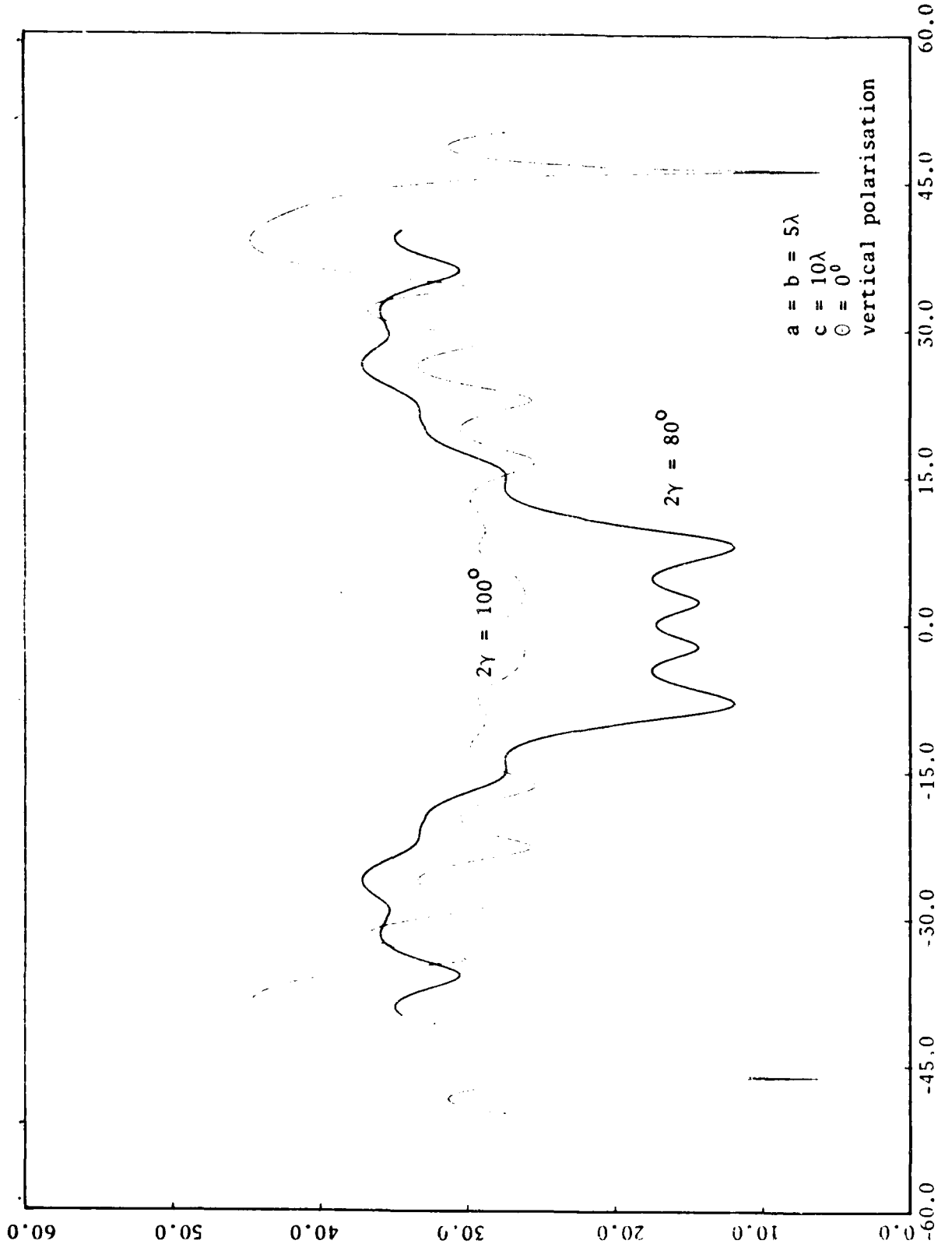

Figure 4. Comparison of RCS for reflector angles 80^{o} and 100^{o}

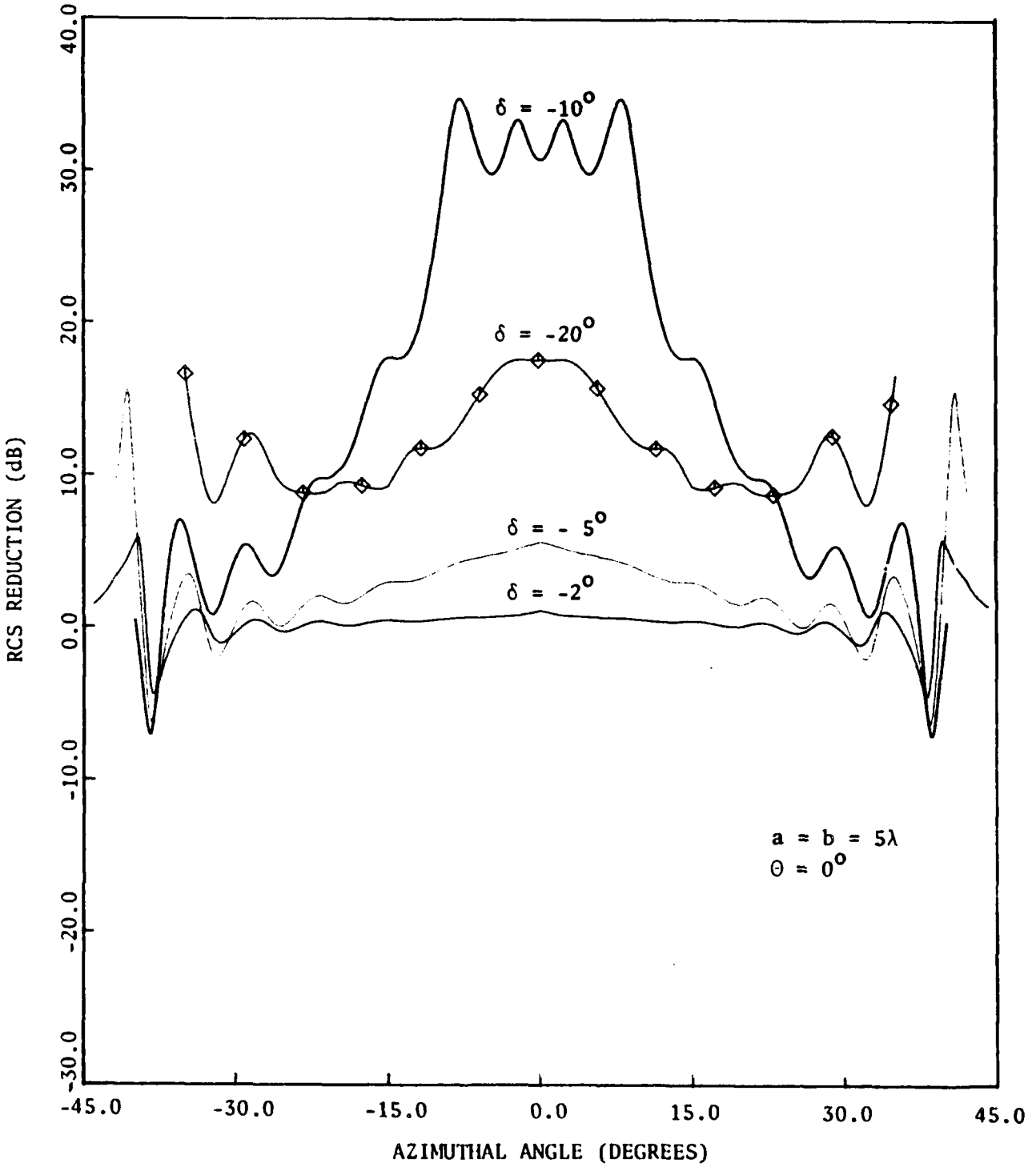

Figure 5. Reduction in RCS for $\delta = -2^{\circ}$, -5°, -10° and -20° (vertical polarisation)

ERL-0325-TR
Figure 6

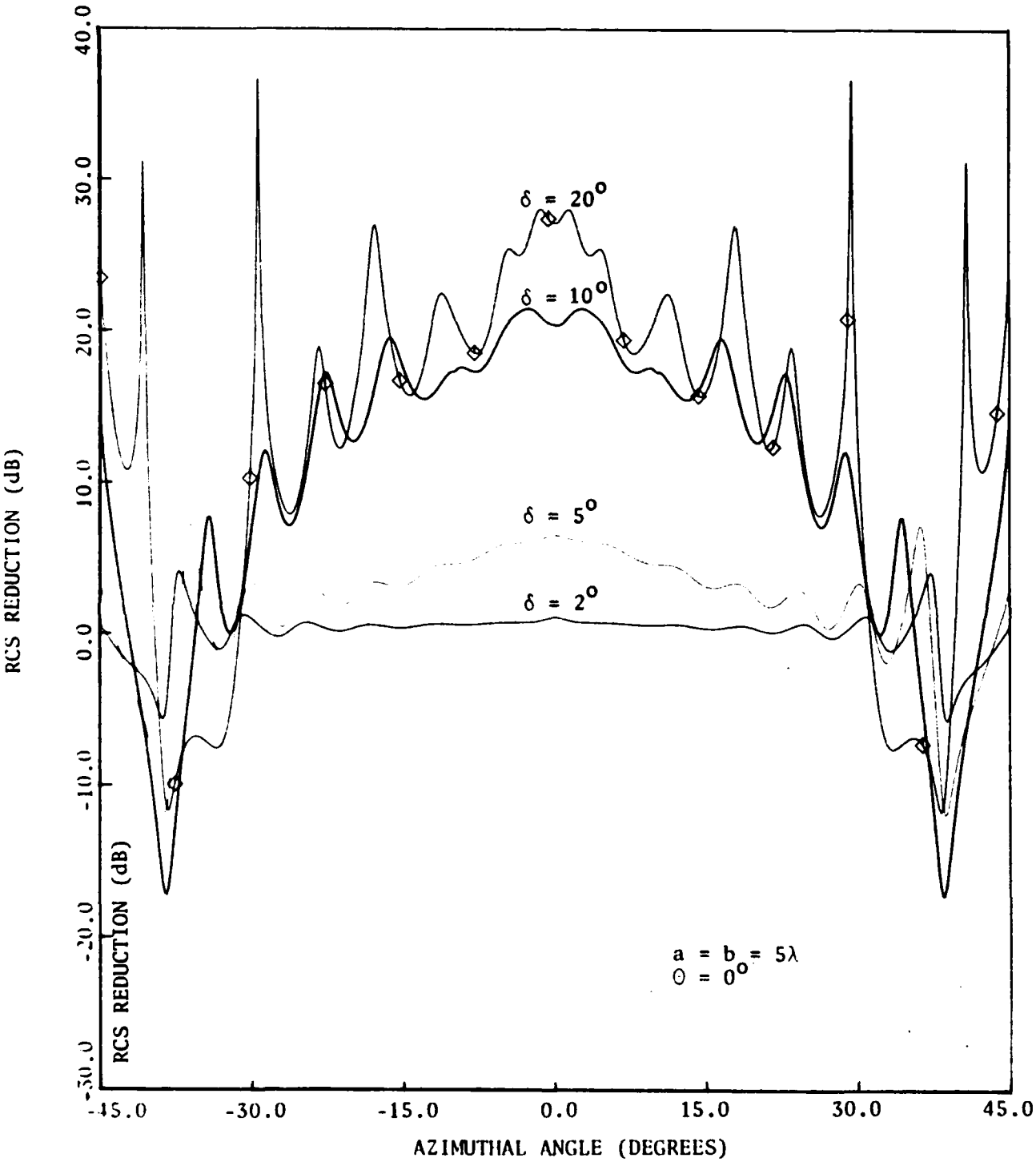

Figure 6. Reduction in RCS for $\delta = 2^{\circ}$, 5°, 10° and 20° (vertical polarisation)

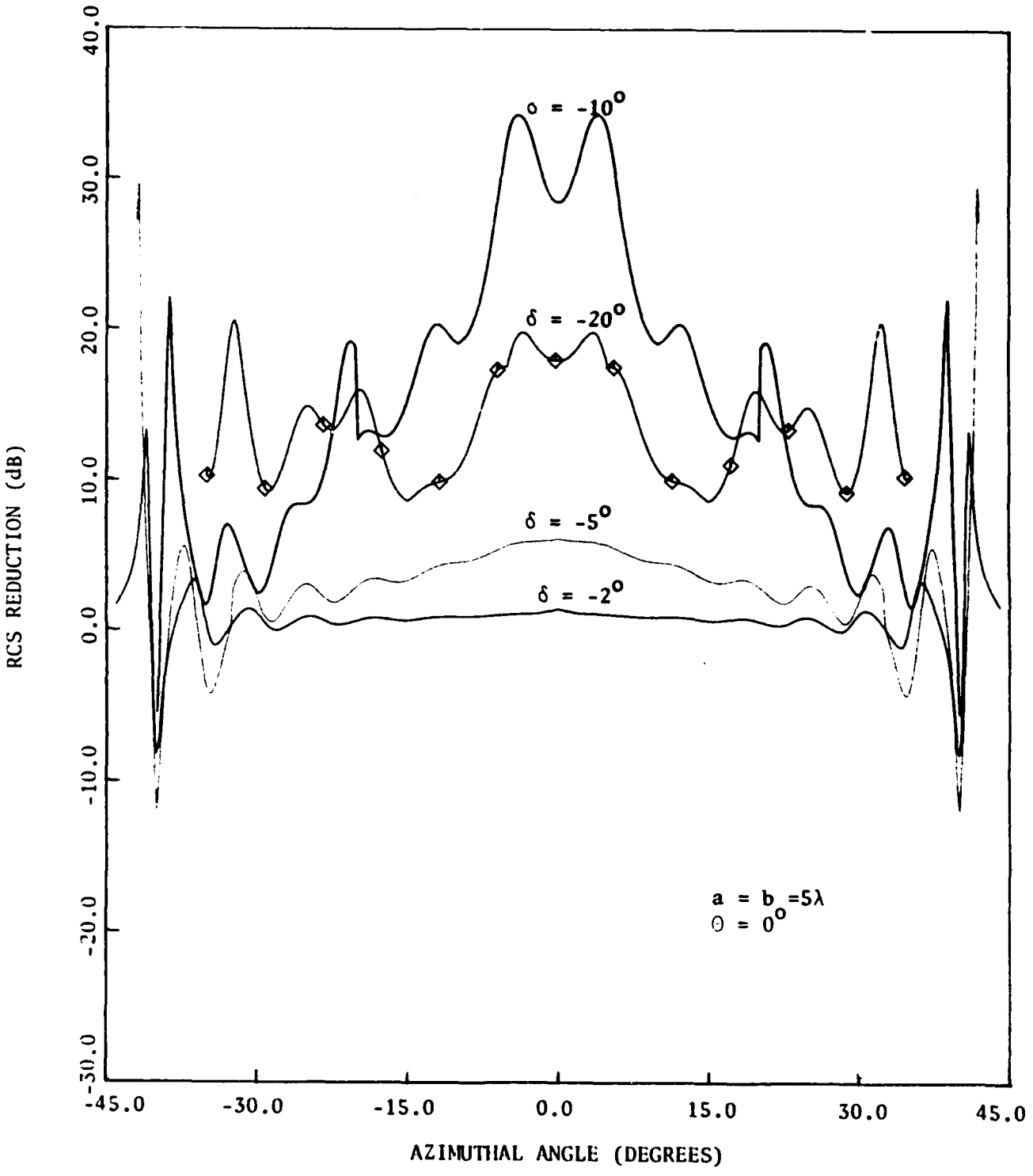

Figure 7. Reduction in RCS for $\delta = -2^{o}$, -5^{o}, -10^{o} and -20^{o} (horizontal polarisation)

ERL-0325-TR
Figure 8

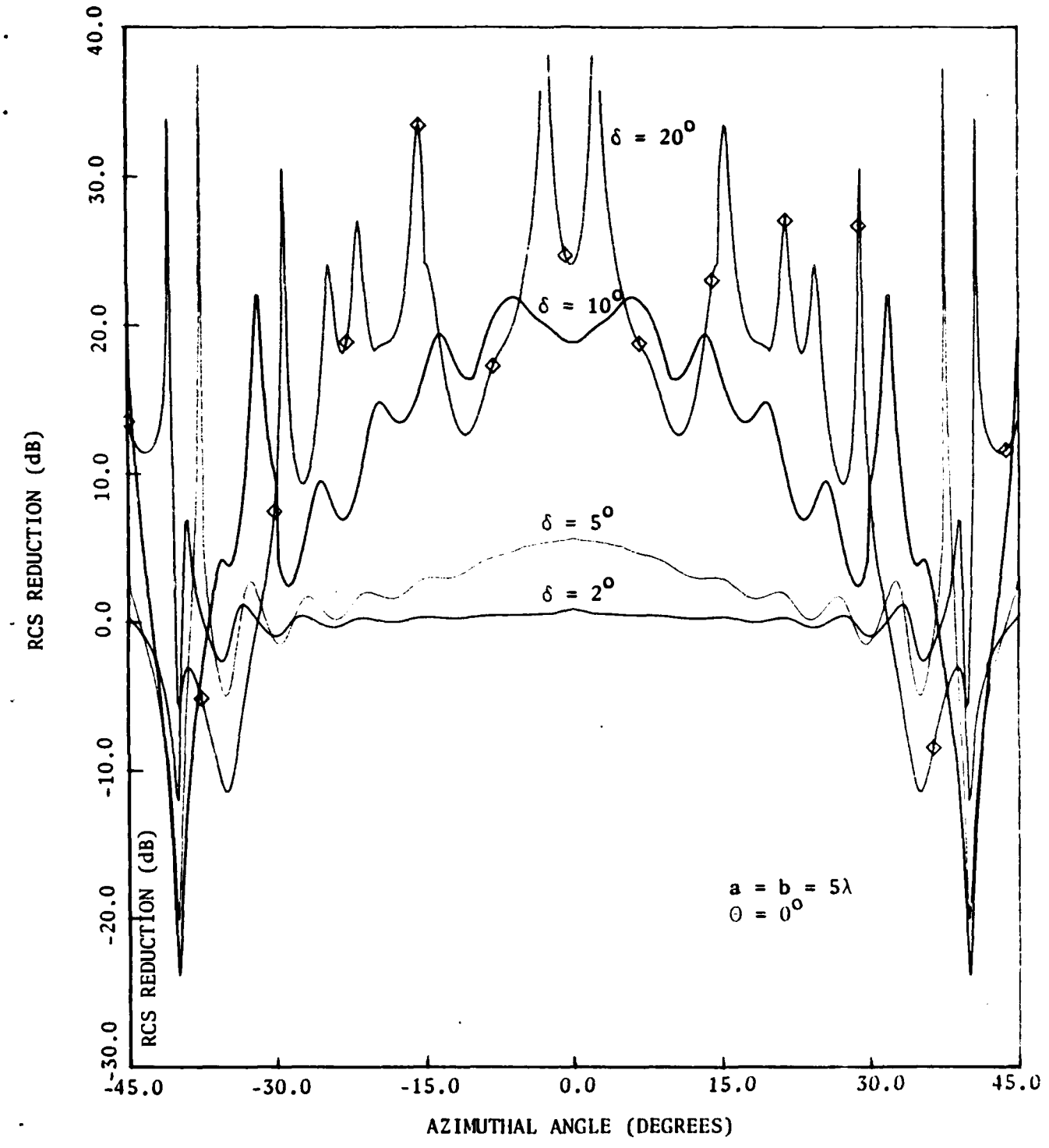

Figure 8. Reduction in RCS for $\delta = 2^{o}$, 5^{o}, 10^{o} and 20^{o} (horizontal polarisation)

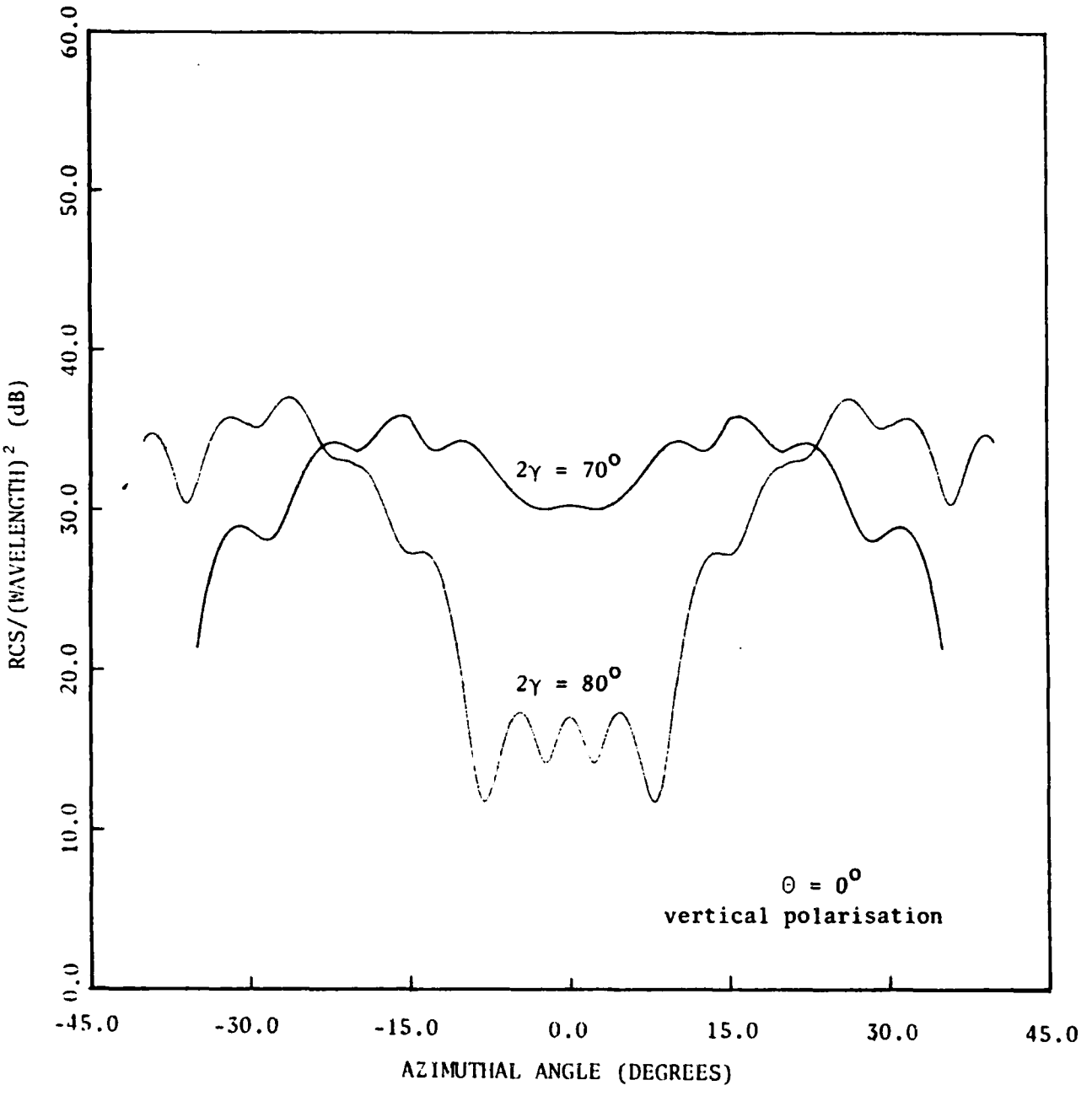

Figure 9. RCS of 70^o and 80^o reflectors, a = b = 5λ, c = 10λ

ERL-0325-TR
Figure 10

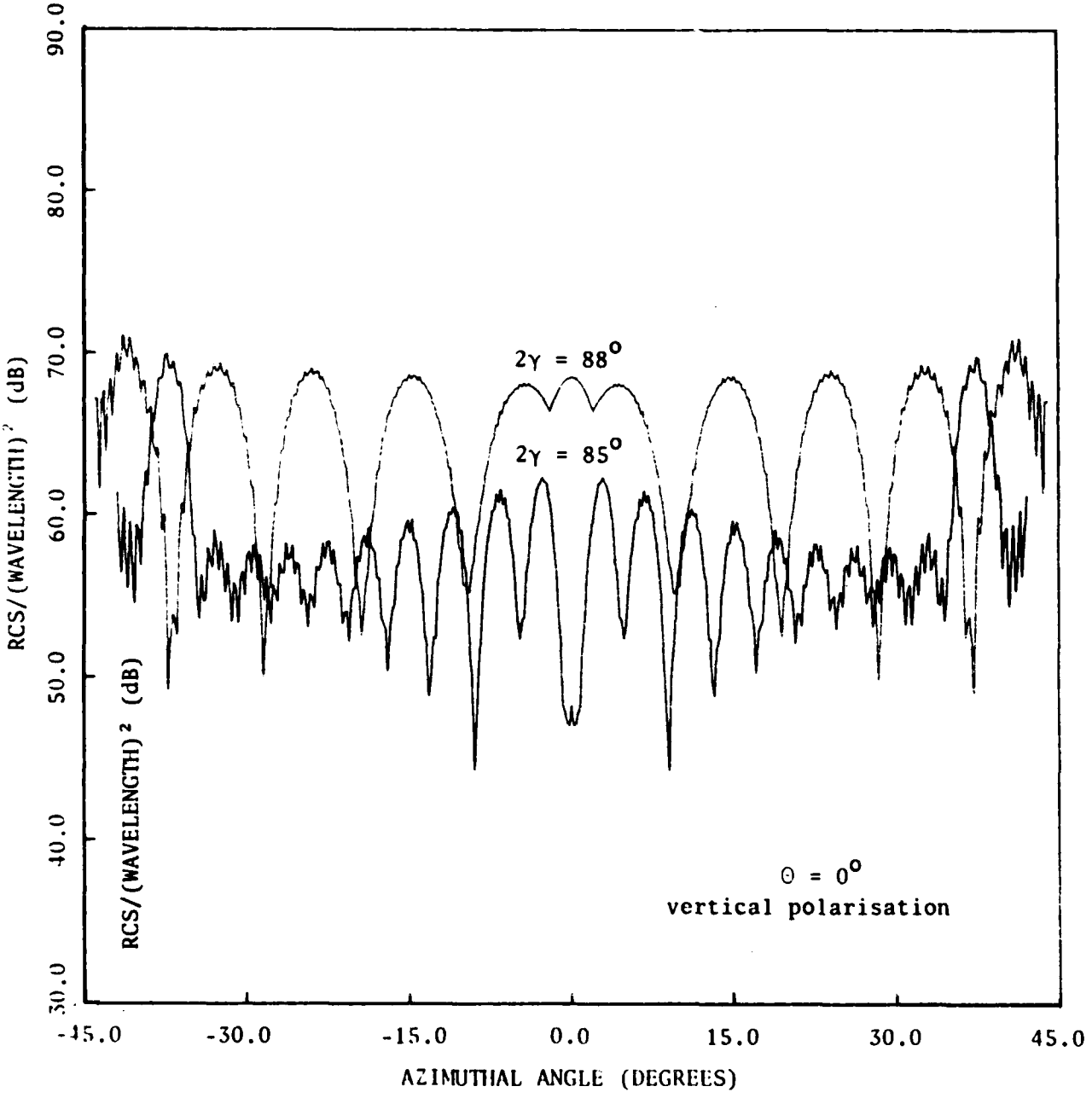

Figure 10. RCS of 85° and 88° reflectors, a = b = c = 100λ

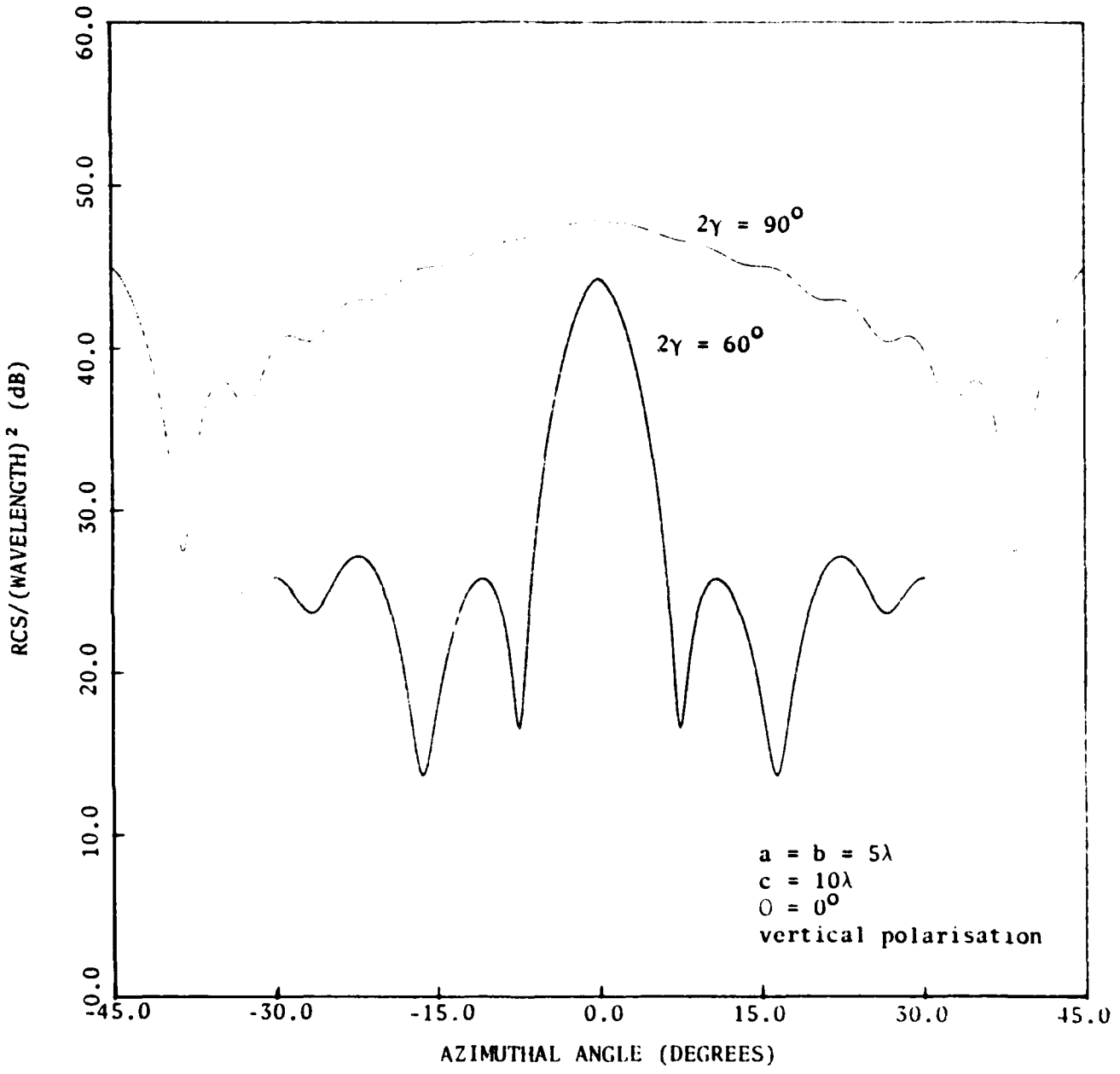

Figure 11. RCS pattern for the special case, reflector angle = 60°, compared with the orthogonal reflector

ERL-0325-TR
Figure 12

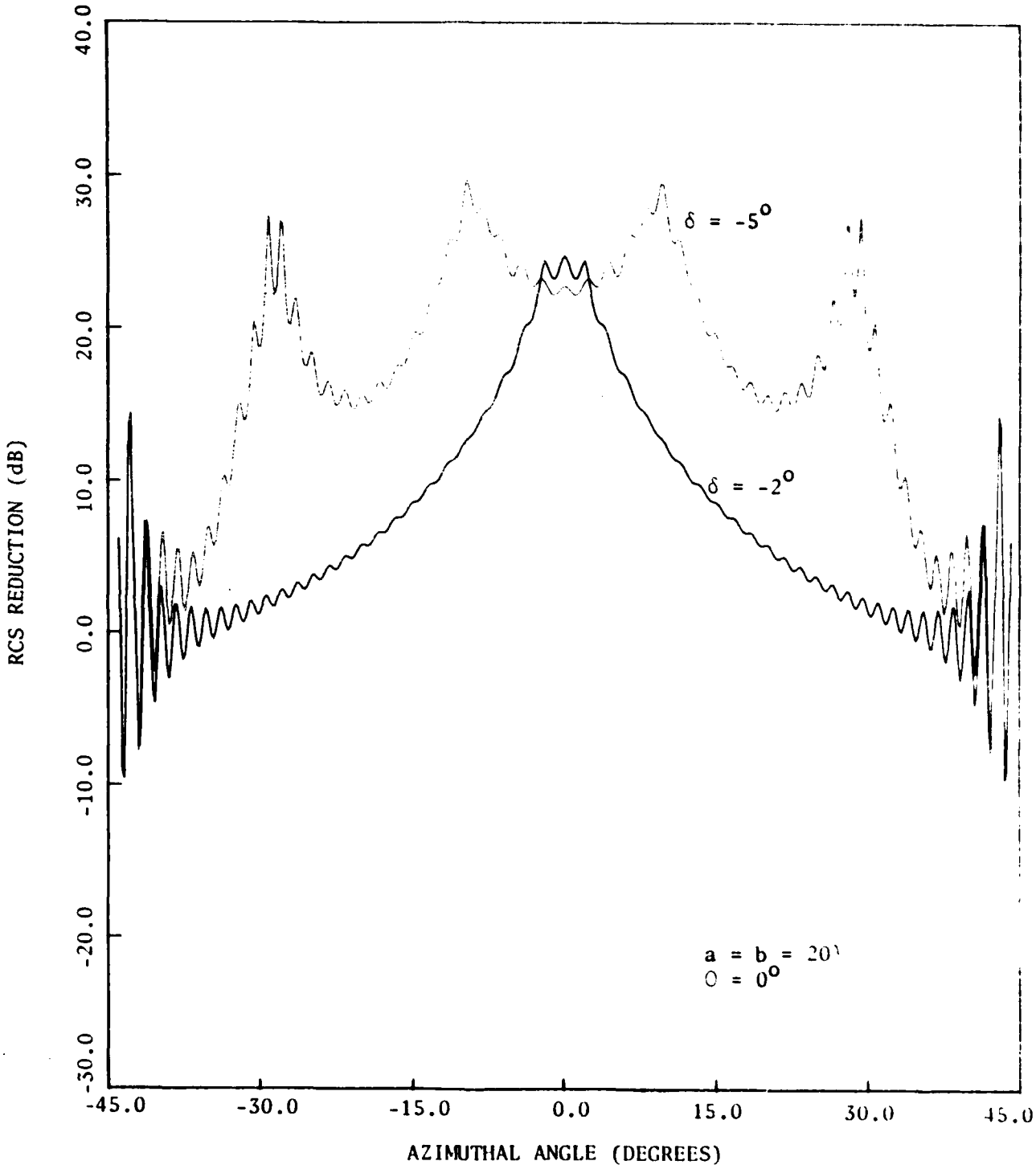

Figure 12. Reduction in RCS for $\delta = -2^{\circ}$ and -5° (vertical polarisation)
$a = b = 20\lambda$

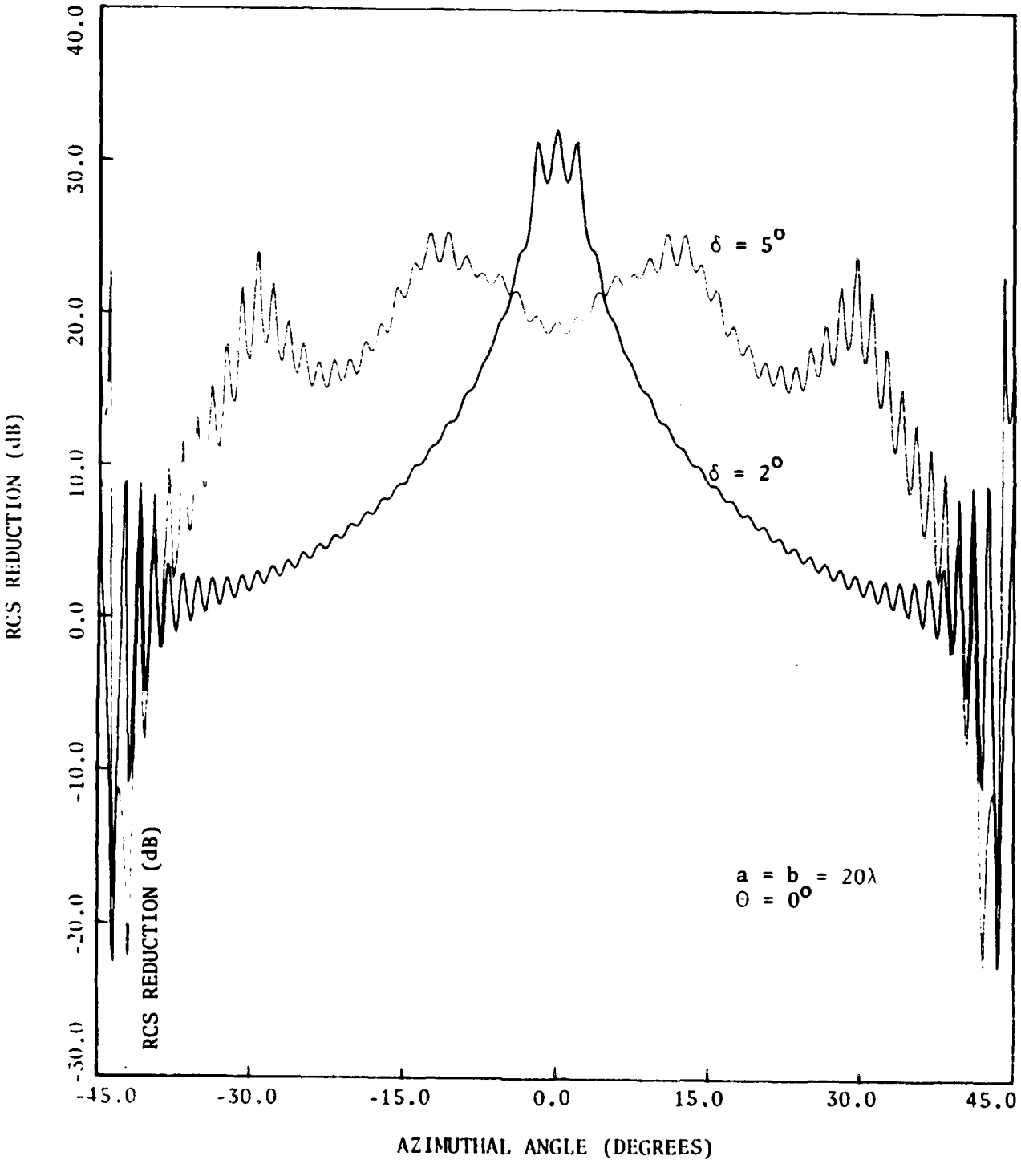

Figure 13. Reduction in RCS for $\delta = 2^{\circ}$ and 5° (vertical polarisation)
$a - b = 20\lambda$

ERL-0325-TR
Figure 14

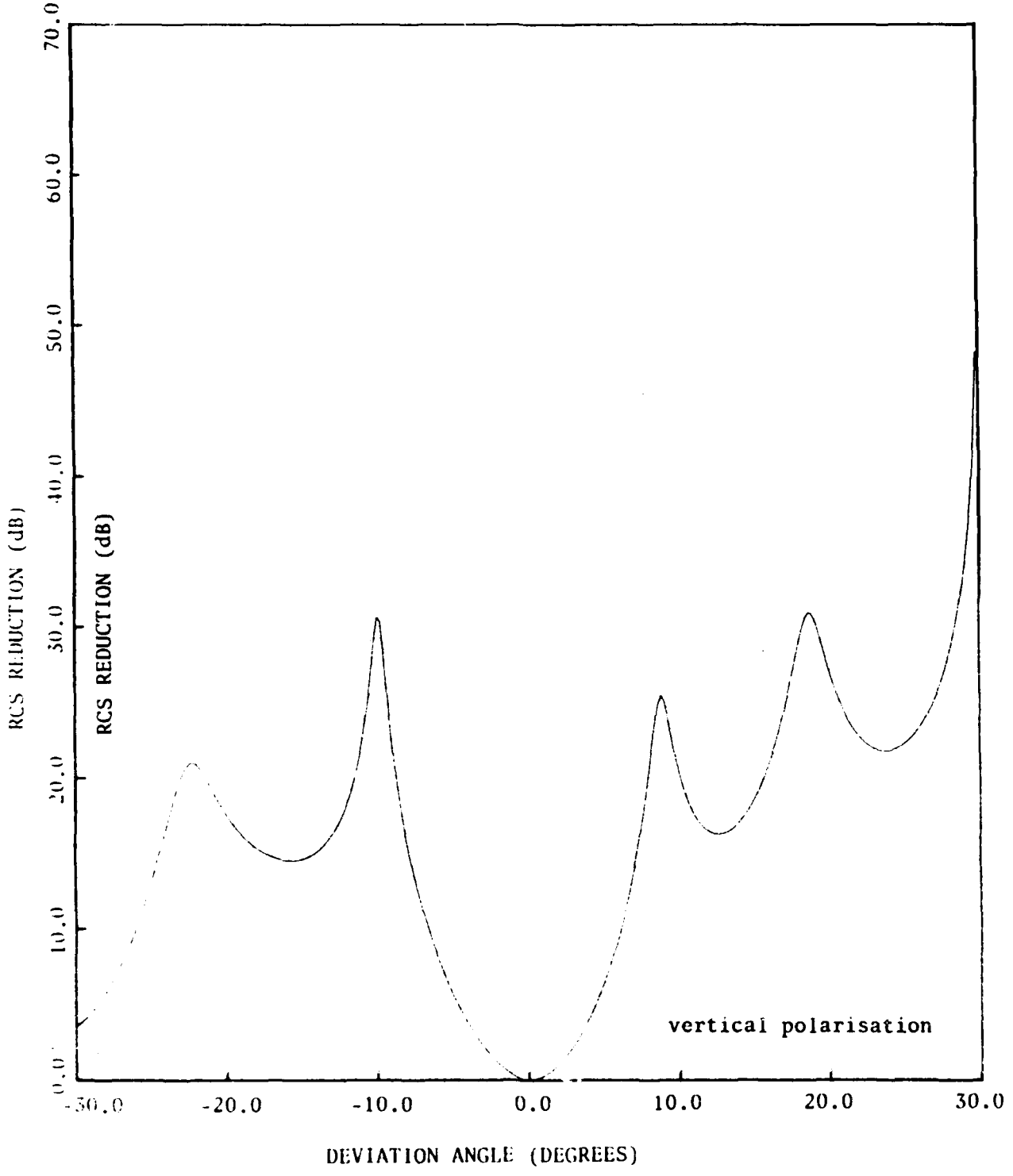

Figure 14. RCS reduction as a function of δ at $\Phi = \theta = 0^{o}$ for a = b = 5λ

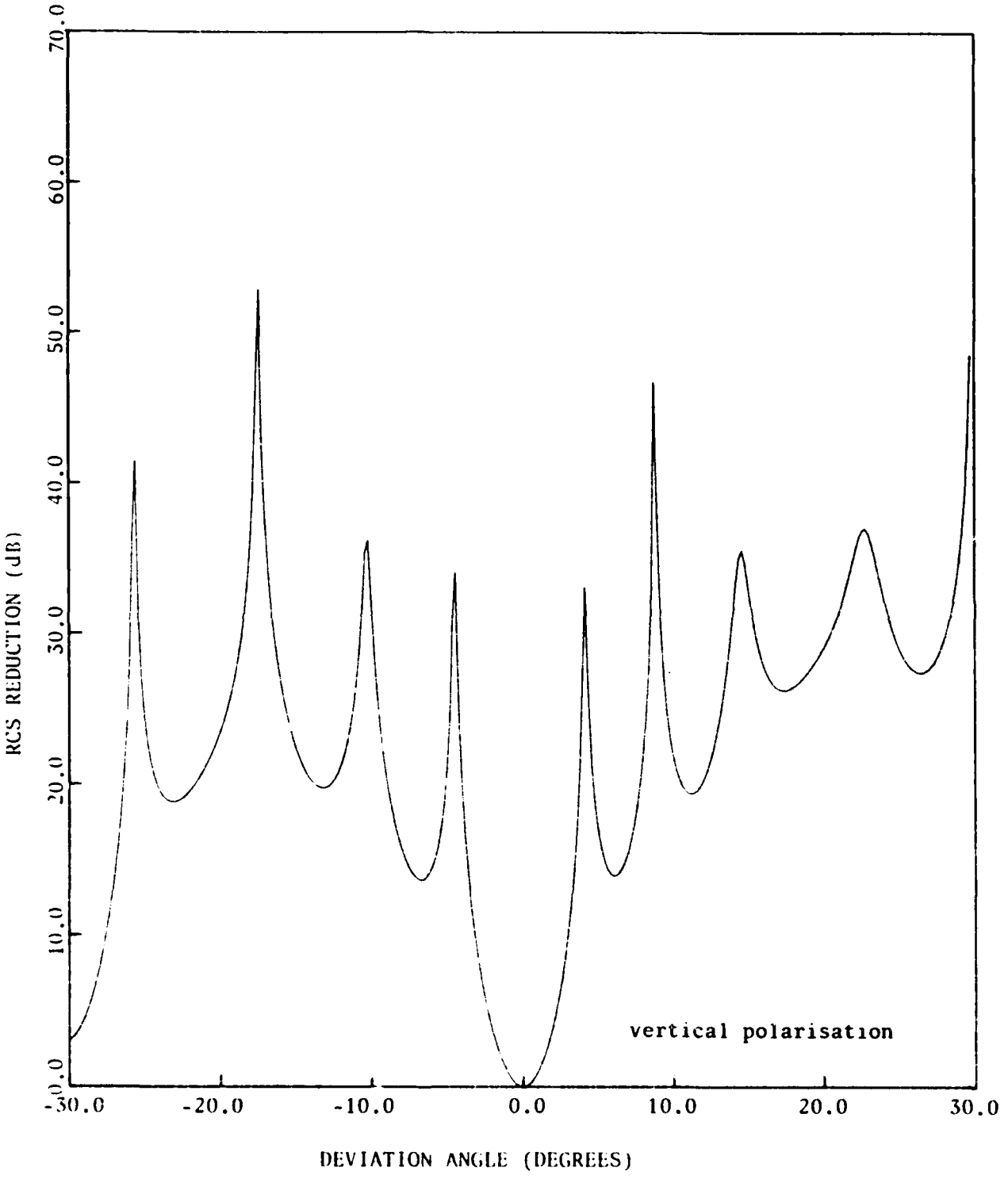

Figure 15. RCS reduction as a function of θ at $\phi = 0^{o}$ for a = b = 10λ

ERL-0325-TR
Figure 16

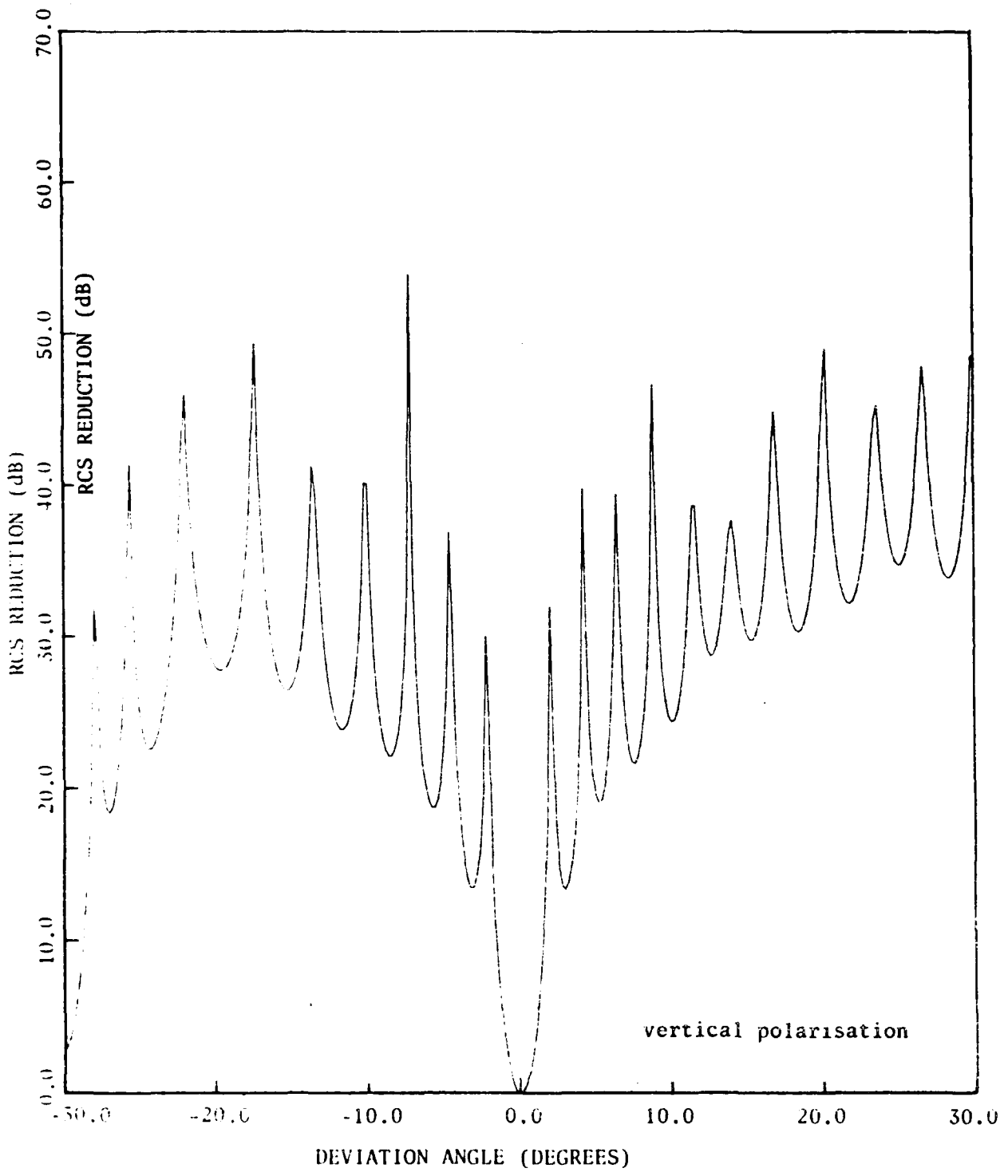

Figure 16. RCS reduction as a function of δ at $\phi = \theta = 0^{o}$ for $a = b = 20\lambda$

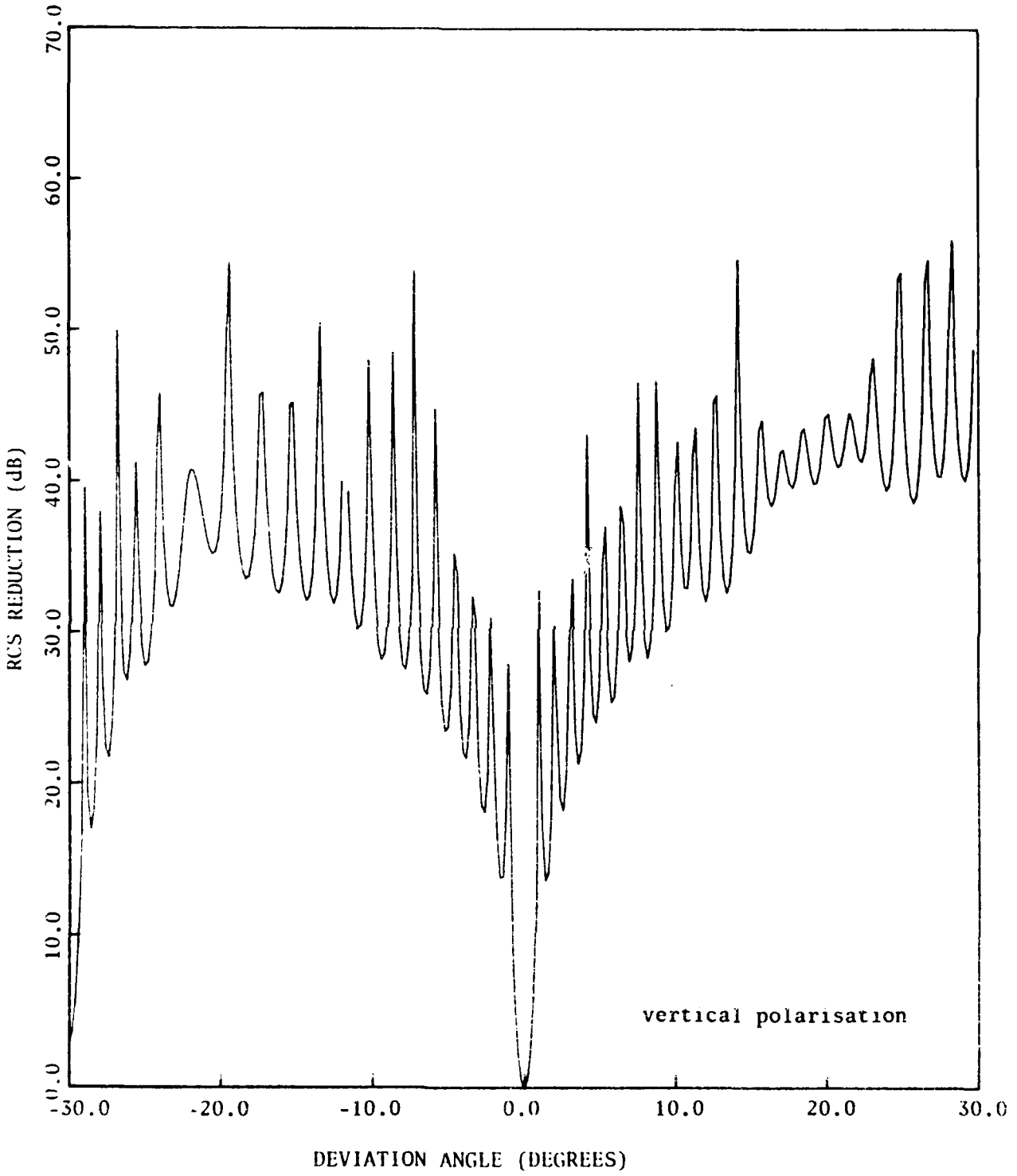

Figure 17. RCS reduction as a function of δ at $\phi = \theta = 0^{\circ}$ for $a = b = 40\lambda$

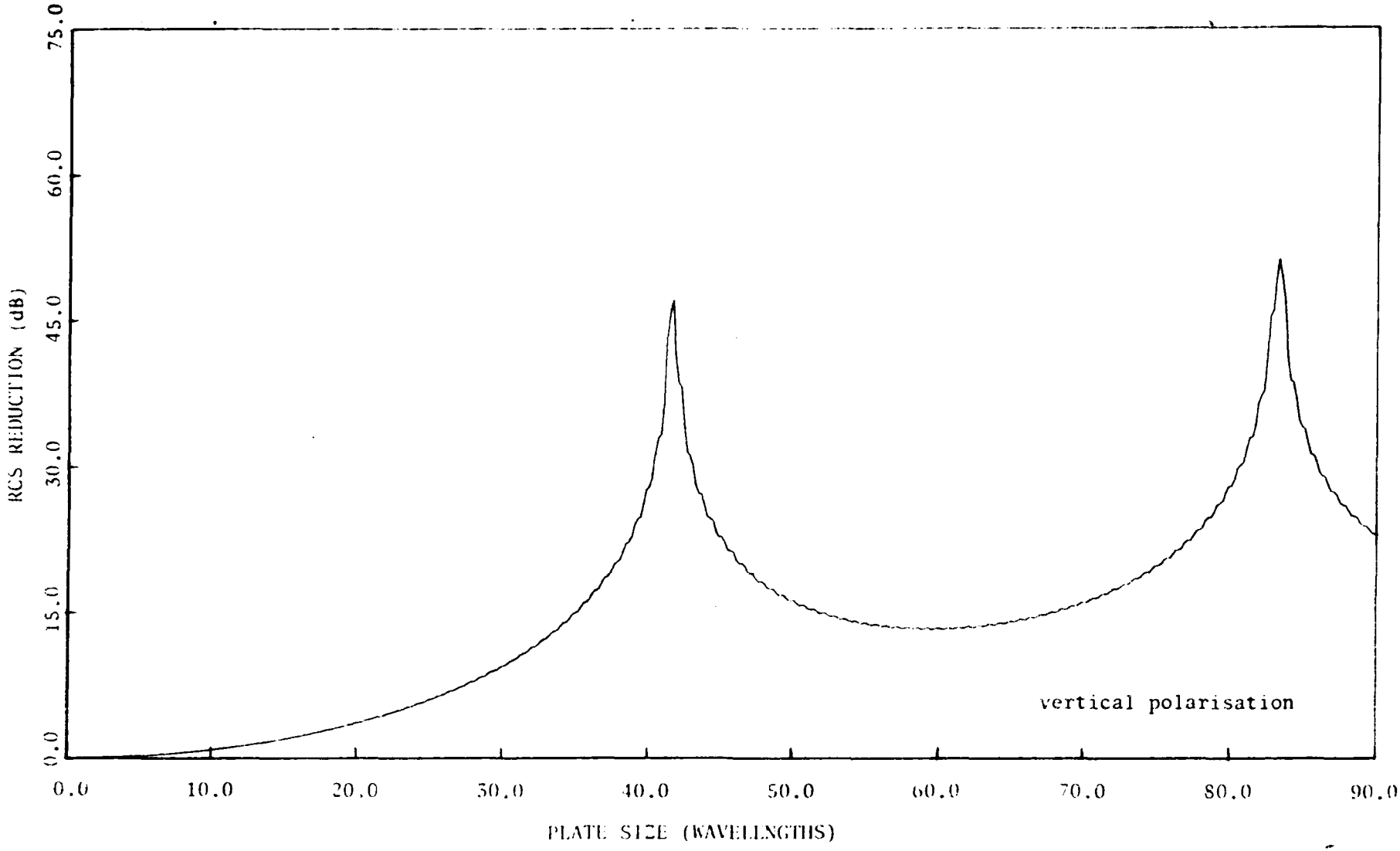

Figure 18. RCS reduction as a function of plate size at $\zeta = \quad = 0^{o}$ for $\lambda = -1^{o}$

ERL-0325-TR
Figure 18

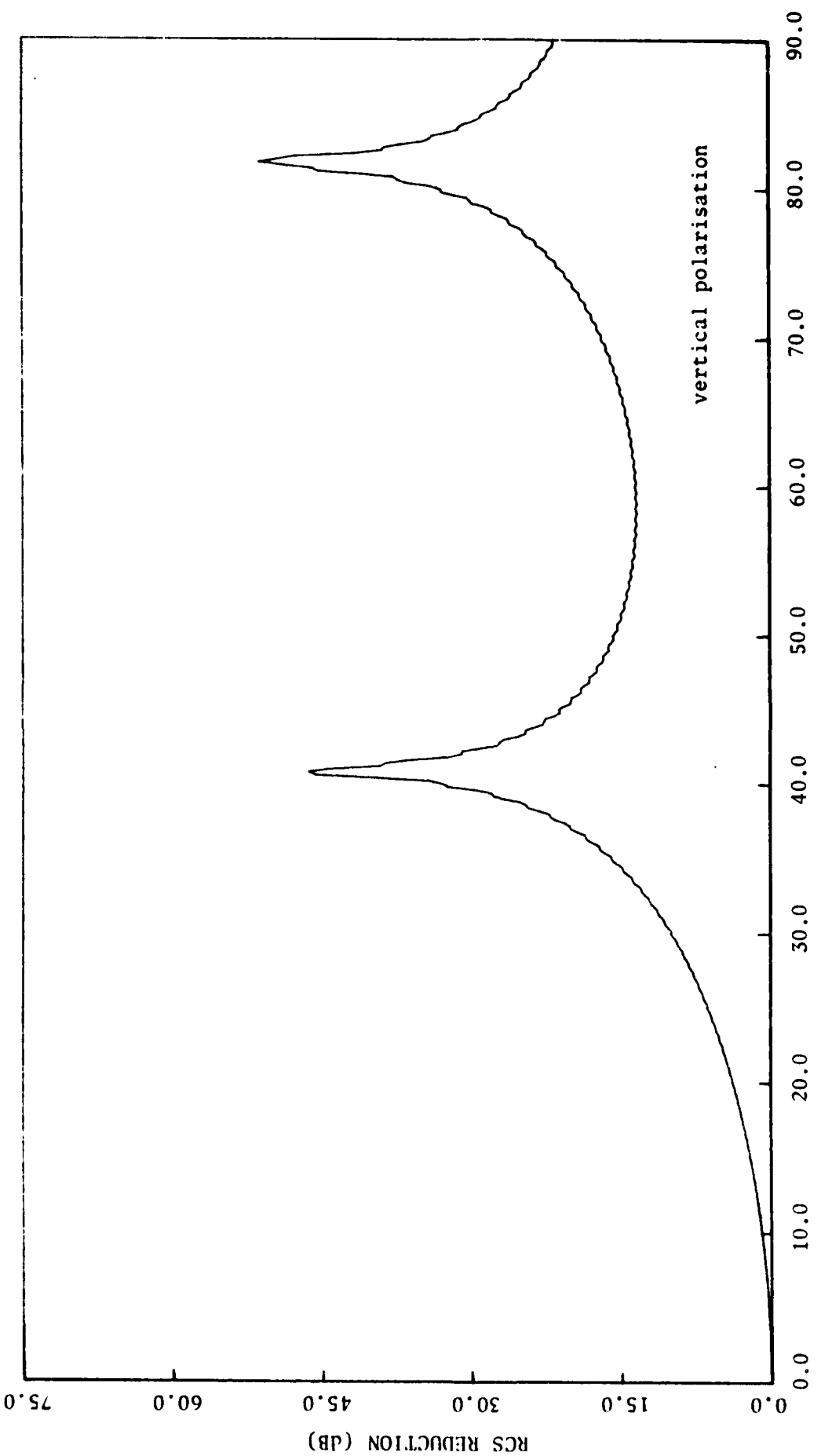

Figure 19. RCS reduction as a function of plate size at $\phi = \theta = 0^{o}$ for $\delta = 1^{o}$

ERL-0325-TR
Figure 20

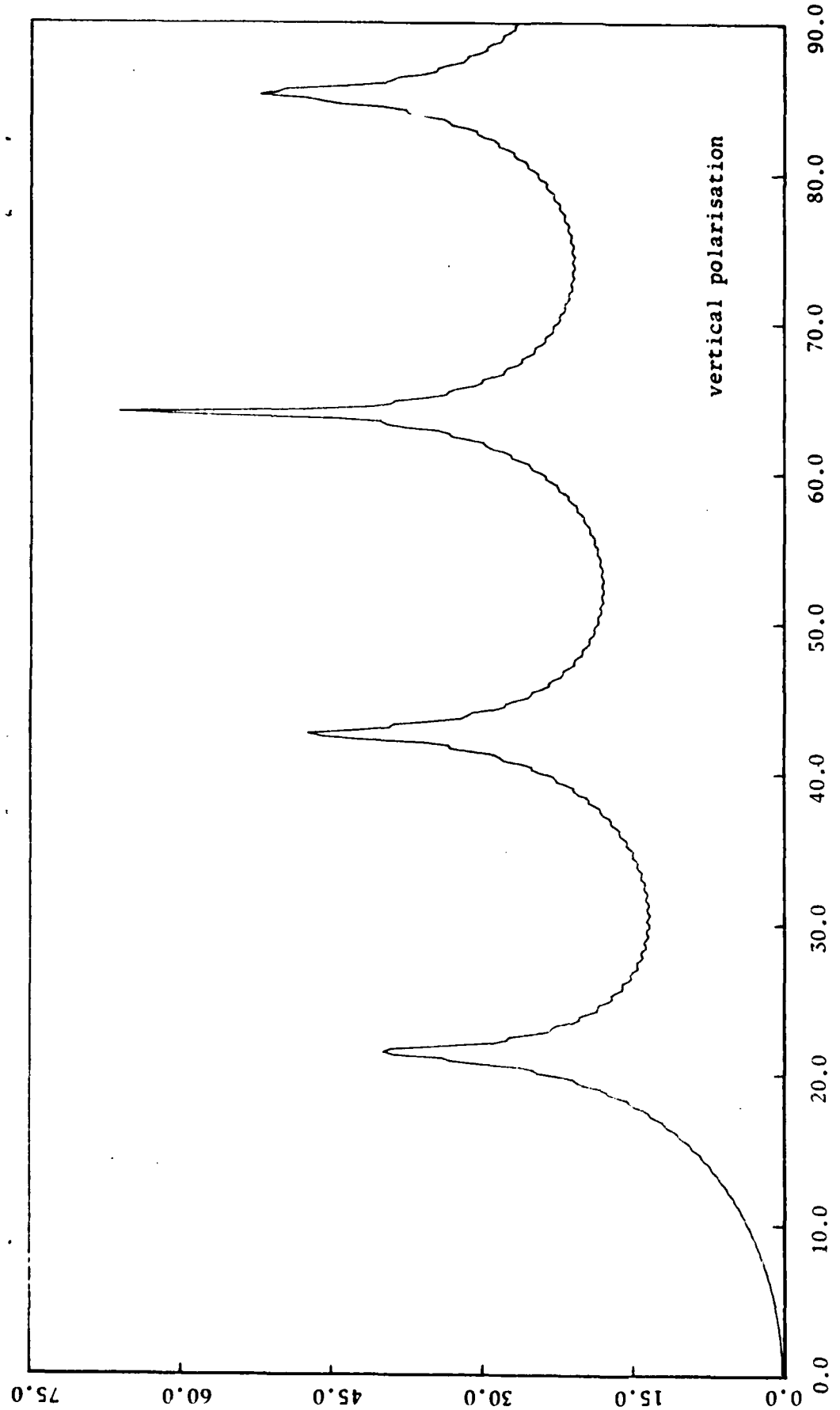

Figure 20. RCS reduction as a function of plate size at $\phi = 0 = 0^{o}$ for $\delta = -2^{o}$

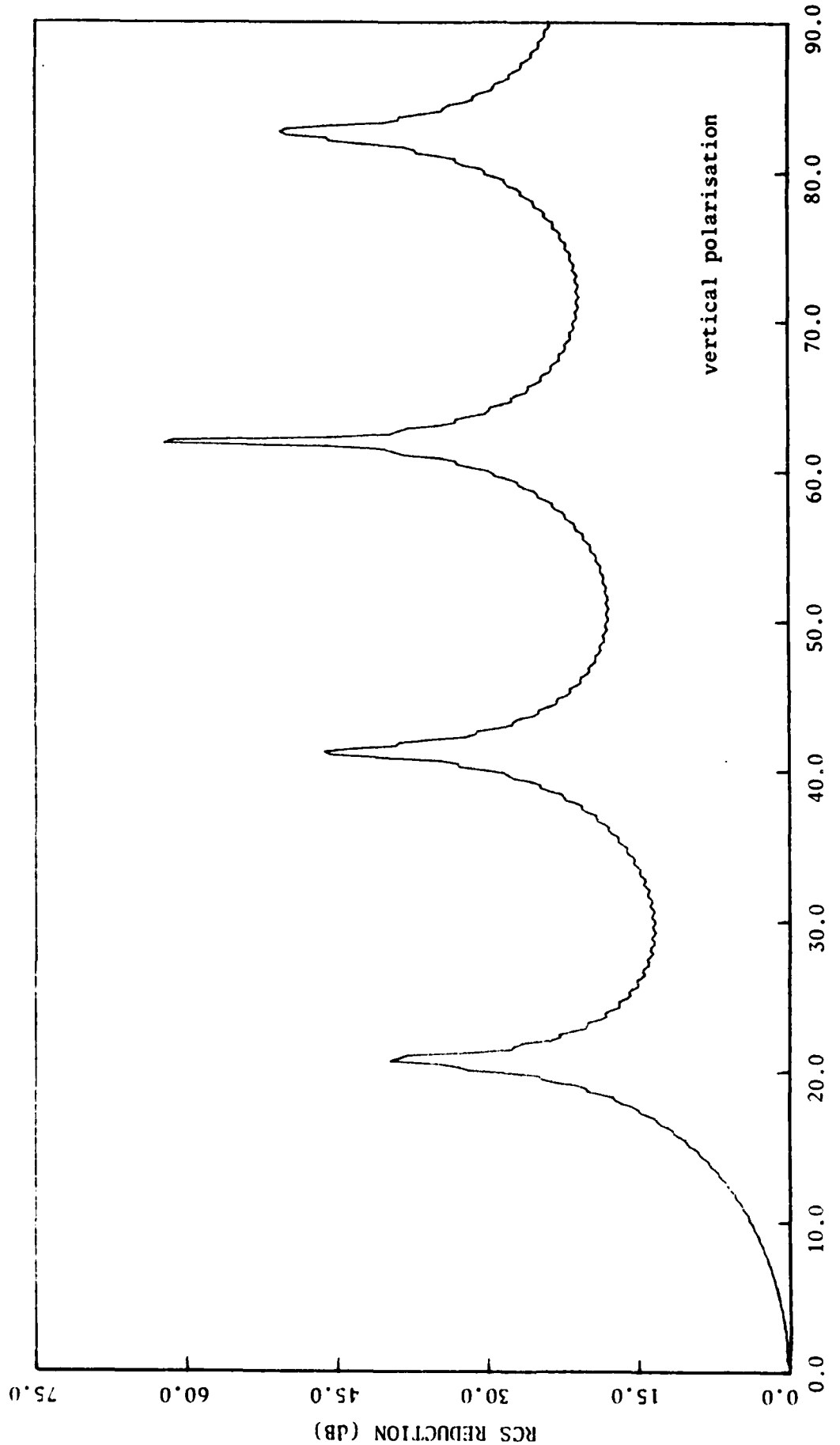

Figure 21. RCS reduction as a function of plate size at $\phi = \Theta = 0^{o}$ for $\delta = 2^{o}$

ERL-0325-TR
Figure 22

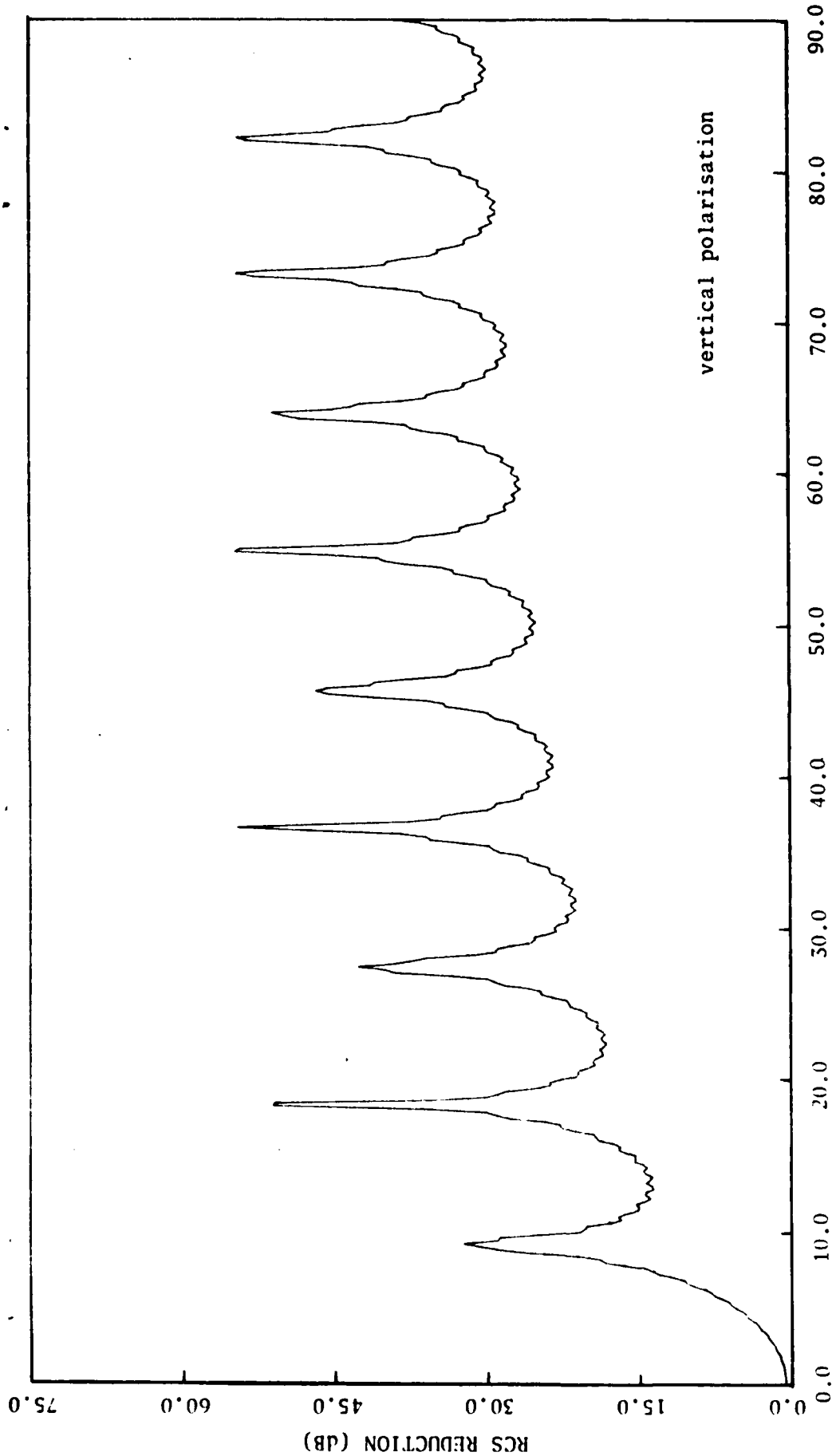

Figure 22. RCS reduction as a function of plate size at $\phi = 0 = 0^{o}$ for $\delta = -5^{o}$

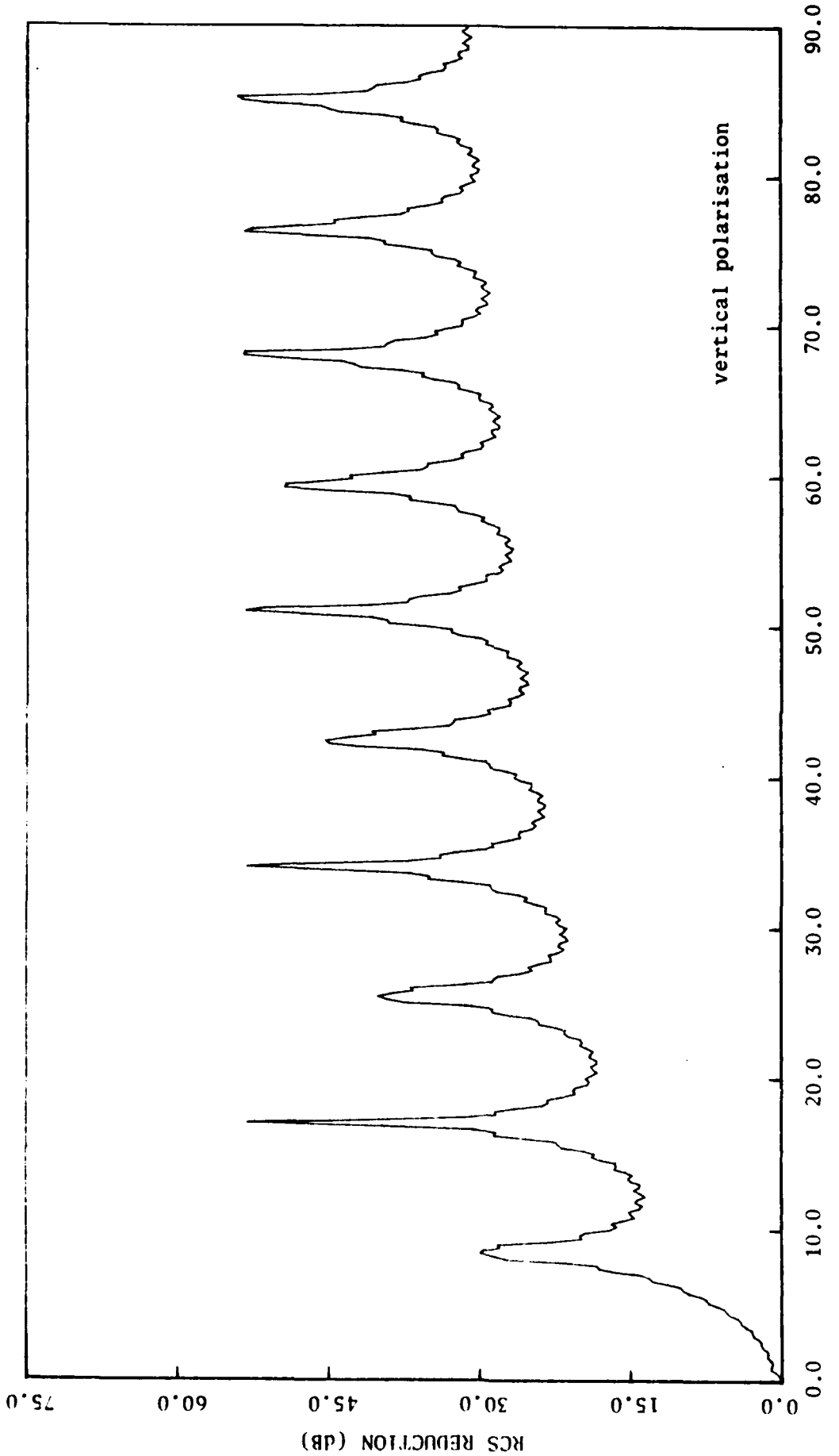

Figure 23. RCS reduction as a function of plate size at $\phi = 0 = 0^{o}$ for $\delta = 5^{o}$

ERL-0325-TR
Figure 24

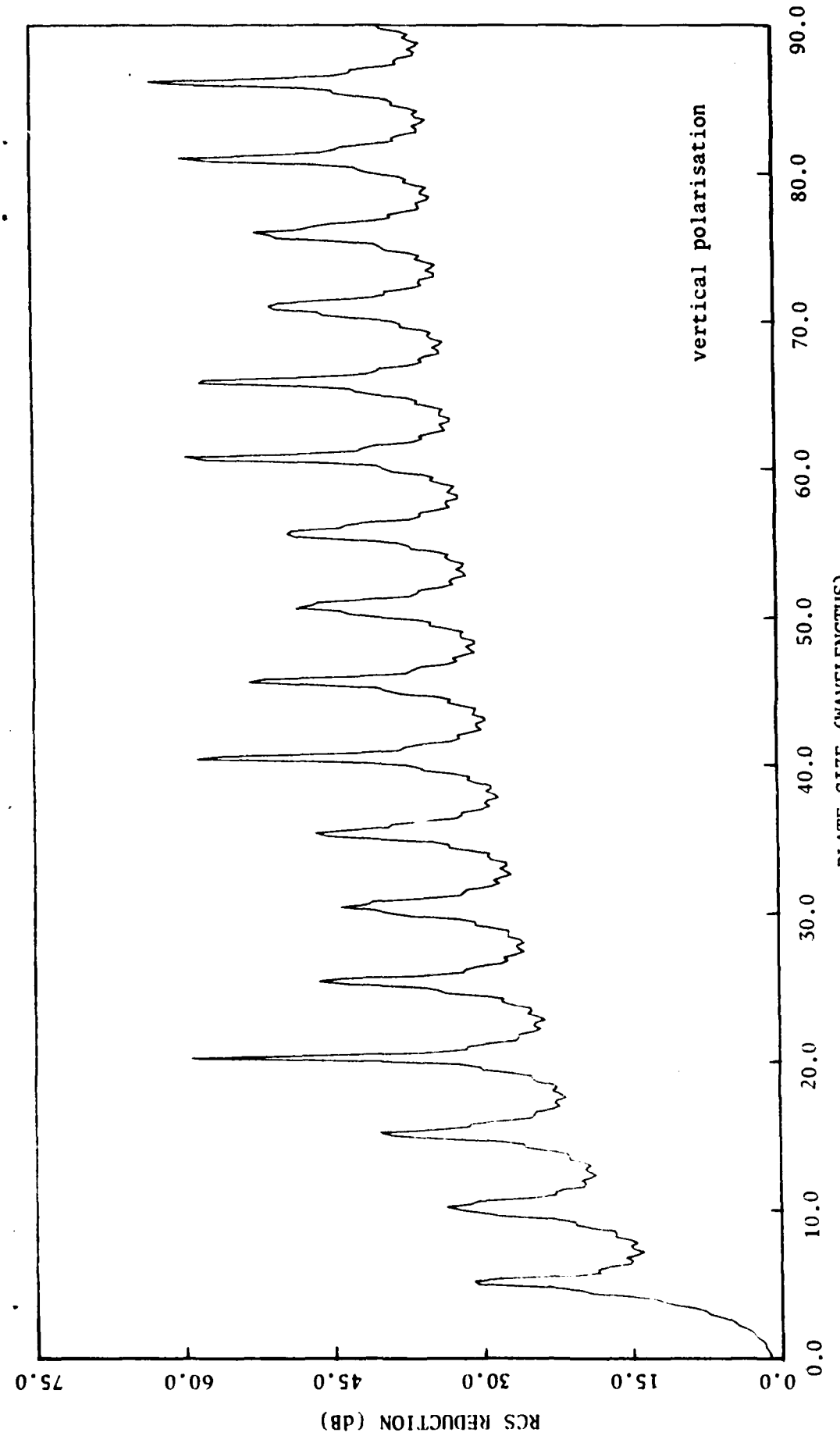

Figure 24 RCS reduction as a function of plate size at $\phi = \theta = 0^{o}$ for $\delta = -10^{o}$

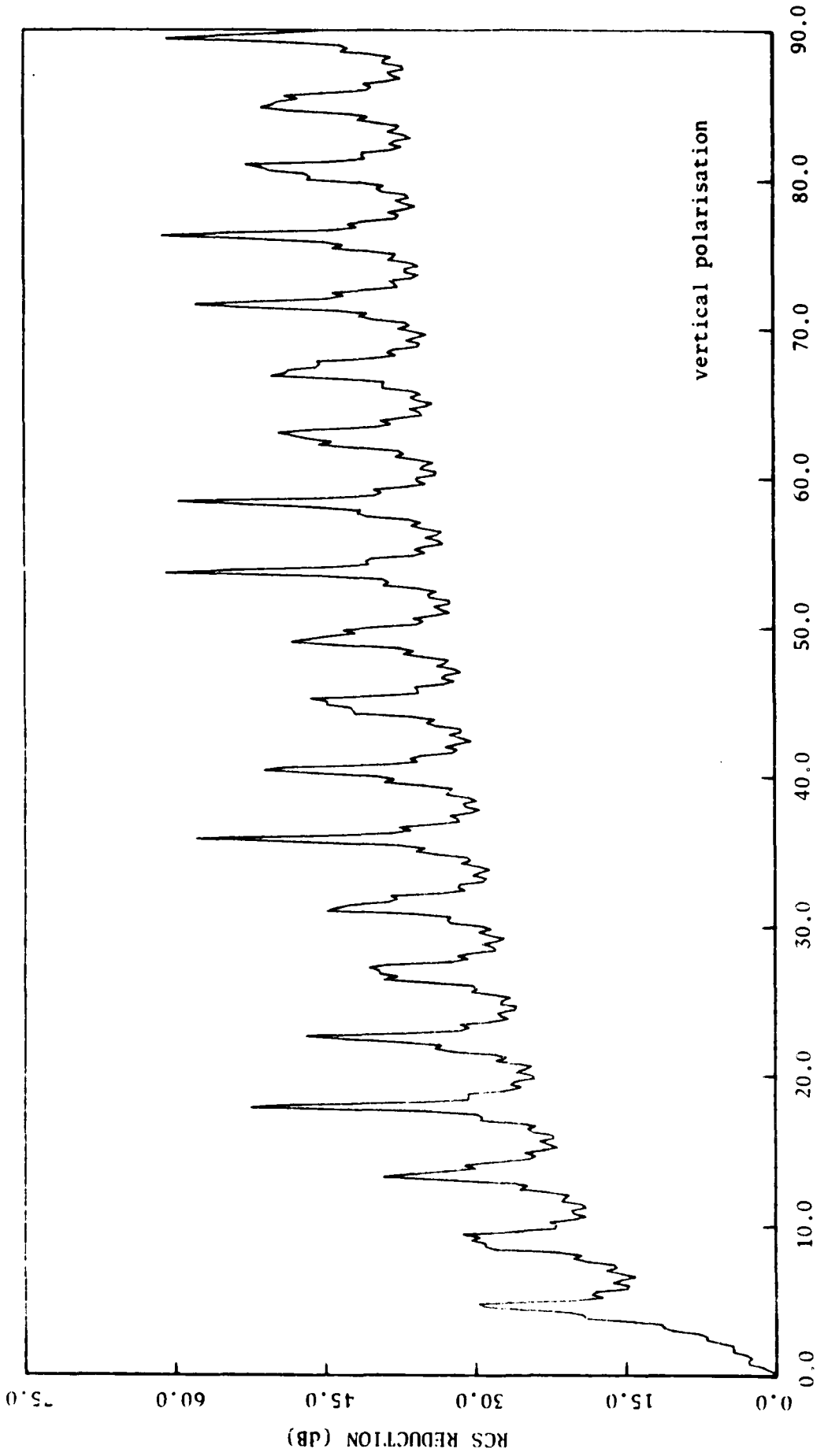

Figure 25. RCS reduction as a function of plate size at $\phi = \Theta = 0^{o}$ for $\delta = 10^{o}$

ERL-0325-TR
Figure 26

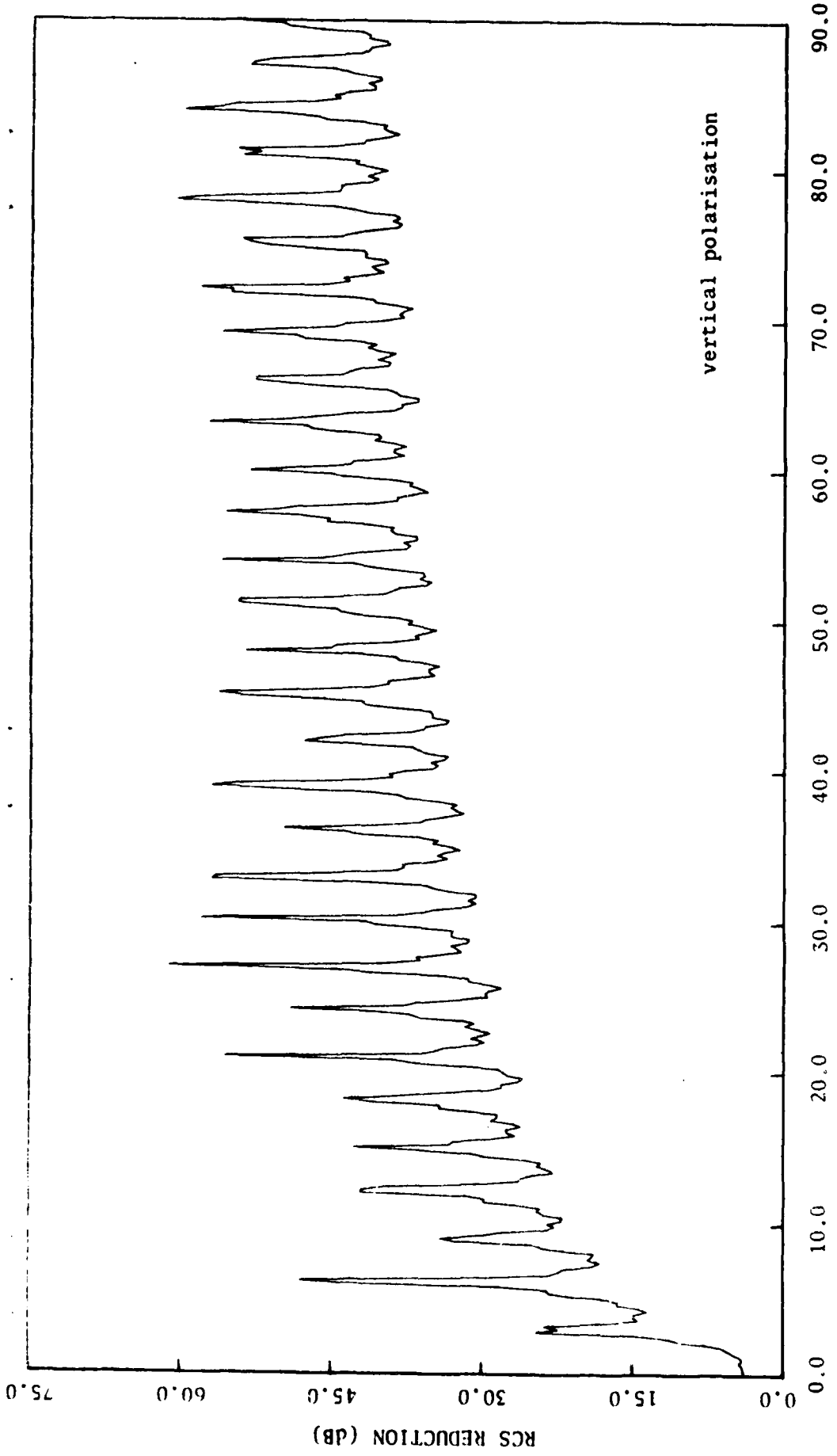

Figure 26. RCS reduction as a function of plate size at $\phi = \theta = 0^{o}$ for $\delta = -20^{o}$

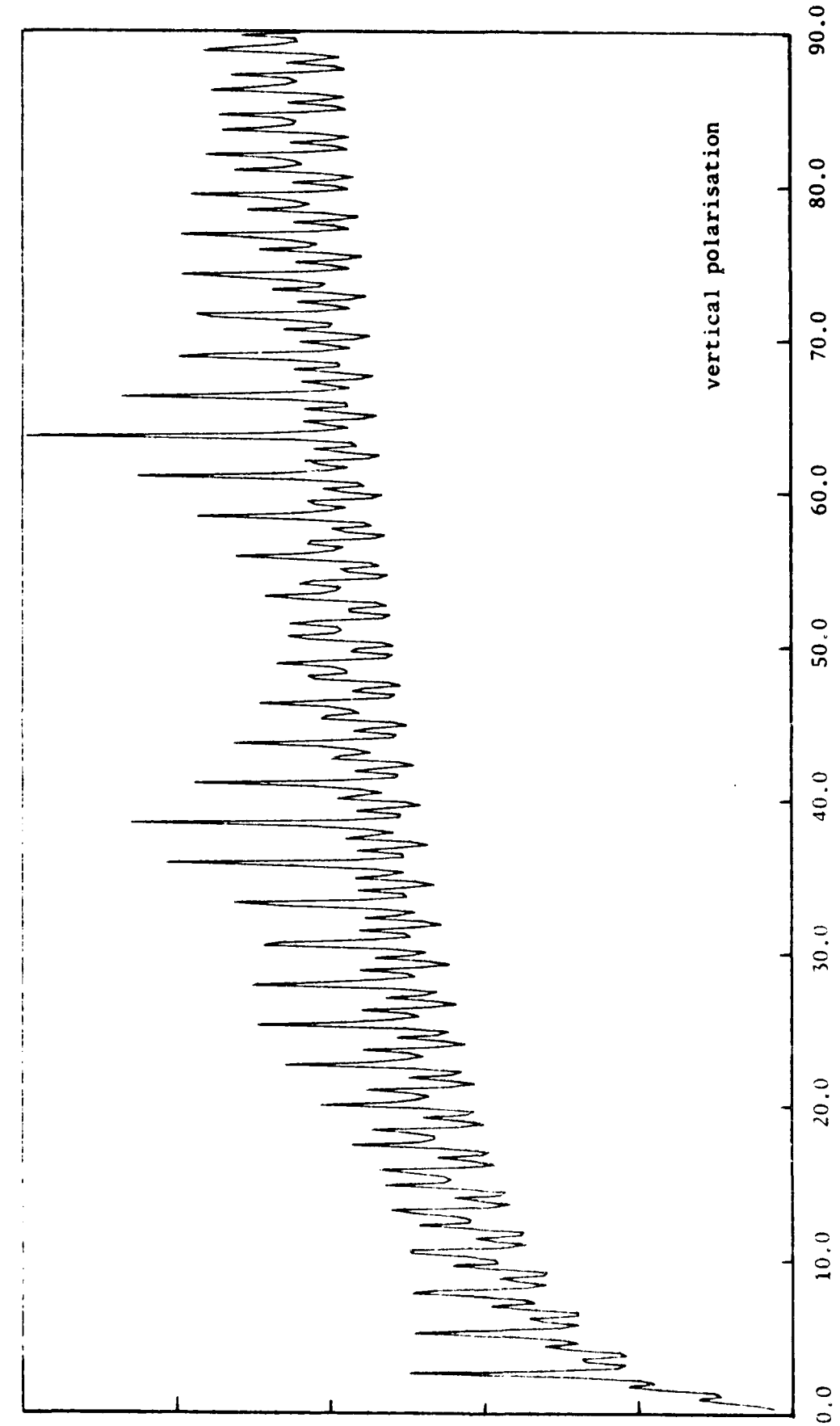

Figure 27. RCS reduction as a function of plate size at $\phi = \theta = 0^{o}$ for $\delta = 20^{o}$

ERL-0325-TR
Figure 28

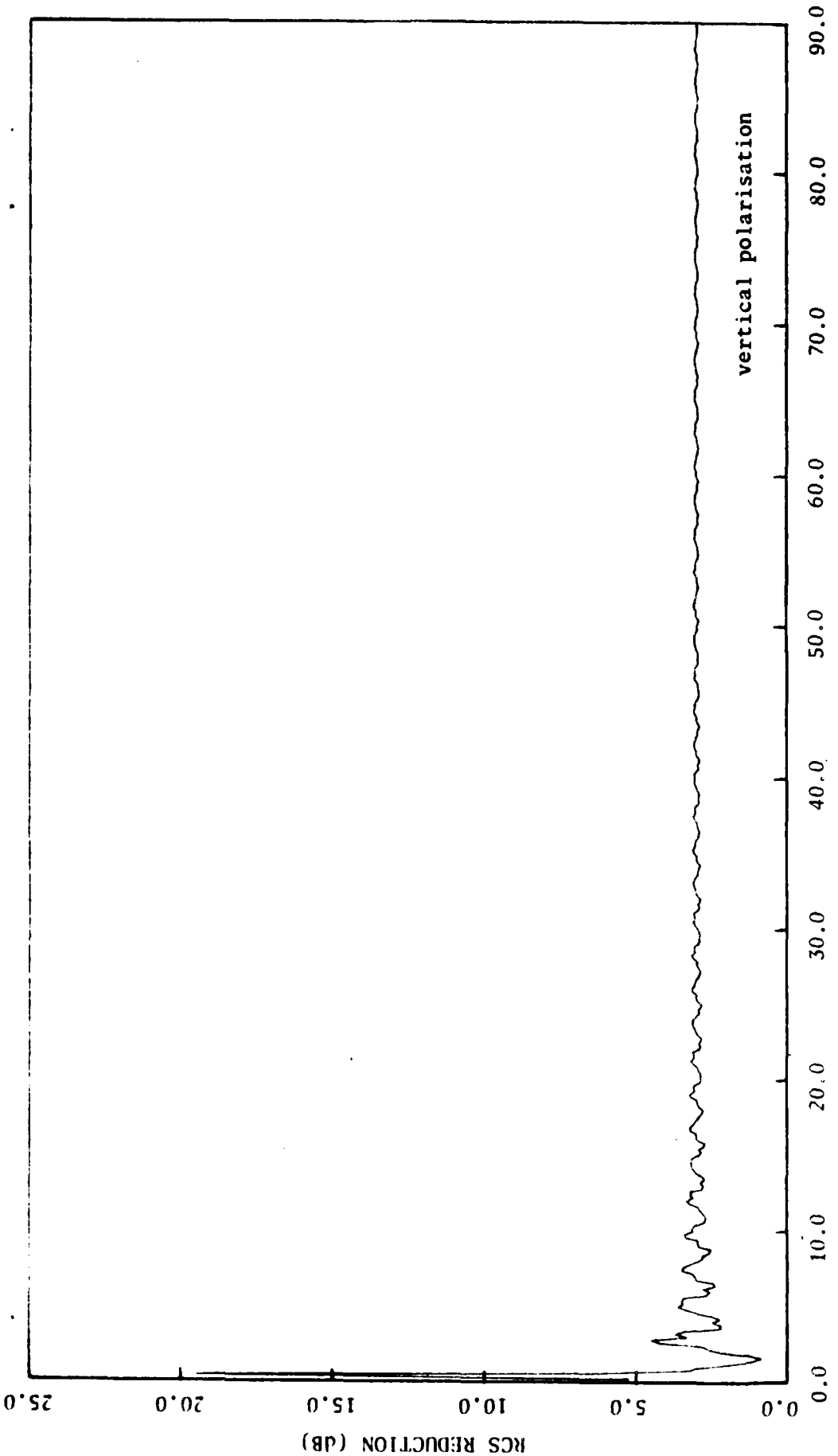

Figure 28. RCS reduction as a function of plate size at $\phi = 0 = 0^{o}$ for $\delta = -30^{o}$

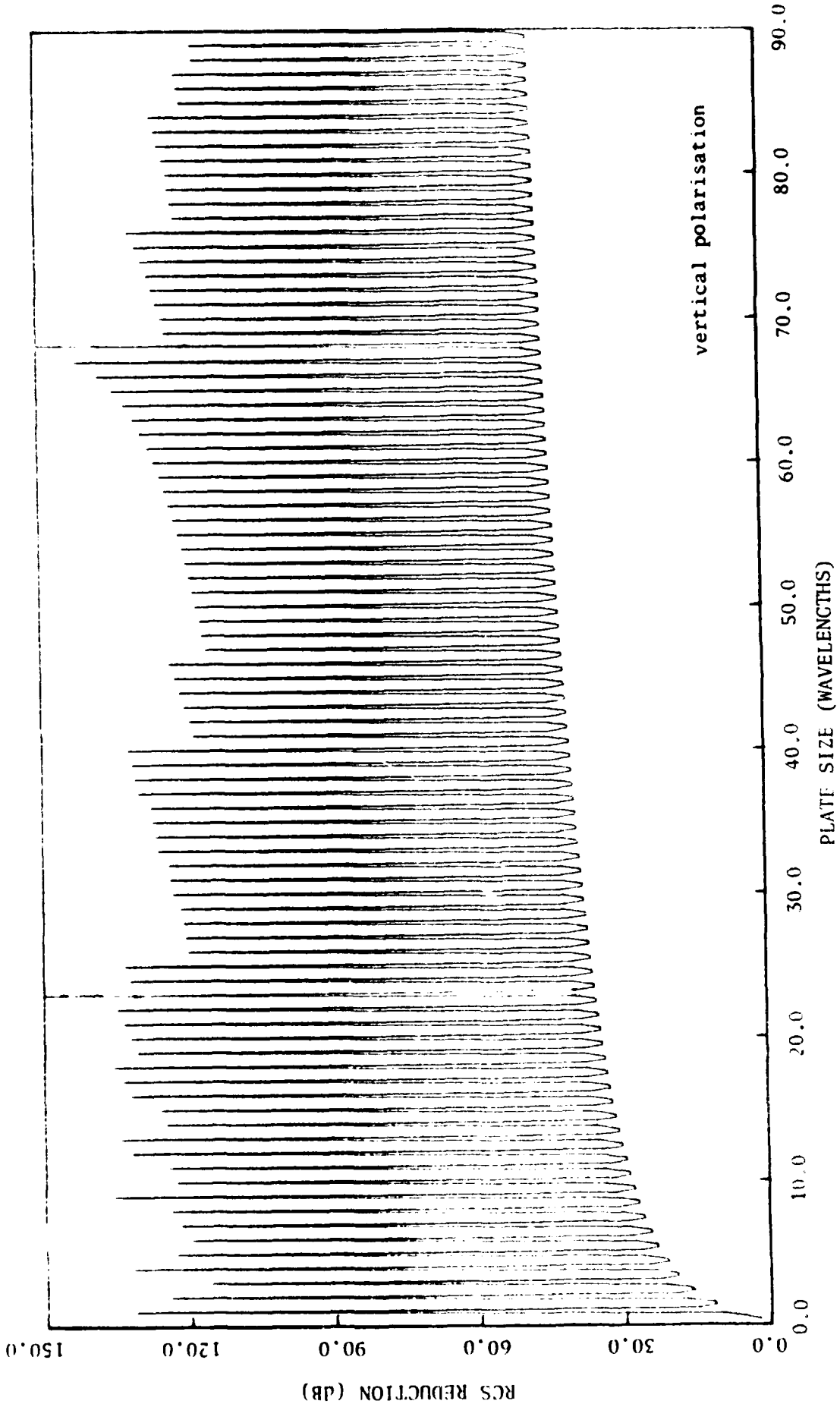

Figure 29. RCS reduction as a function of plate size at $\phi = 0 = 0^{o}$ for $\delta = 30^{o}$

ERL-0325-TR
Figure 30

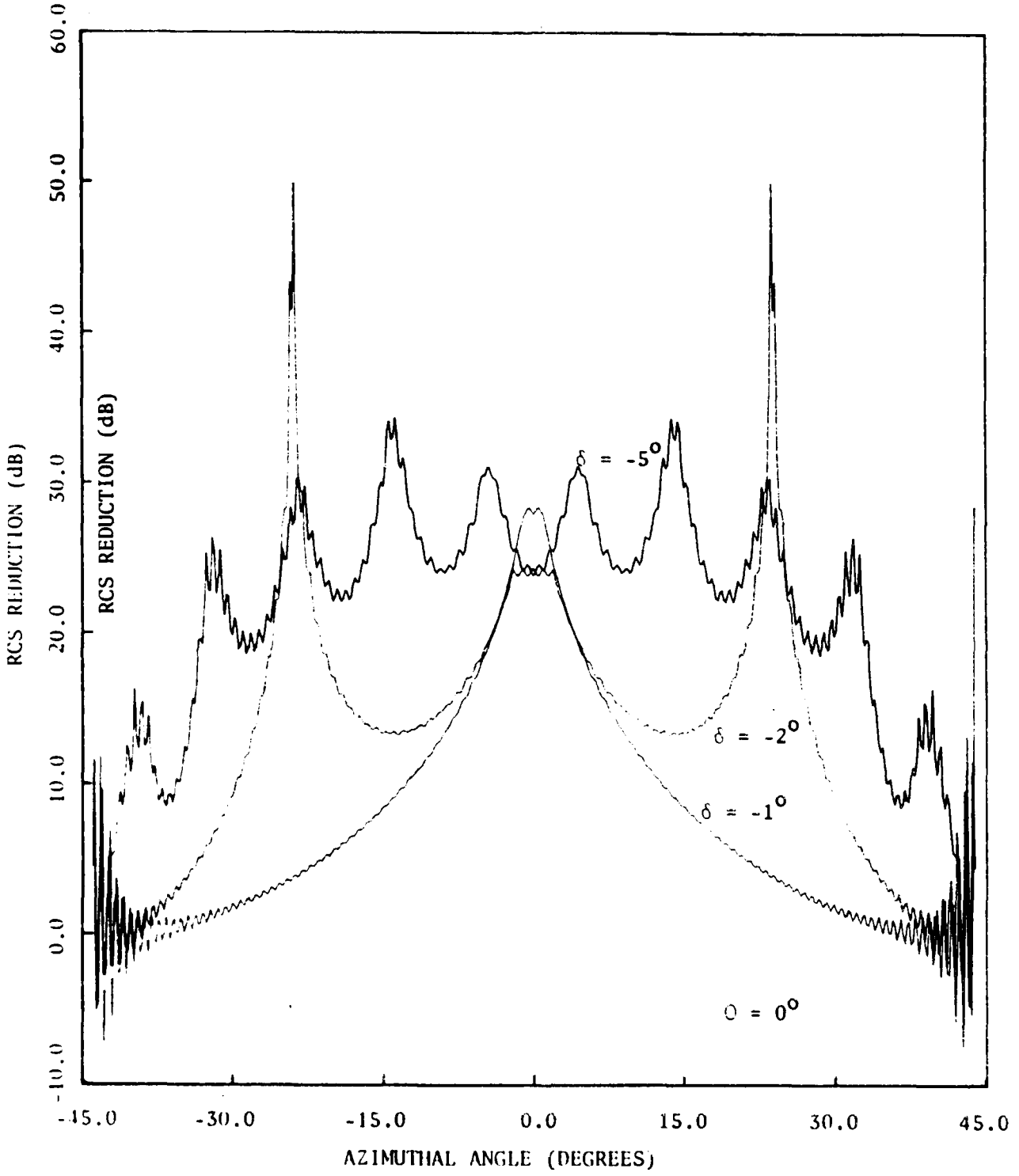

Figure 30. Reduction in RCS for $\delta = -1^{\circ}, -2^{\circ}$ and -5° (vertical polarisation). $a = b = 40\lambda$

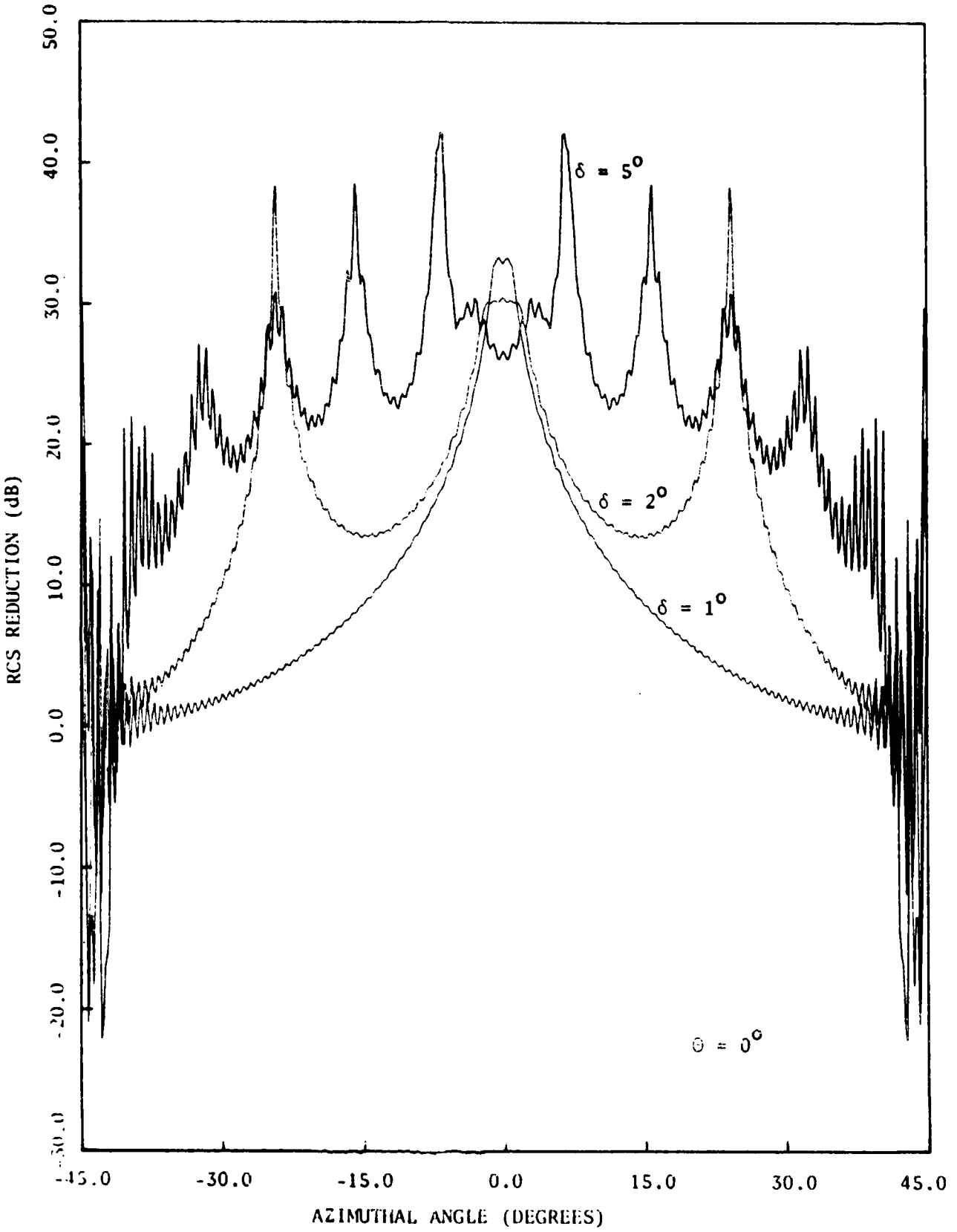

Figure 31. Reduction in RCS for $\delta = 1^{\circ}$, 2° and 5° (vertical polarisation). $a = b = 40\lambda$

ERL-0325-TR
Figure 32

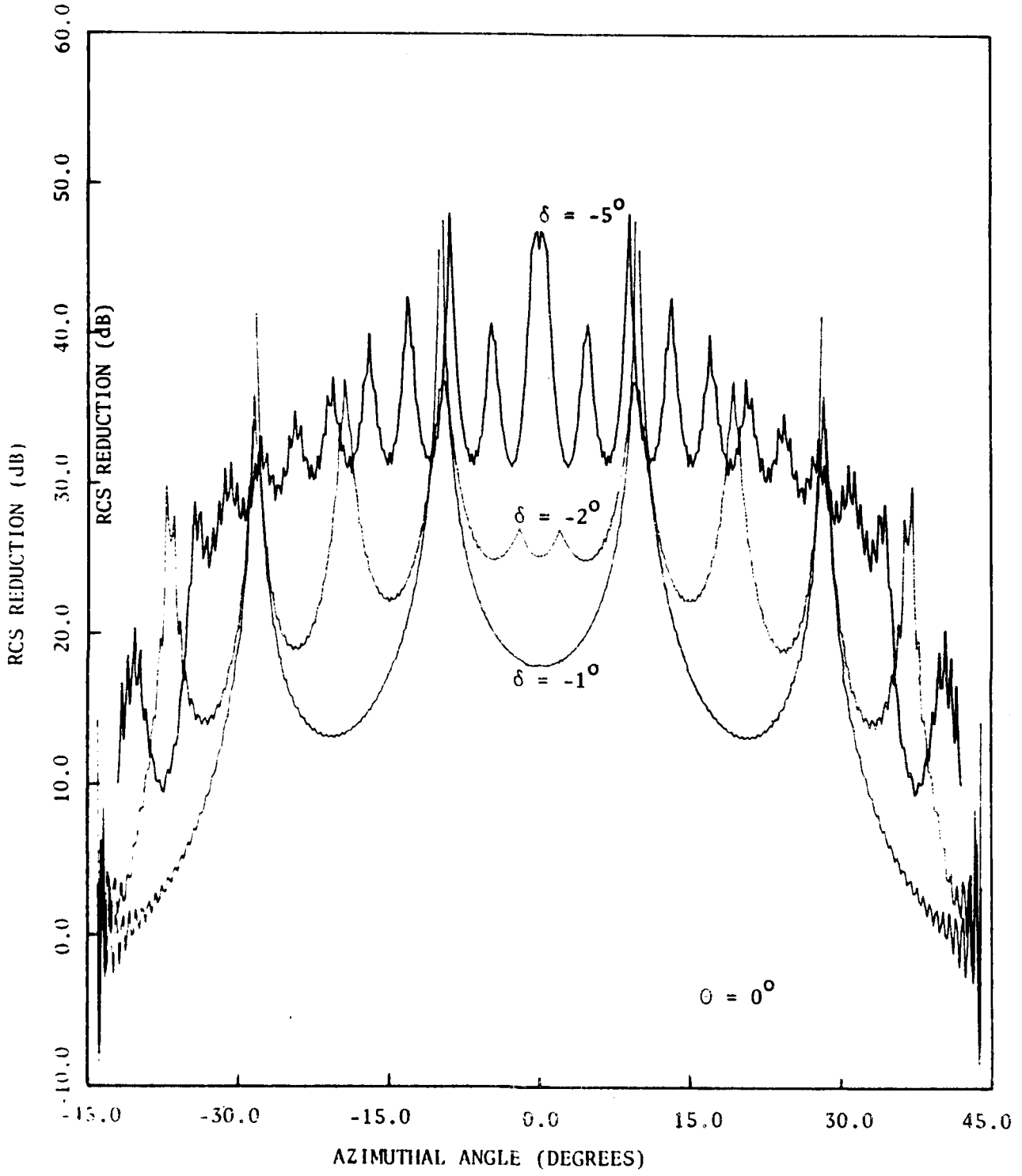

Figure 32. Reduction in RCS for $\delta = -1^{\circ}$, -2° and -5° (vertical polarisation) $a = b = 100\lambda$

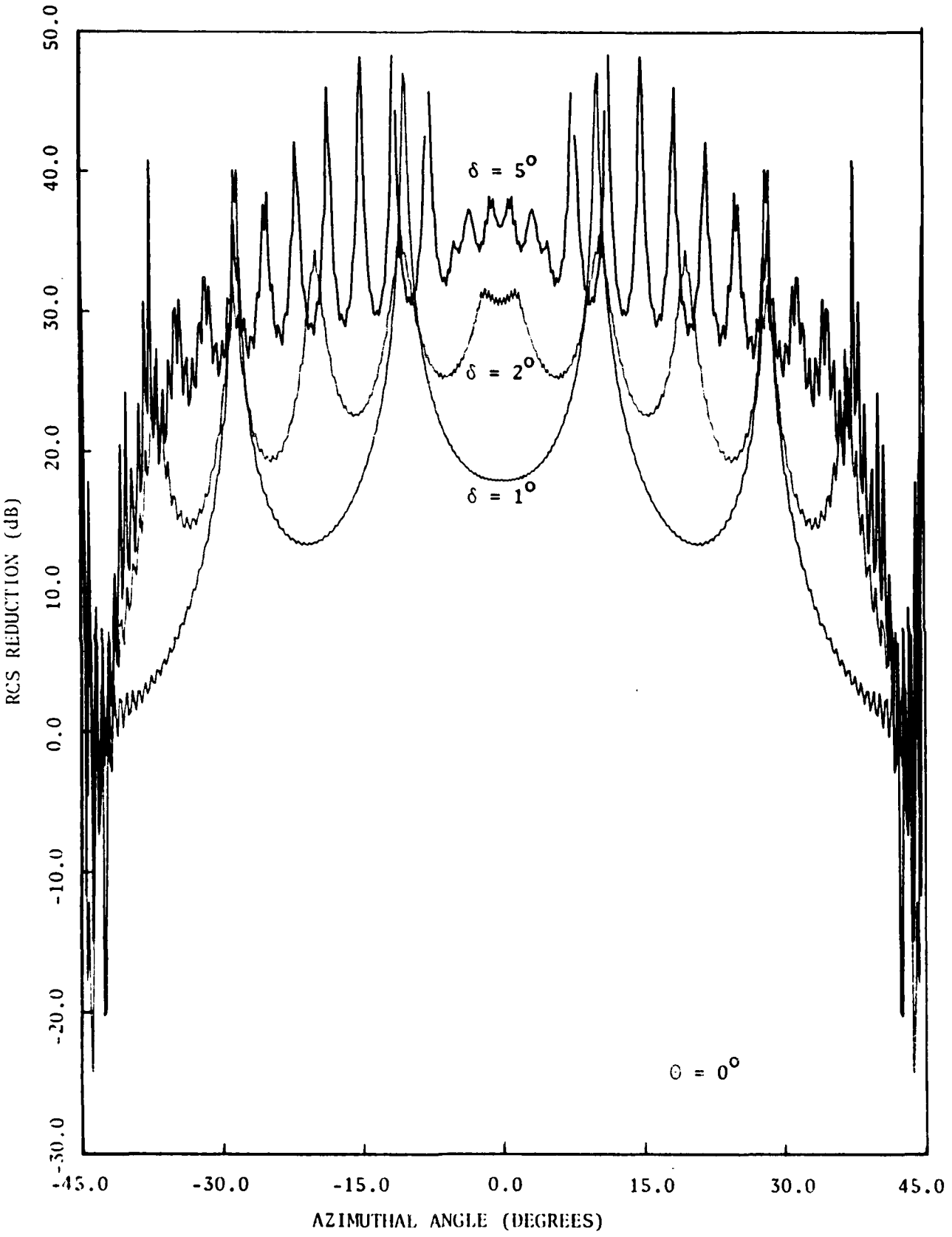

Figure 33. Reduction in RCS for $\delta = 1^{\circ}$, 2° and 5° (vertical polarisation). $a = b = 100\lambda$

ERL-0325-TR
Figure 34

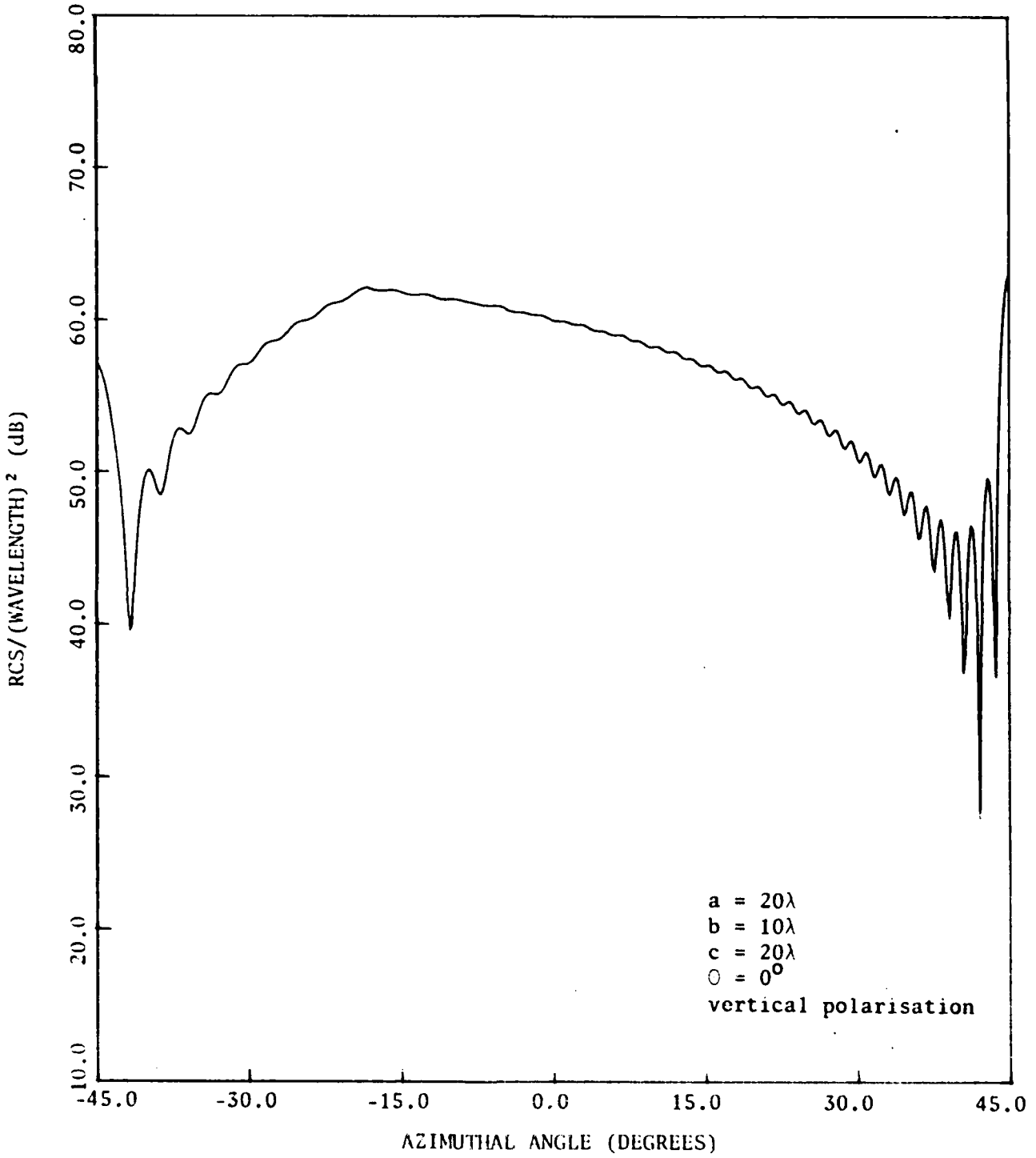

Figure 34. RCS for an asymmetric reflector with reflector angle 90°

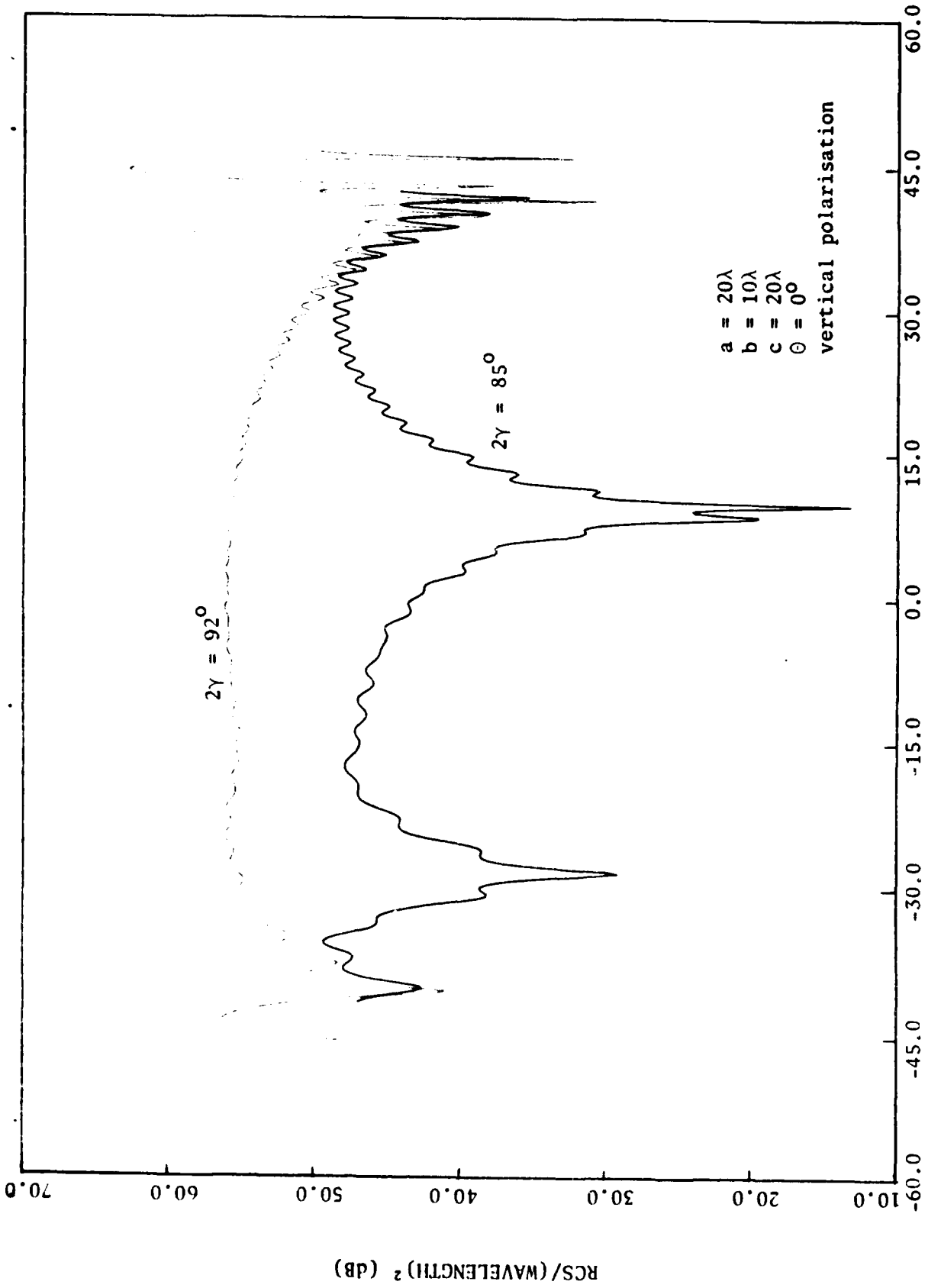

Figure 35. RCS for asymmetric reflectors with reflector angles 85° and 92°

ERL-0325-TR
Figure 36

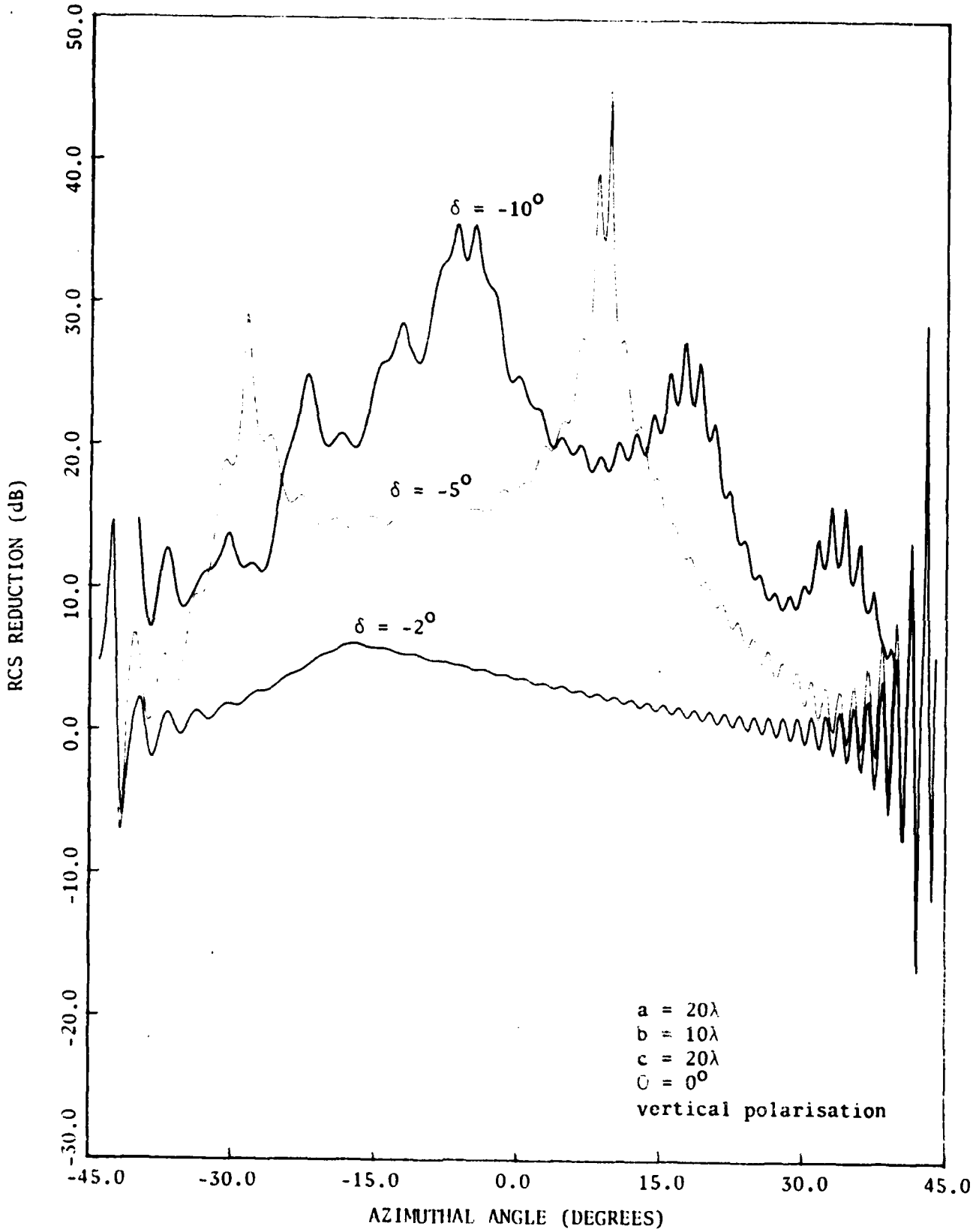

Figure 36. Reduction in RCS for asymmetric reflectors with δ = -2°, -5° and -10°

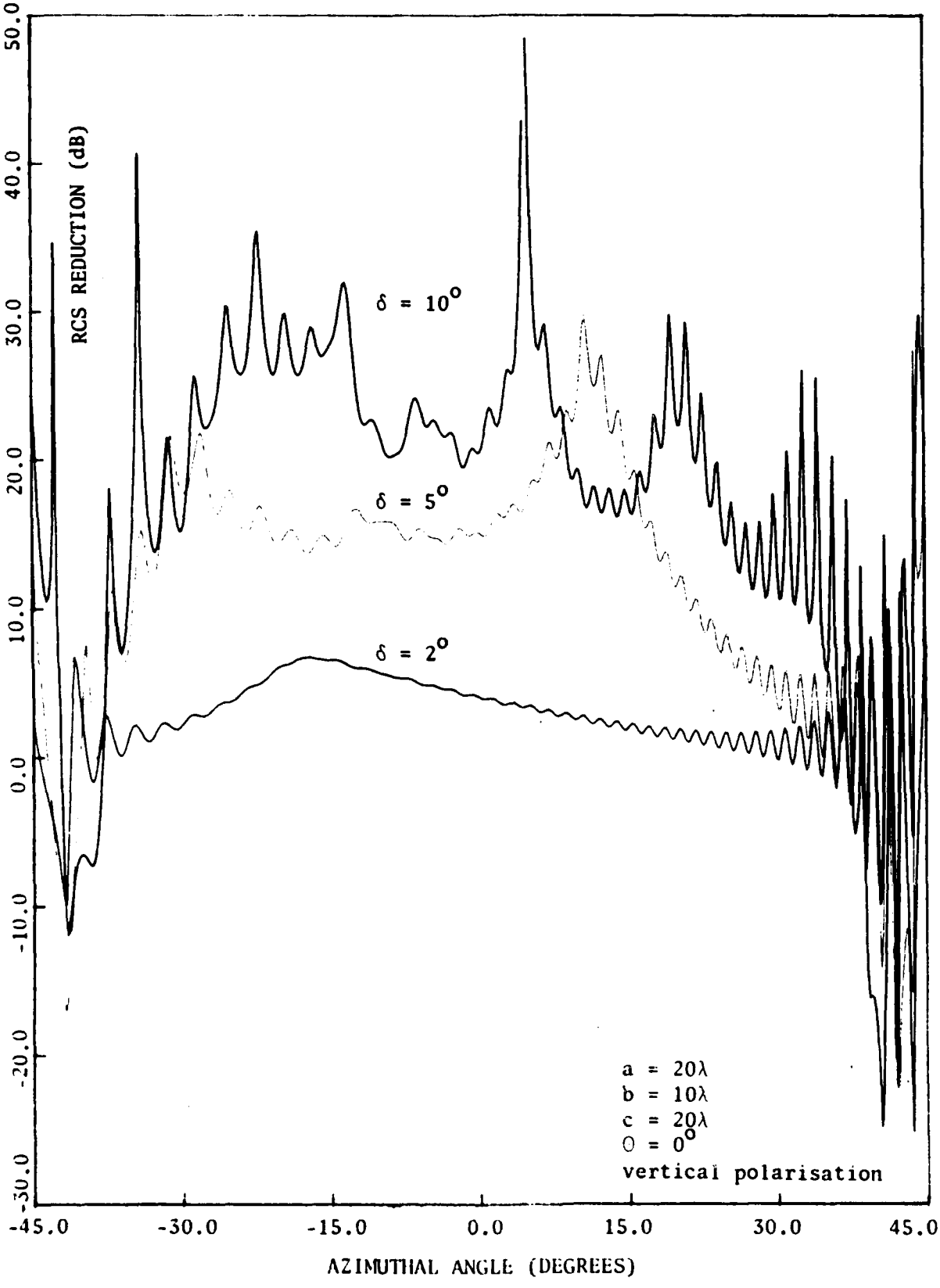

RCS REDUCTION (dB)

Figure 37. Reduction in RCS for asymmetric reflectors for $\delta = 2^{o}$, 5^{o} and 10^{o}

ERL-0325-TR
Figure 38

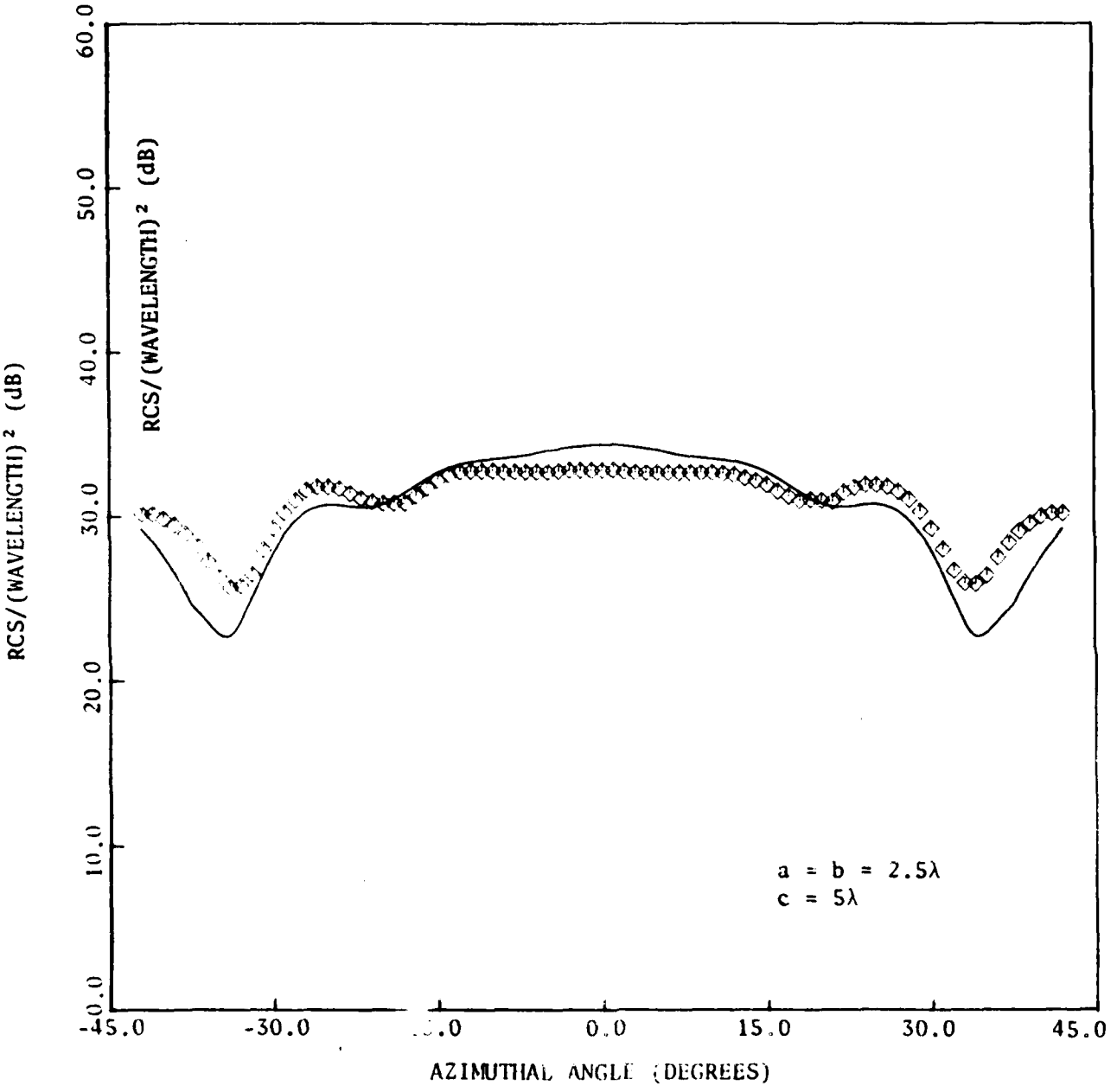

Figure 38. Comparison of theory with experiment for $a/\lambda = 2.5$, $\theta = 0^{\circ}$, $2\gamma = 85^{\circ}$ (vertical polarisation)

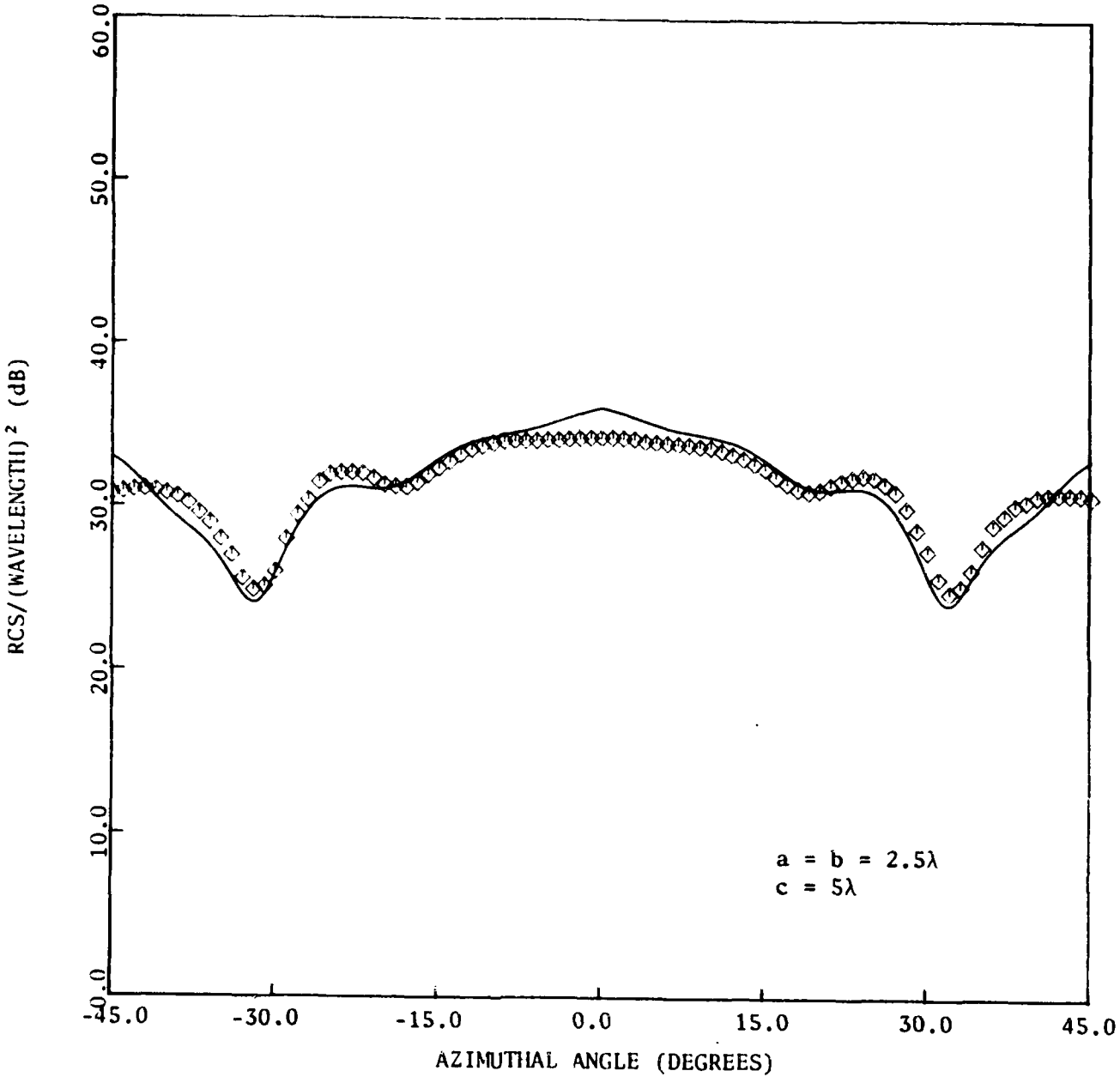

Figure 39. Comparison of theory with experiment for $a/\lambda = 2.5$, $\theta = 0^{o}$, $2\gamma = 90^{o}$ (vertical polarisation)

ERL-0325-TR
Figure 40

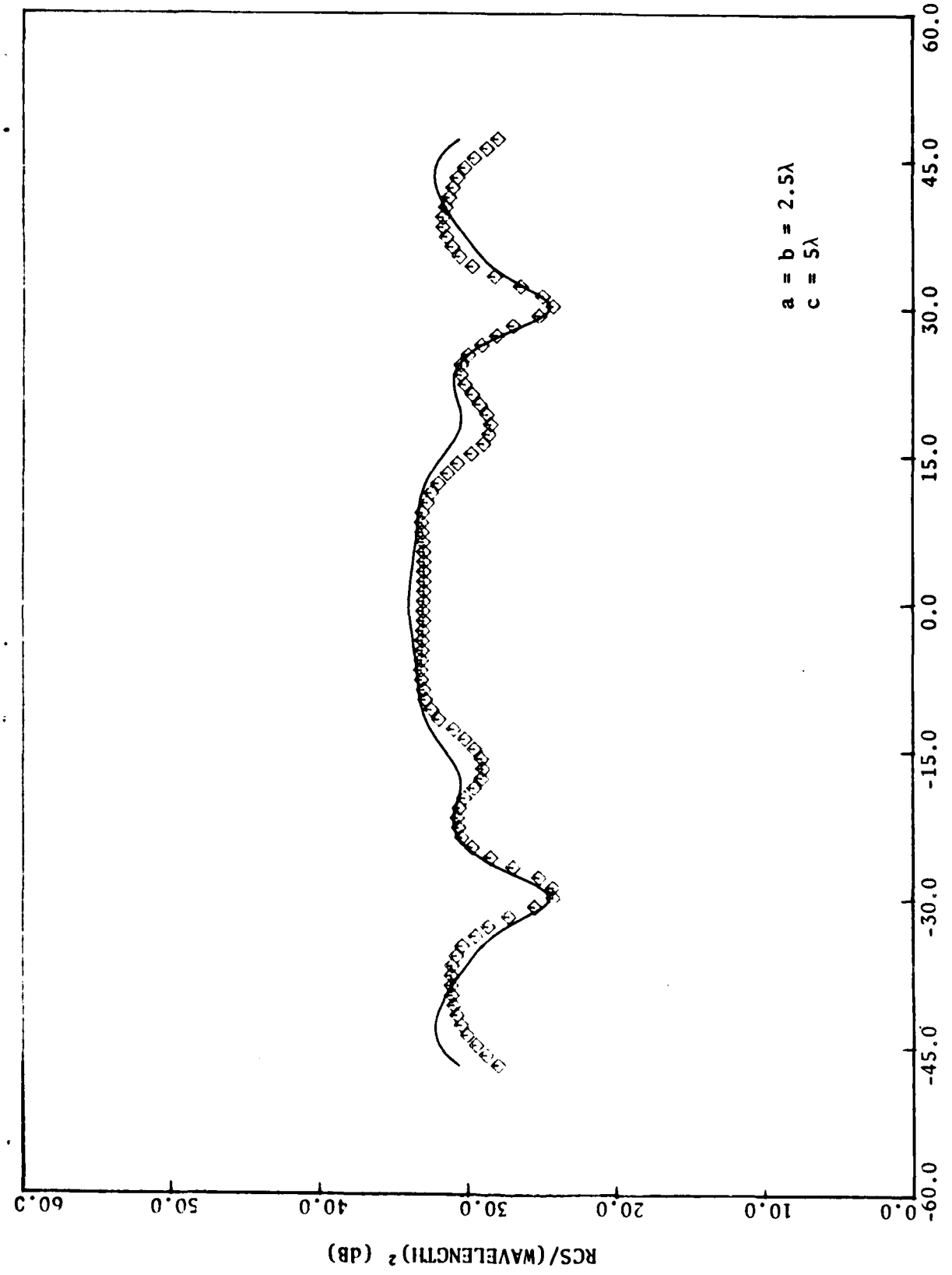

Figure 40. Comparison of theory with experiment for $a/\lambda = 2.5$, $\Theta = 0^{\circ}$, $2\gamma = 95^{\circ}$ (vertical polarisation)

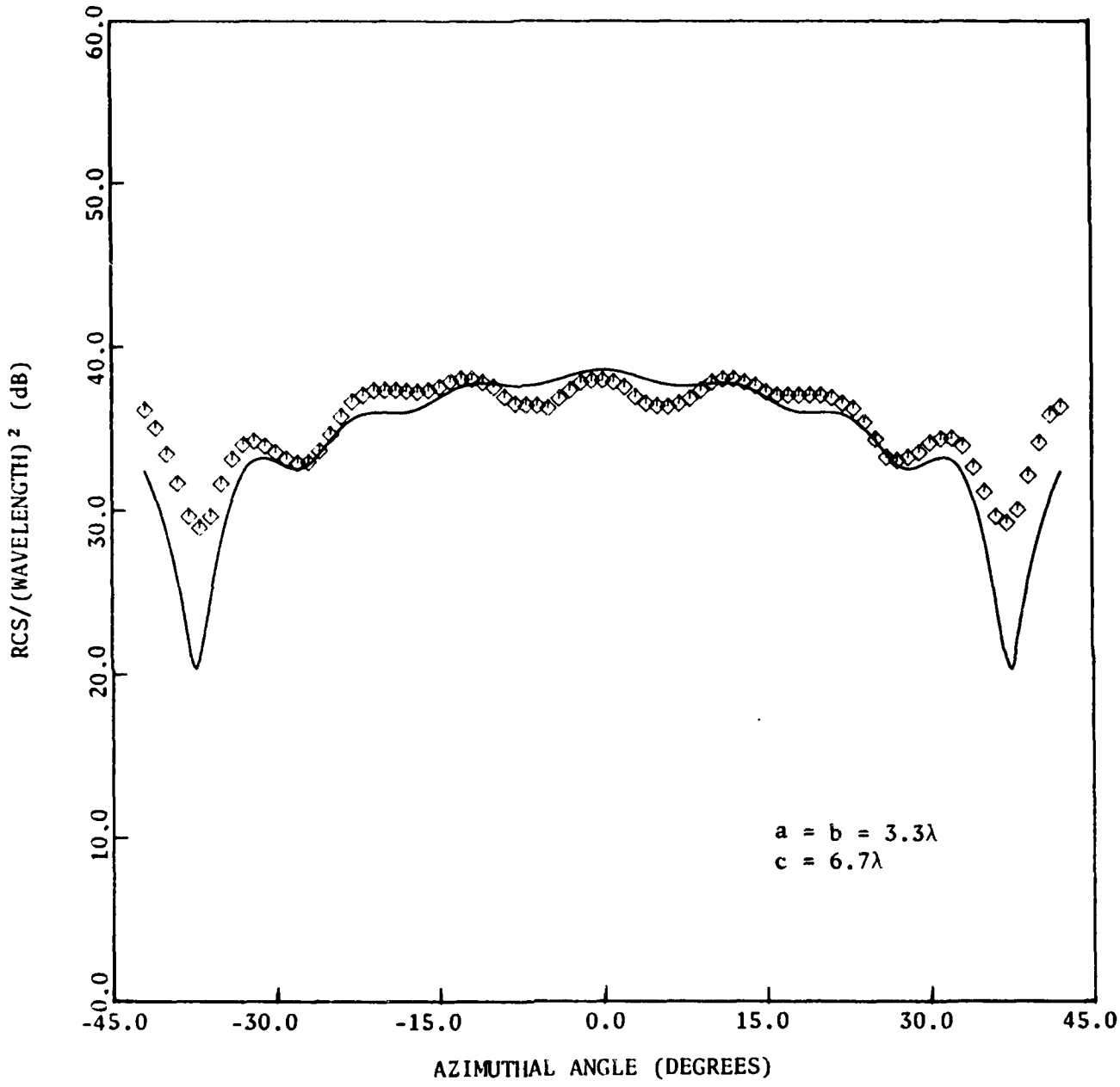

Figure 41. Comparison of theory with experiment for $a/\lambda = 3.3$, $\Theta = 0^{o}$, $2\gamma = 85^{o}$ (vertical polarisation)

ERL-0325-TR
Figure 42

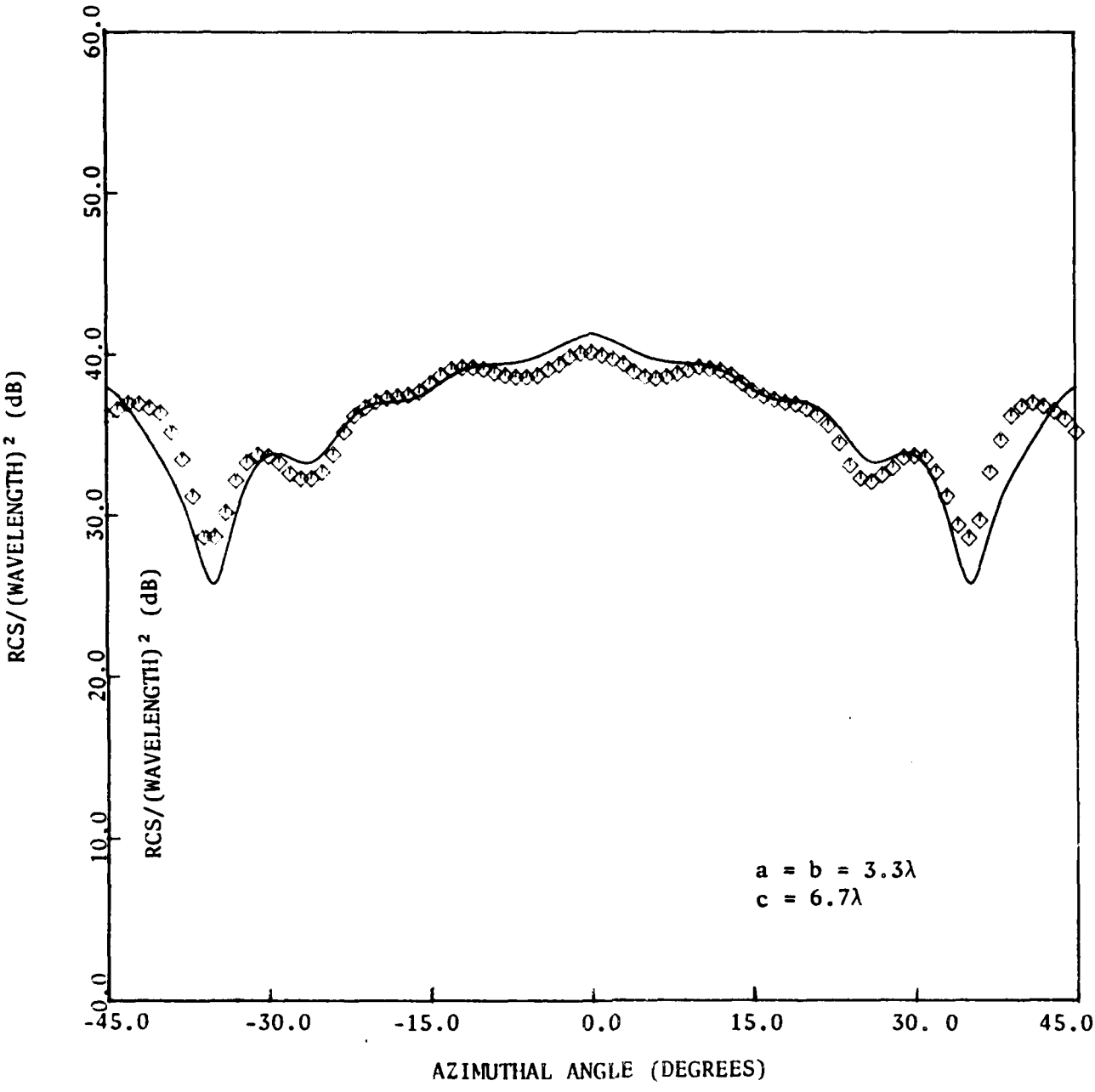

Figure 42. Comparison of theory with experiment for $a/\lambda = 3.3$, $\Theta = 0^{o}$, $2\gamma = 90^{o}$ (vertical polarisation)

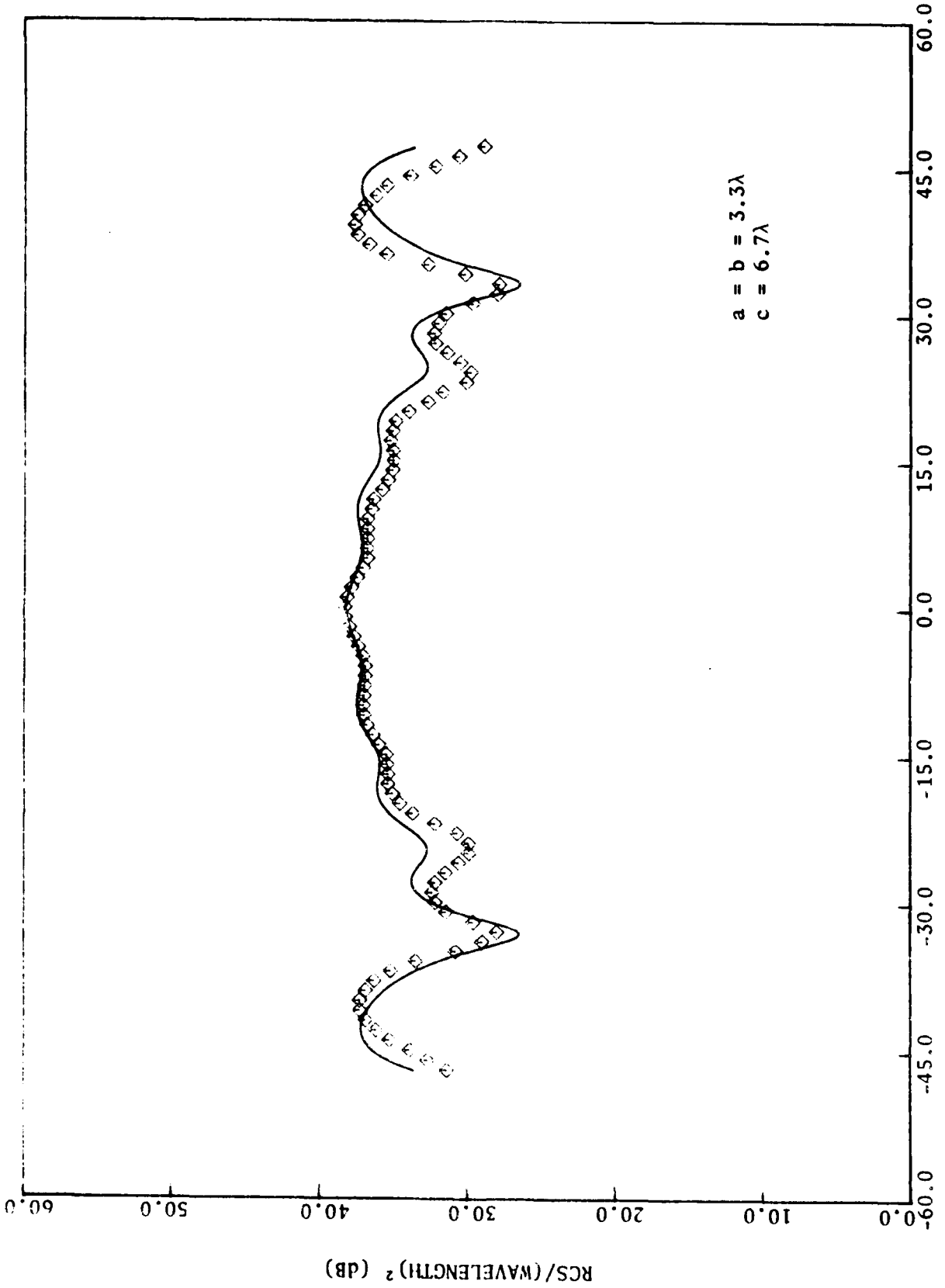

Figure 43. Comparison of theory with experiment for $a/\lambda = 3.3$, $\Theta = 0^{o}$, $2\gamma = 95^{o}$ (vertical polarisation)

ERL-0325-TR
Figure 44

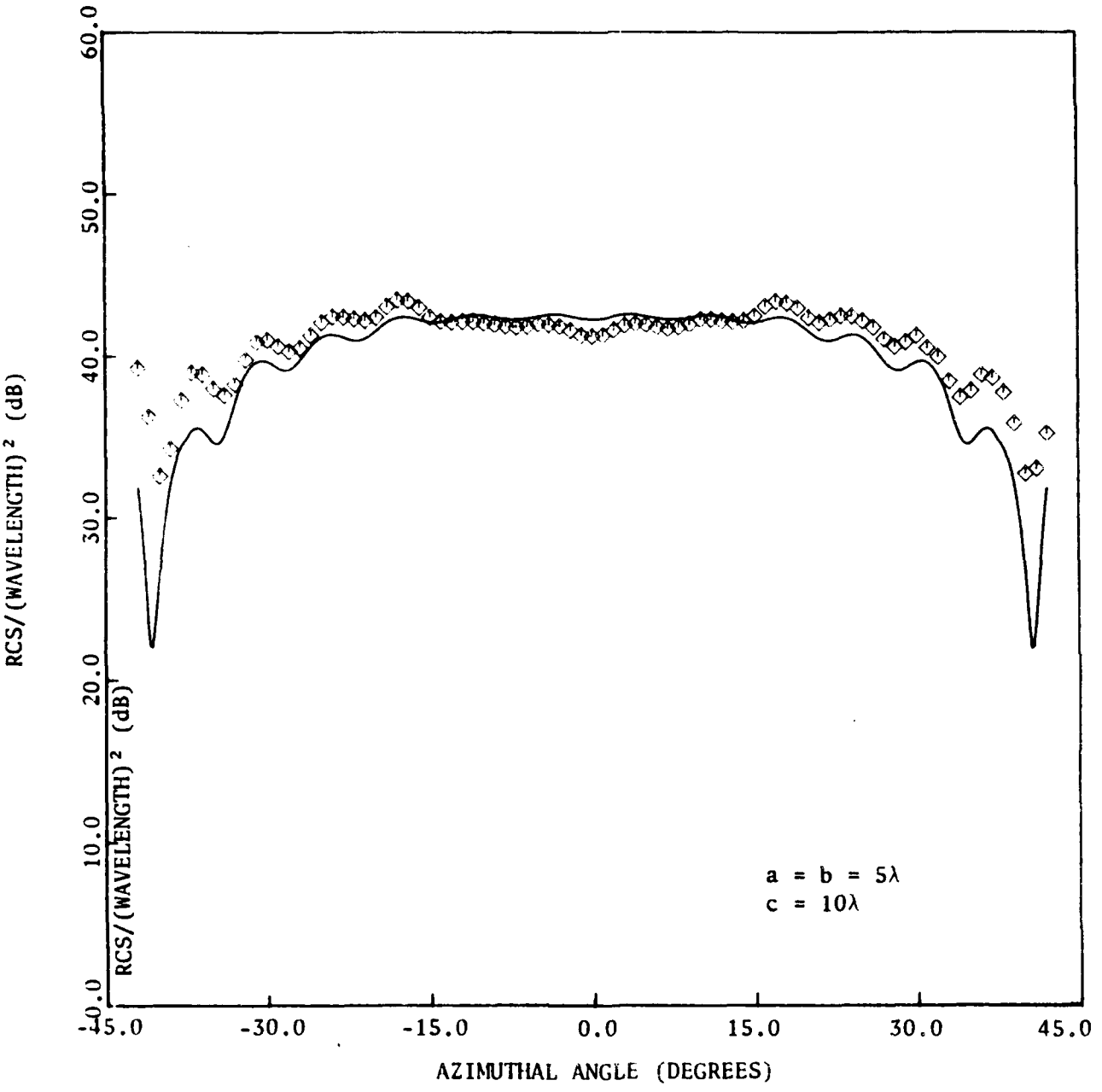

Figure 44. Comparison of theory with experiment for $a/\lambda = 5.0$, $\Theta = 0^{o}$, $2\gamma = 85^{o}$ (vertical polarisation)

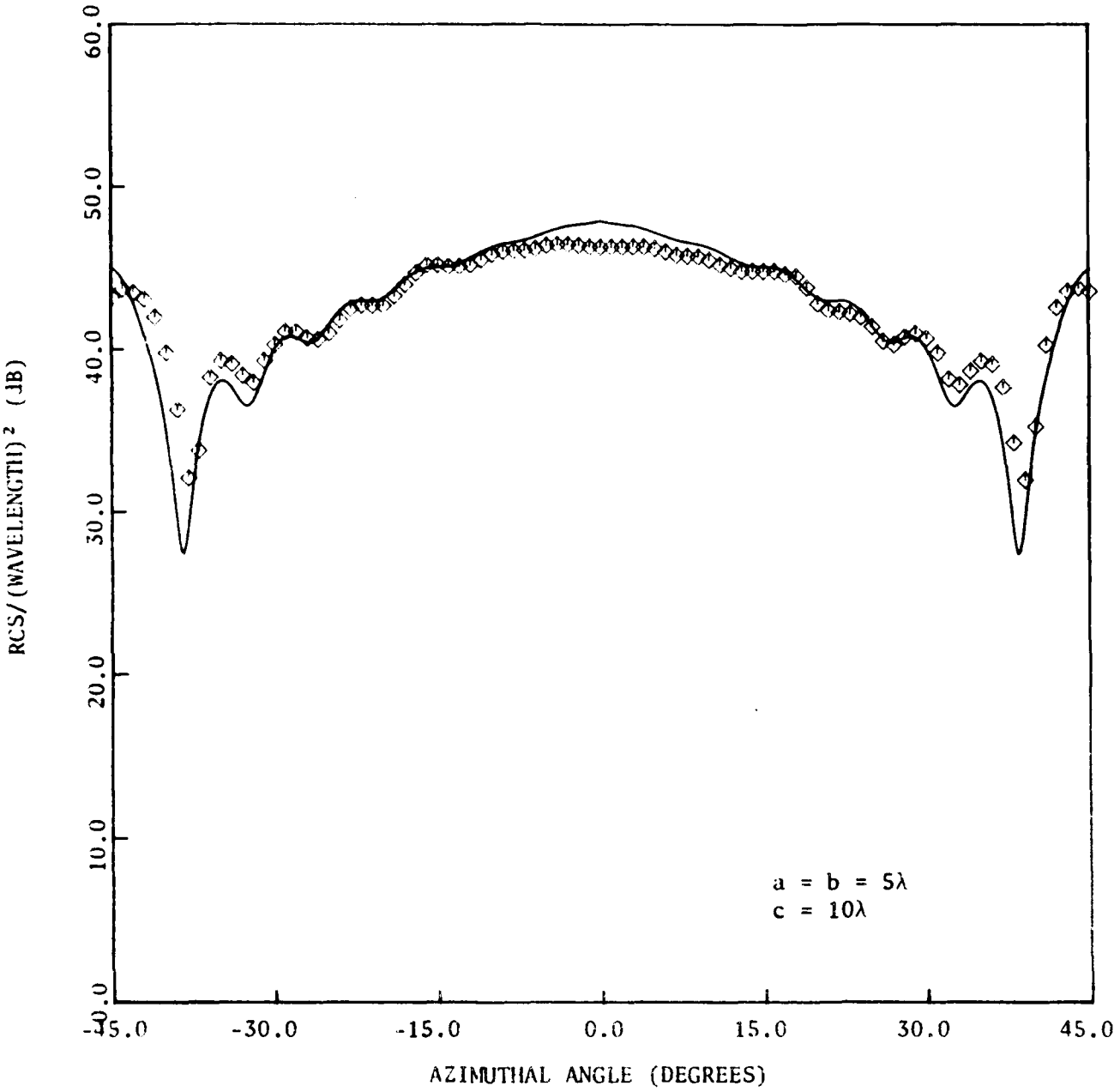

Figure 45. Comparison of theory with experiment for $a/\lambda = 5.0$, $\theta = 0^{\circ}$, $2\gamma = 90^{\circ}$ (vertical polarisation)

ERL-0325-TR
Figure 46

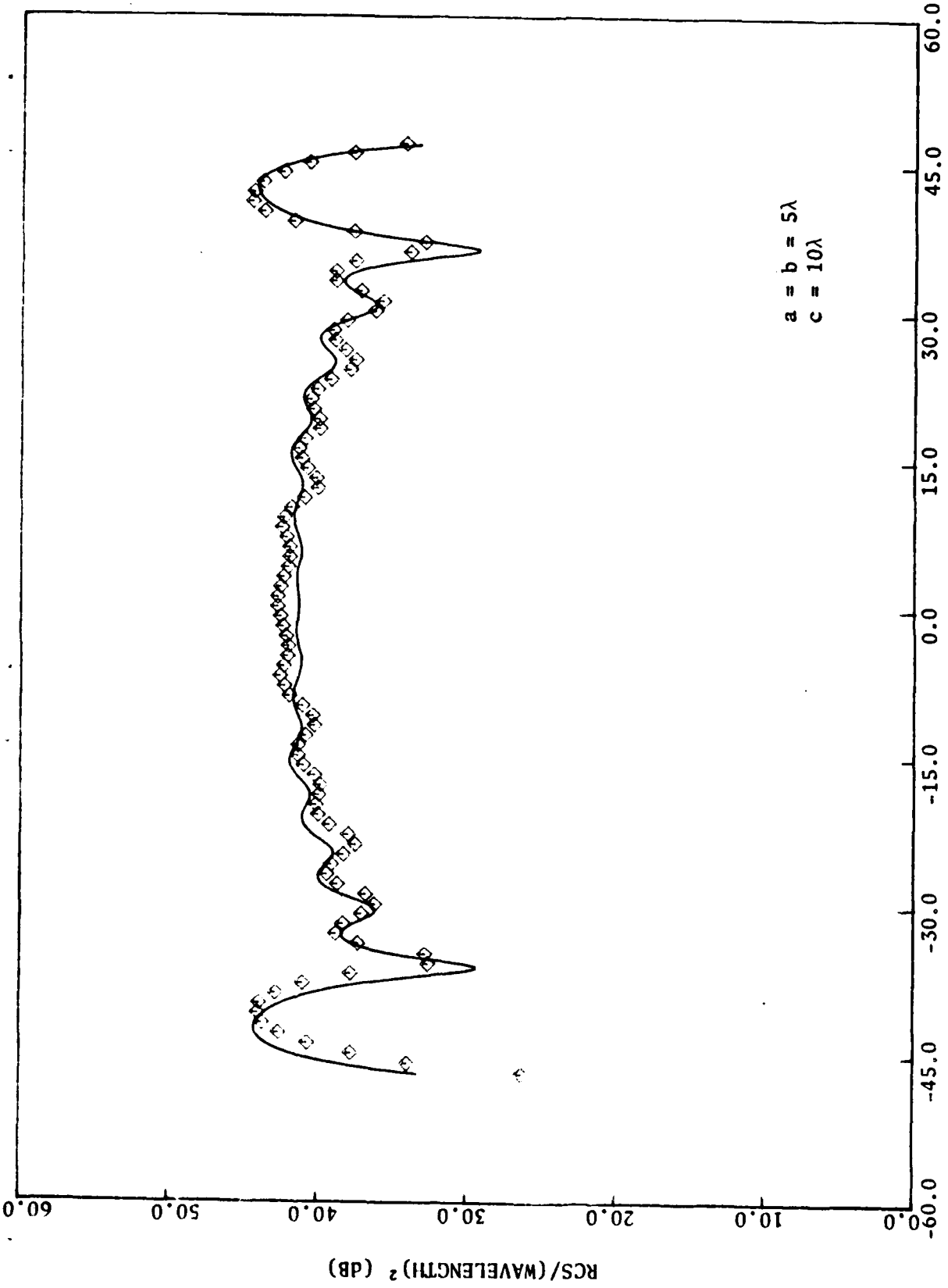

Figure 46. Comparison of theory with experiment for $a/\lambda = 5.0$, $\Theta = 0^{o}$, $2\gamma = 95^{o}$ (vertical polarisation)

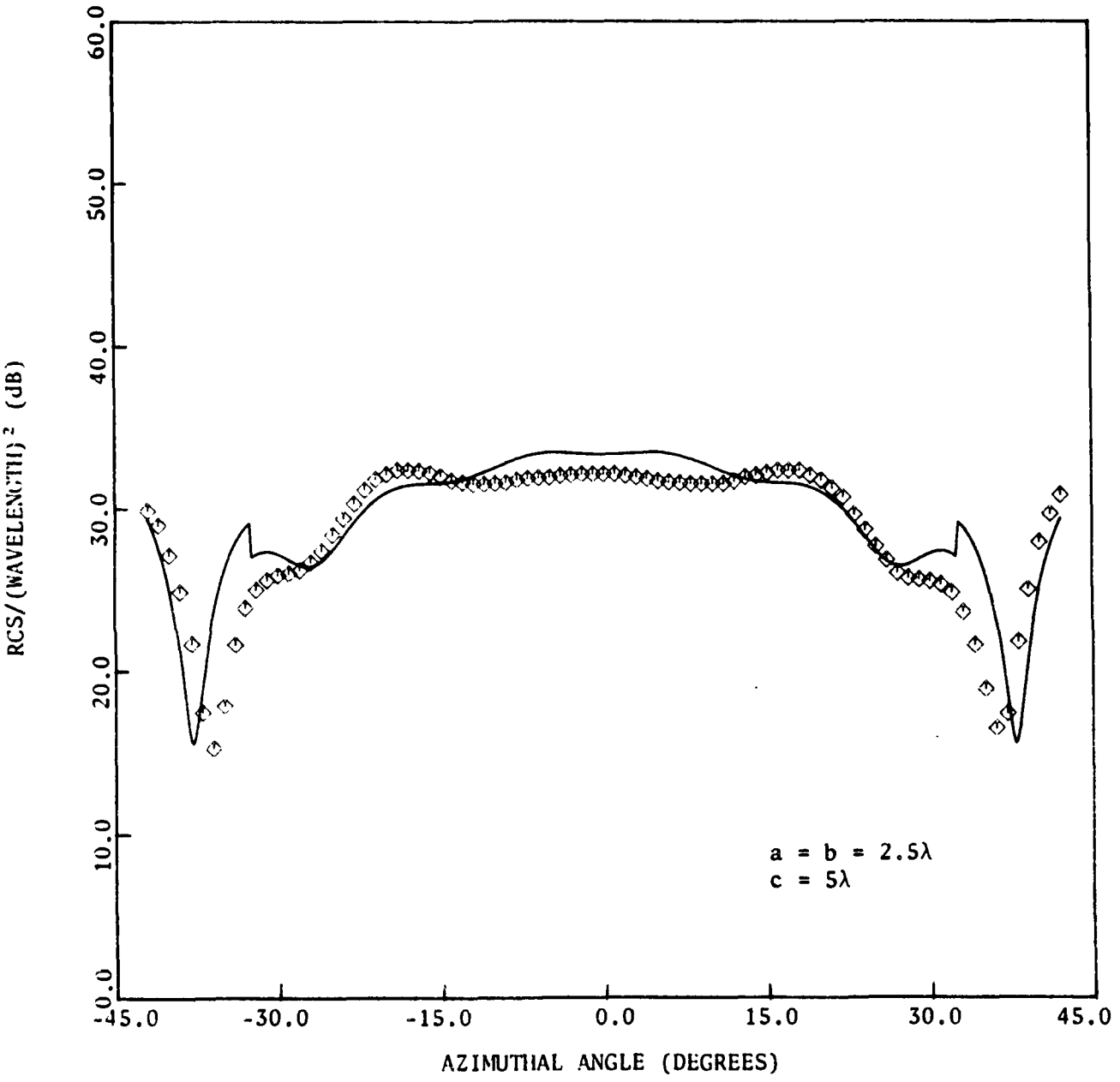

Figure 47. Comparison of theory with experiment for $a/\lambda = 2.5$, $\Theta = 0^{o}$, $2\gamma = 85^{o}$ (horizontal polarisation)

ERL-0325-TR
Figure 48

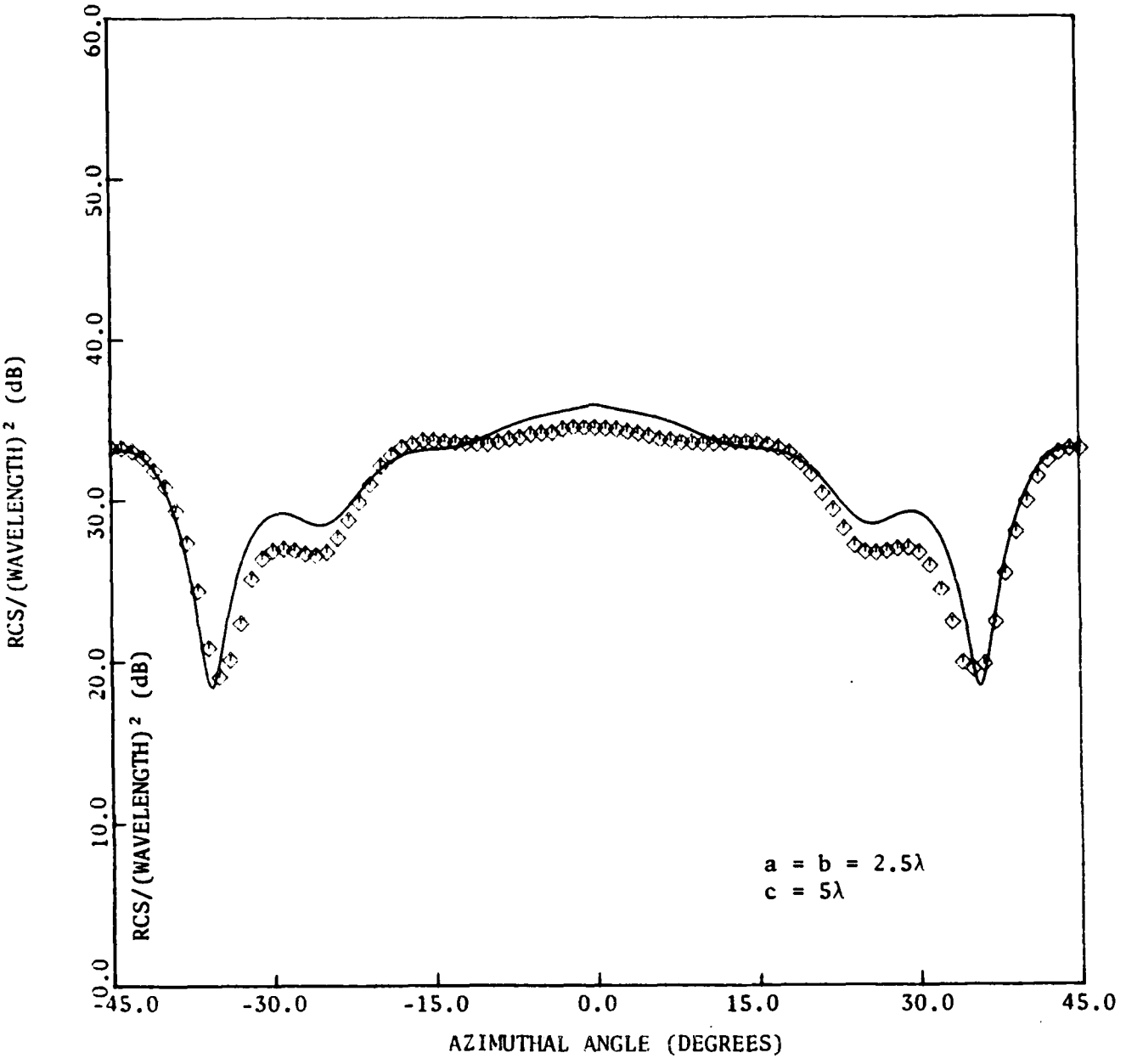

Figure 48. Comparison of theory with experiment for $a/\lambda = 2.5$, $\Theta = 0^{\circ}$, $2\gamma = 90^{\circ}$ (horizontal polarisation)

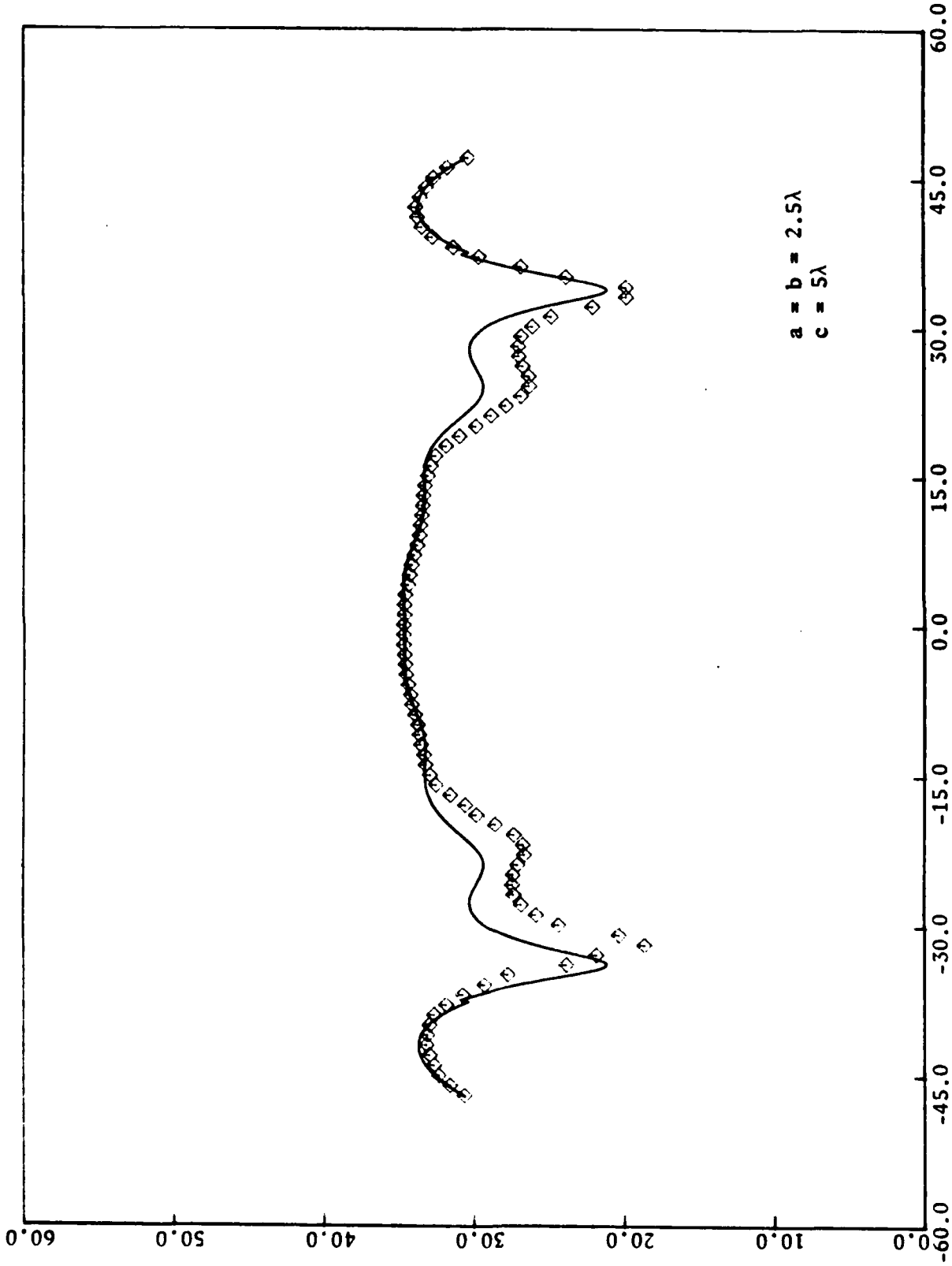

Figure 49. Comparison of theory with experiment for $a/\lambda = 2.5$, $\theta = 0^{o}$, $2\gamma = 95^{o}$ (horizontal polarisation)

ERL-0325-TR
Figure 50

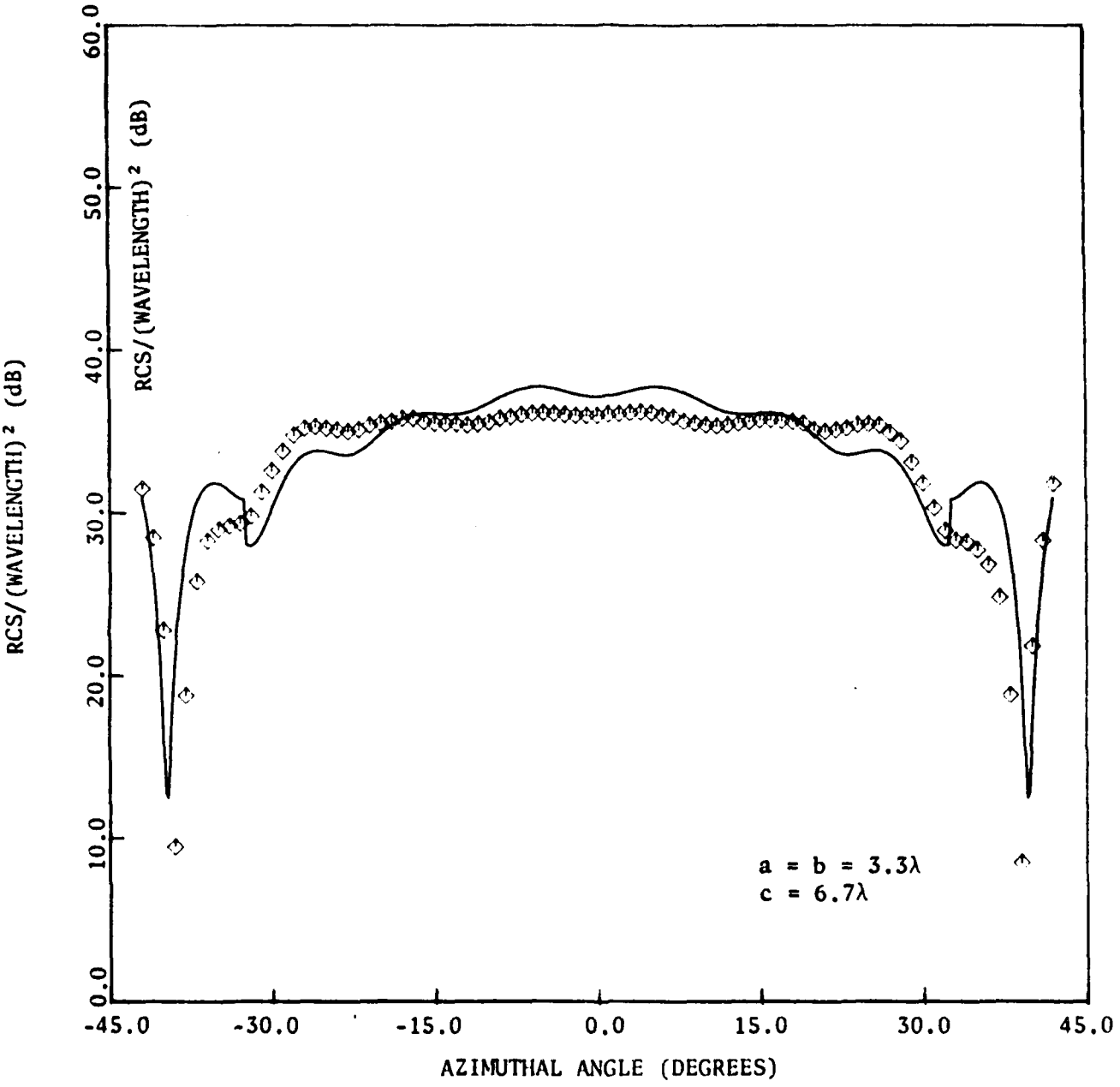

Figure 50. Comparison of theory with experiment for $a/\lambda = 3.3$, $\theta = 0^{\circ}$, $2\gamma = 85^{\circ}$ (horizontal polarisation)

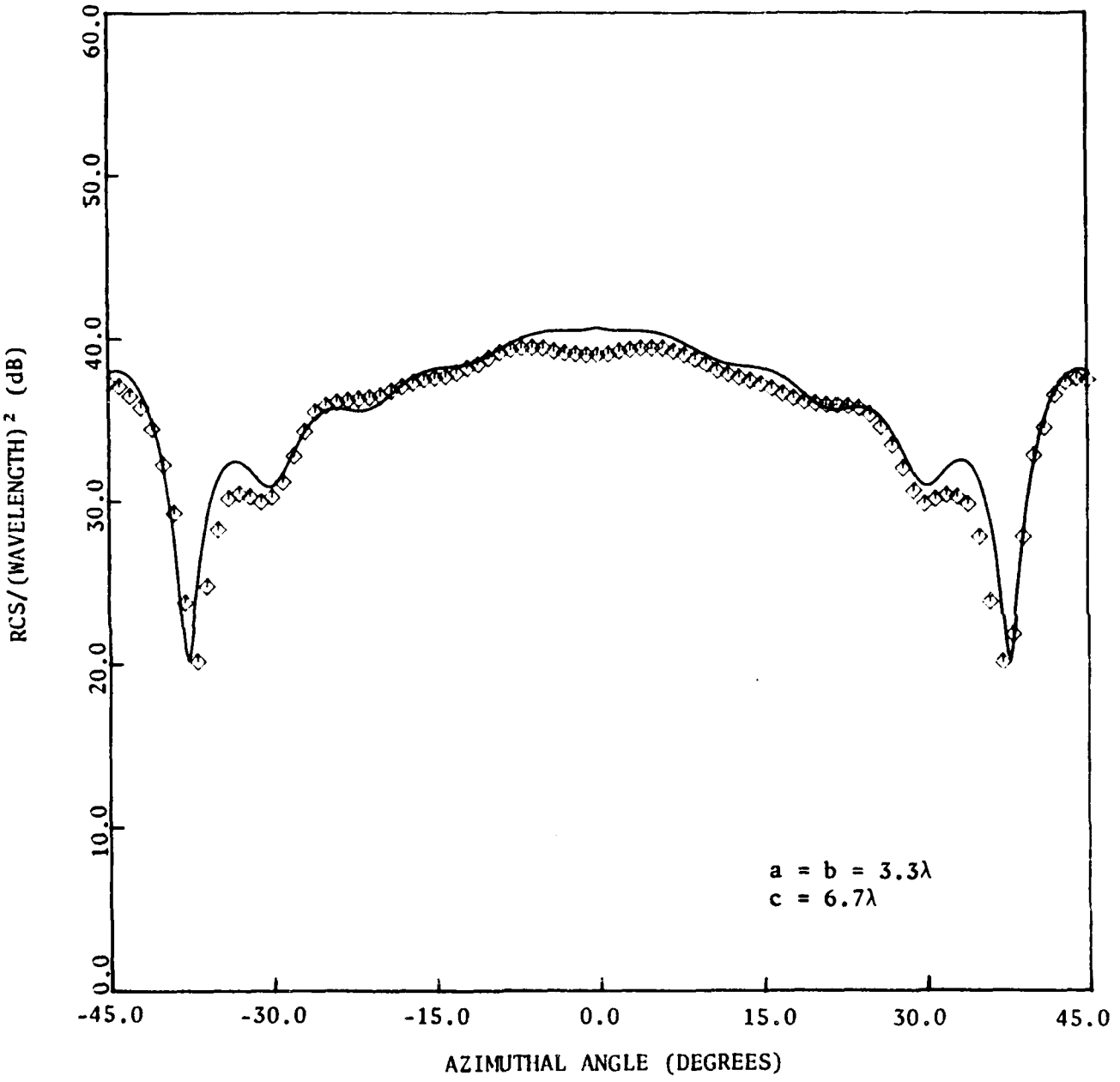

Figure 51. Comparison of theory with experiment for $a/\lambda = 3.3$, $\Theta = 0^{o}$, $2\gamma = 90^{o}$ (horizontal polarisation)

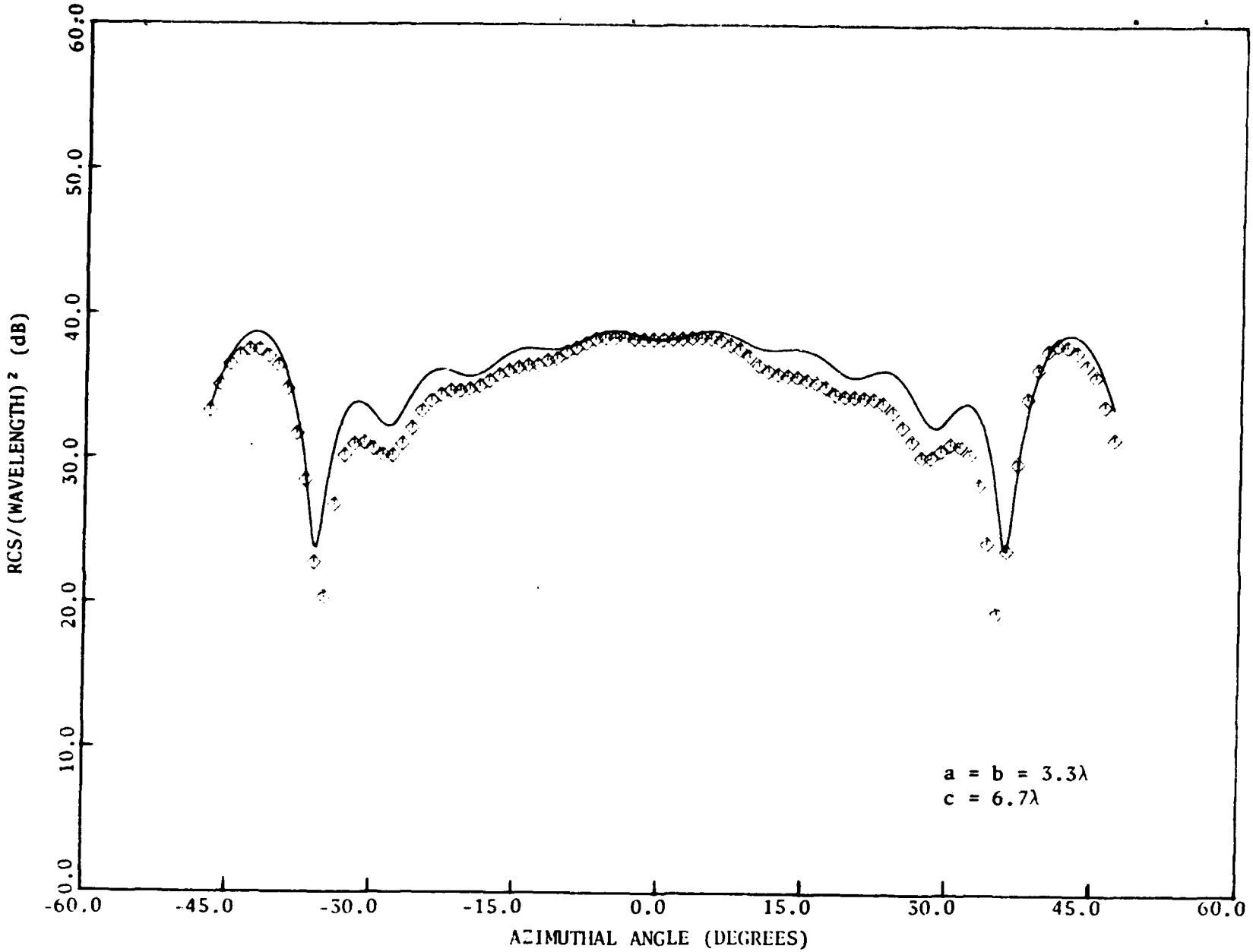

Figure 52. Comparison of theory with experiment for $a/\lambda = 3.3$, $\zeta = 0^{o}$, $2\gamma = 95^{o}$ (horizontal polarisation)

ERL-0325-TR
Figure 52

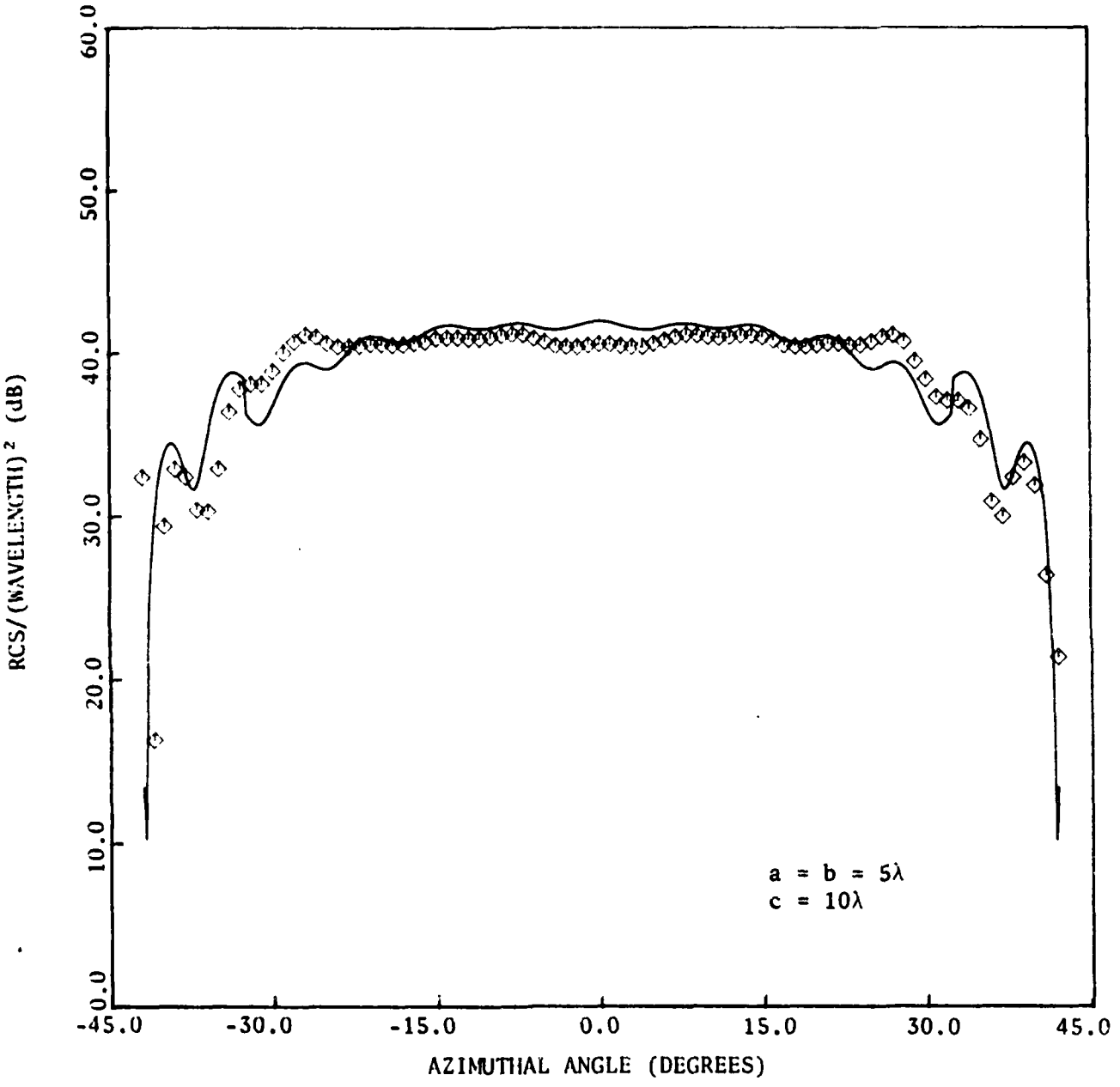

Figure 53. Comparison of theory with experiment for $a/\lambda = 5.0$, $\theta = 0^{\circ}$, $2\gamma = 85^{\circ}$ (horizontal polarisation)

ERL-0325-TR
Figure 54

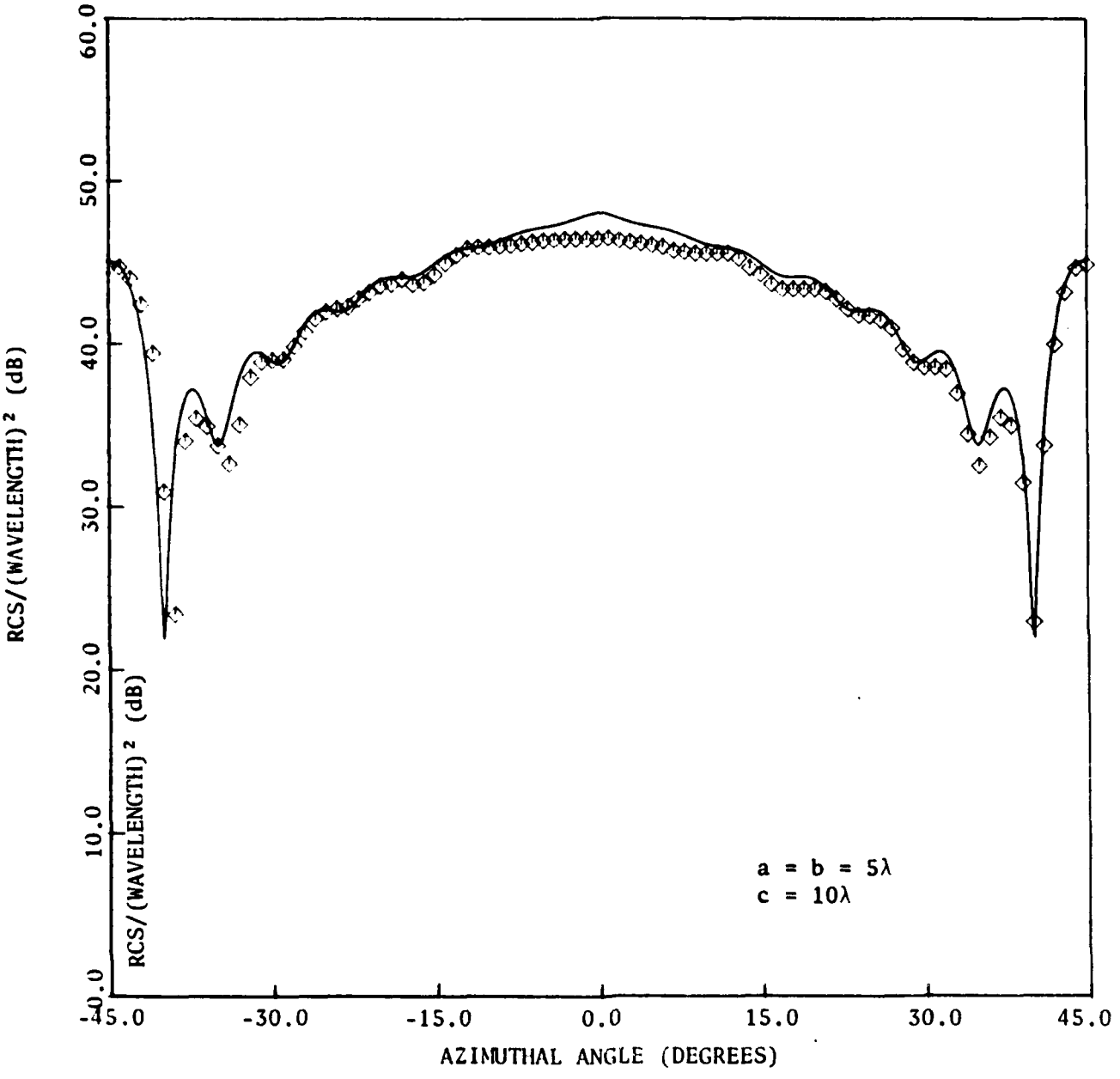

Figure 54. Comparison of theory with experiment for $a/\lambda = 5.0$, $\theta = 0^{o}$, $2\gamma = 90^{o}$ (horizontal polarisation)

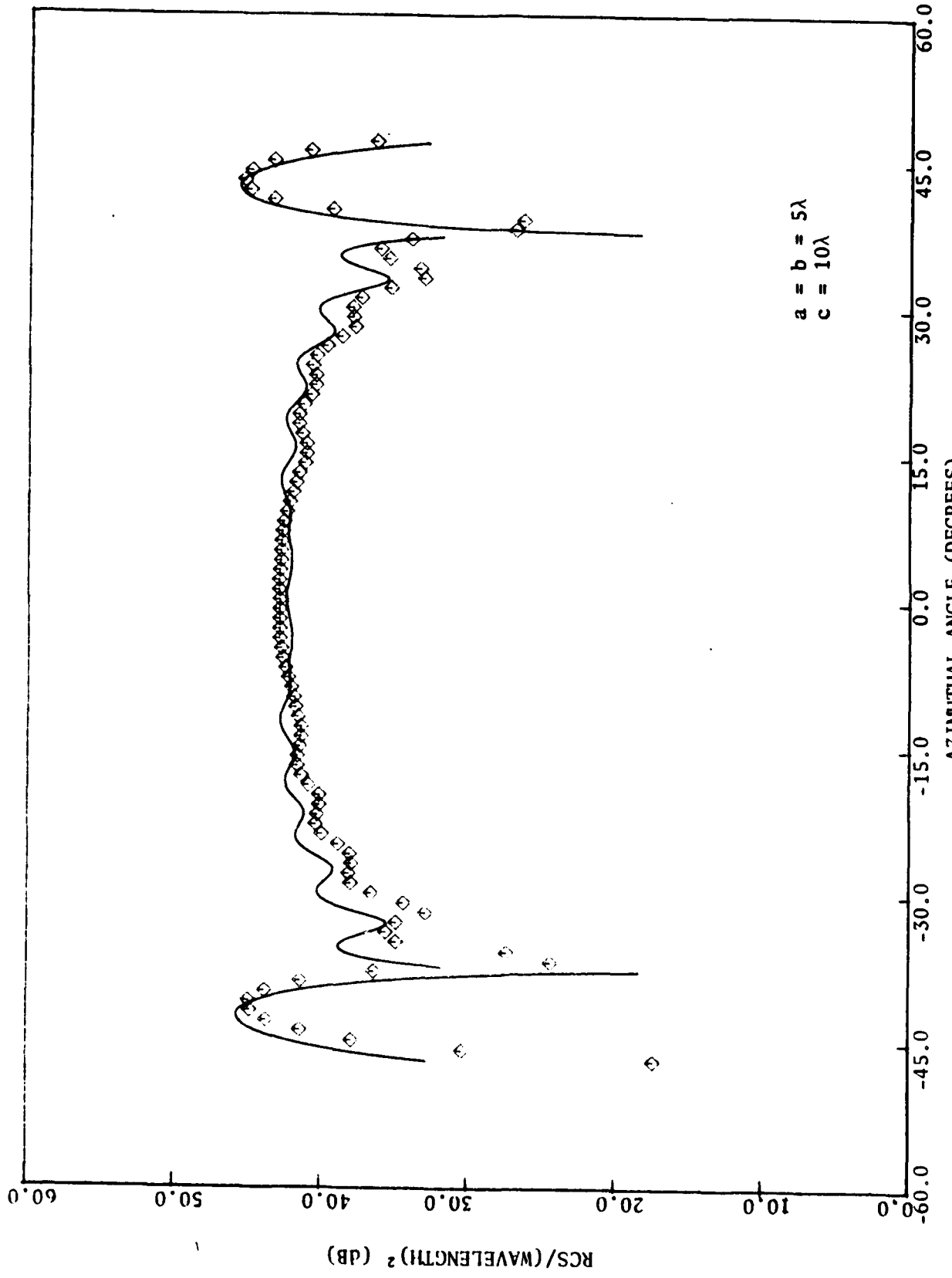

Figure 55. Comparison of theory with experiment for $a/\lambda = 5.0$, $\Theta = 0^{o}$, $2\gamma = 95^{o}$ (horizontal polarisation)

ERL-0325-TR
Figure 56

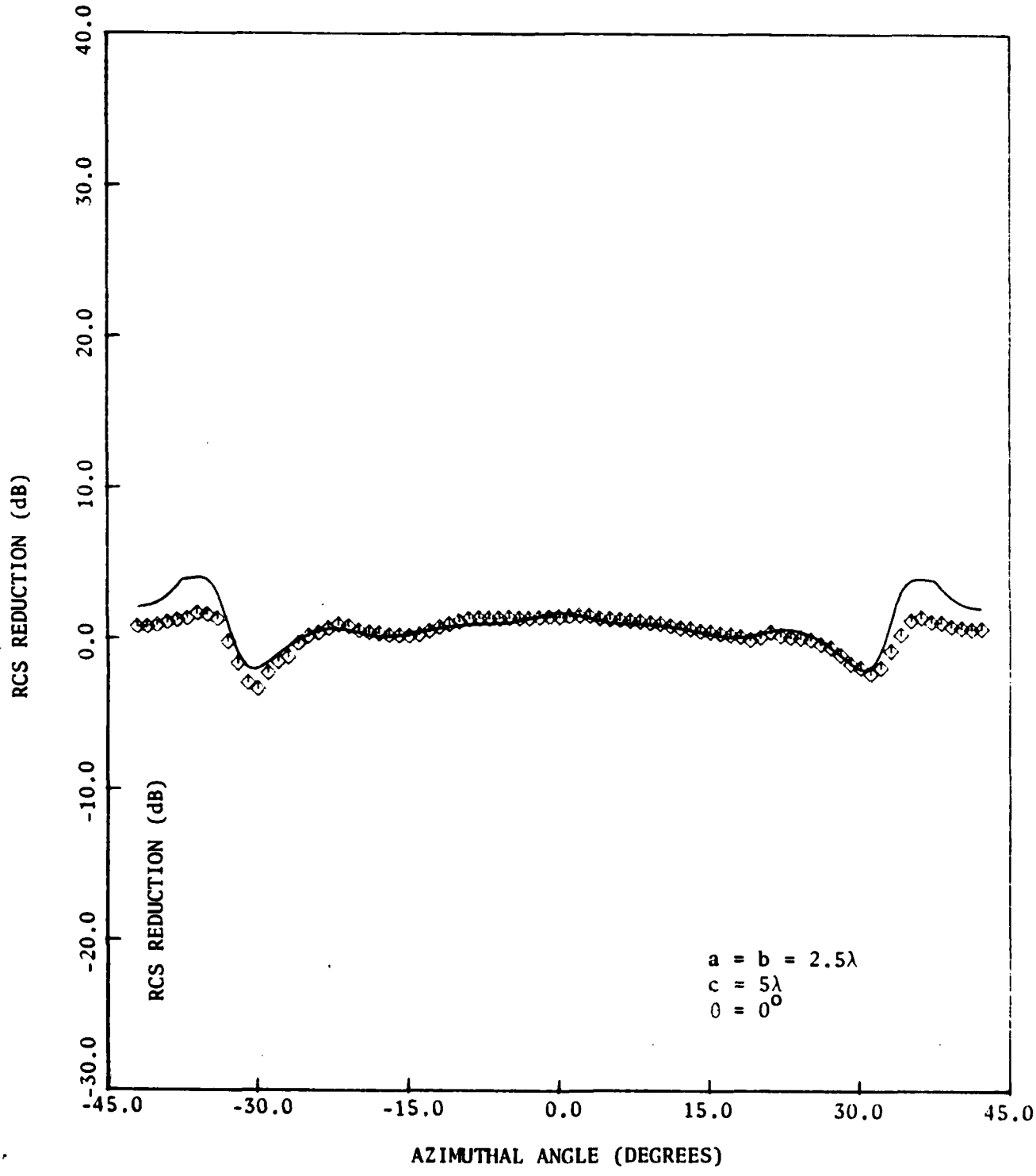

Figure 56. Predicted and measured reduction in RCS for $\delta = -5^{o}$, $a/\lambda = 2.5$ and vertical polarisation

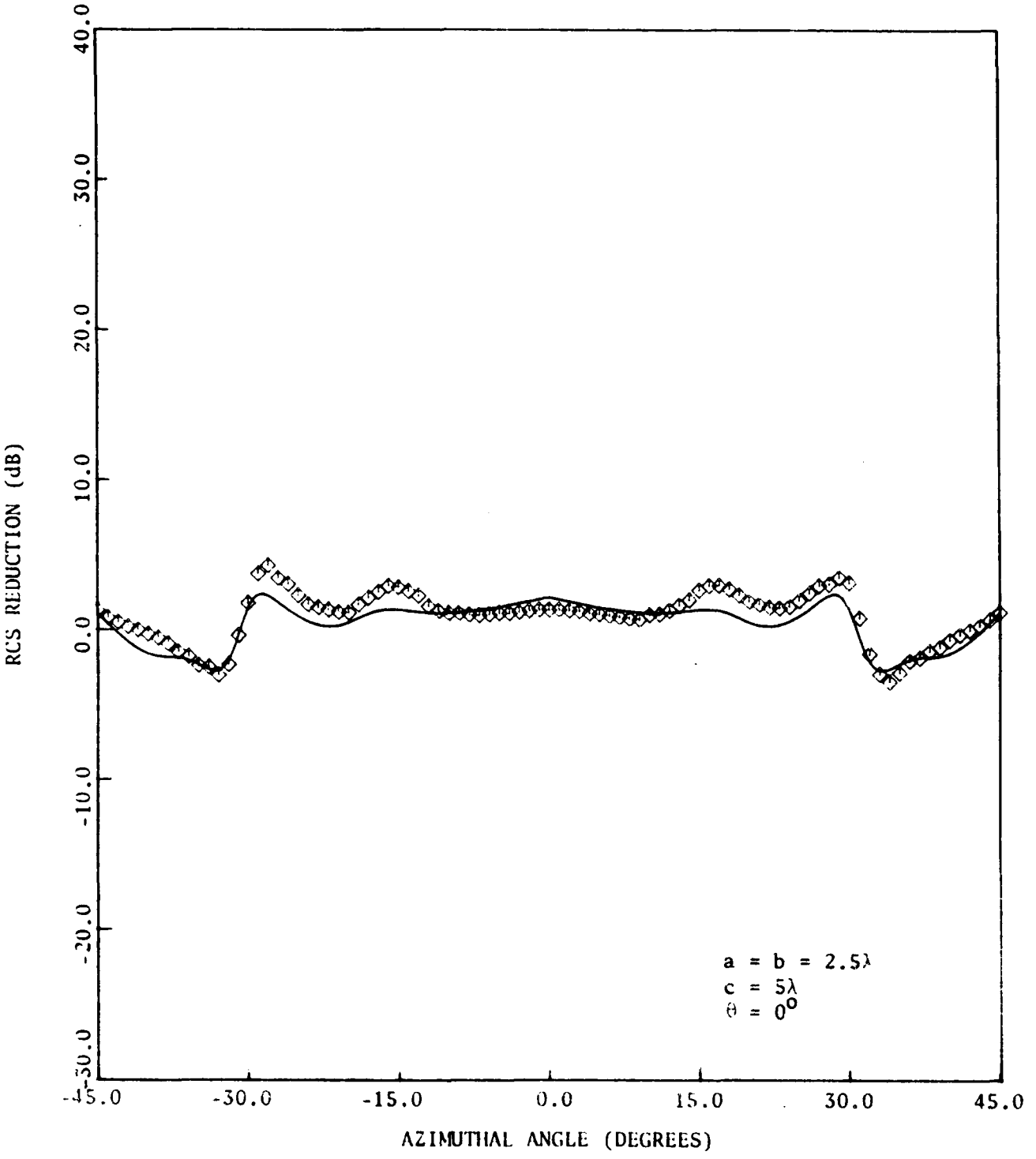

Figure 57. Predicted and measured reduction in RCS for $\delta = 5^{o}$, $a/\lambda = 2.5$ and vertical polarisation

ERL-0325-TR
Figure 58

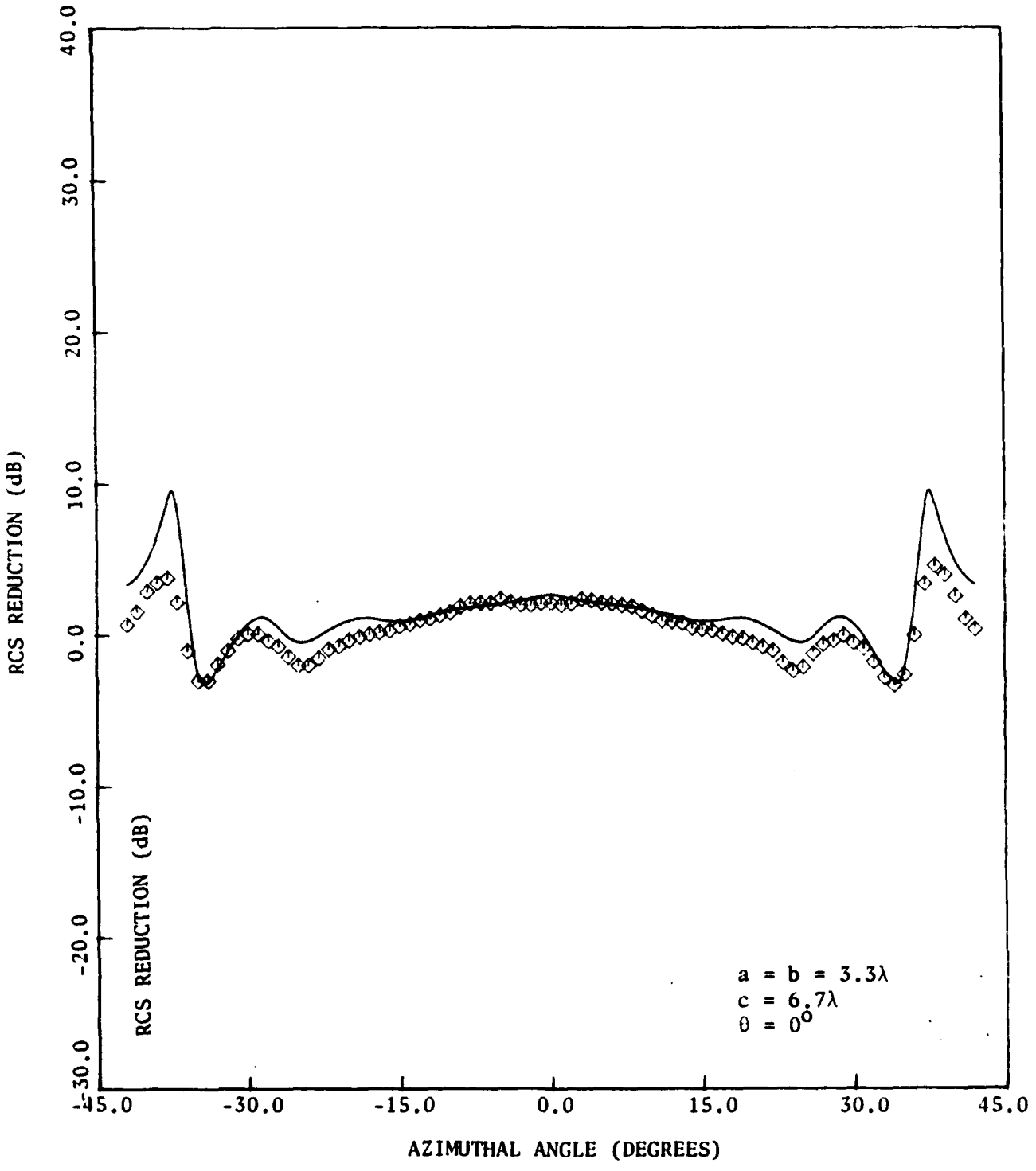

Figure 58. Predicted and measured reduction in RCS for $\delta = -5^{o}$, $a/\lambda = 3.3$ and vertical polarisation

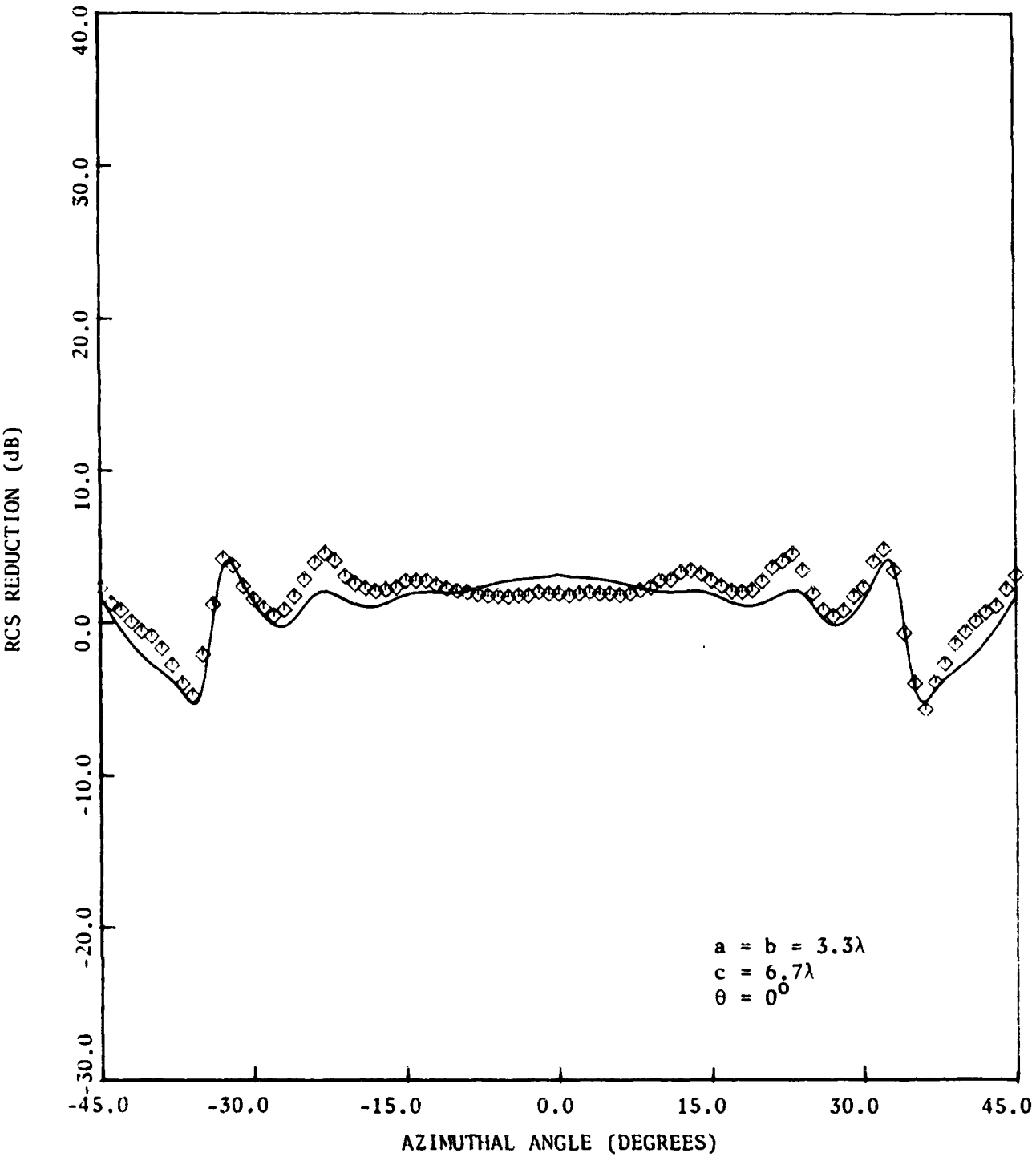

Figure 59. Predicted and measured reduction in RCS for $\delta = 5^{o}$, $a/\lambda = 3.3$ and vertical polarisation

ERL-0325-TR
Figure 60

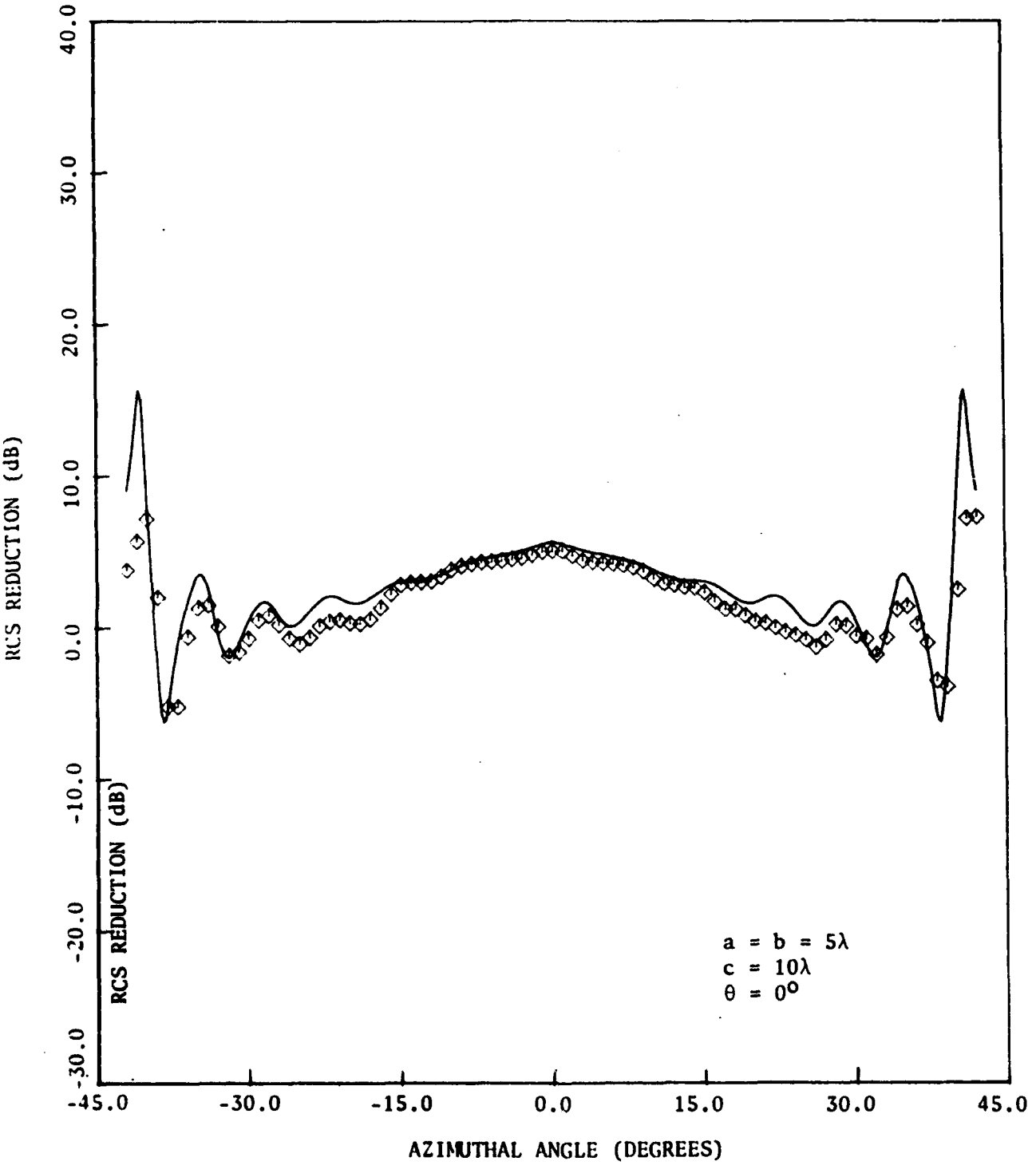

Figure 60. Predicted and measured reduction in RCS for $\delta = -5^{o}$, $a/\lambda = 5.0$ and vertical polarisation

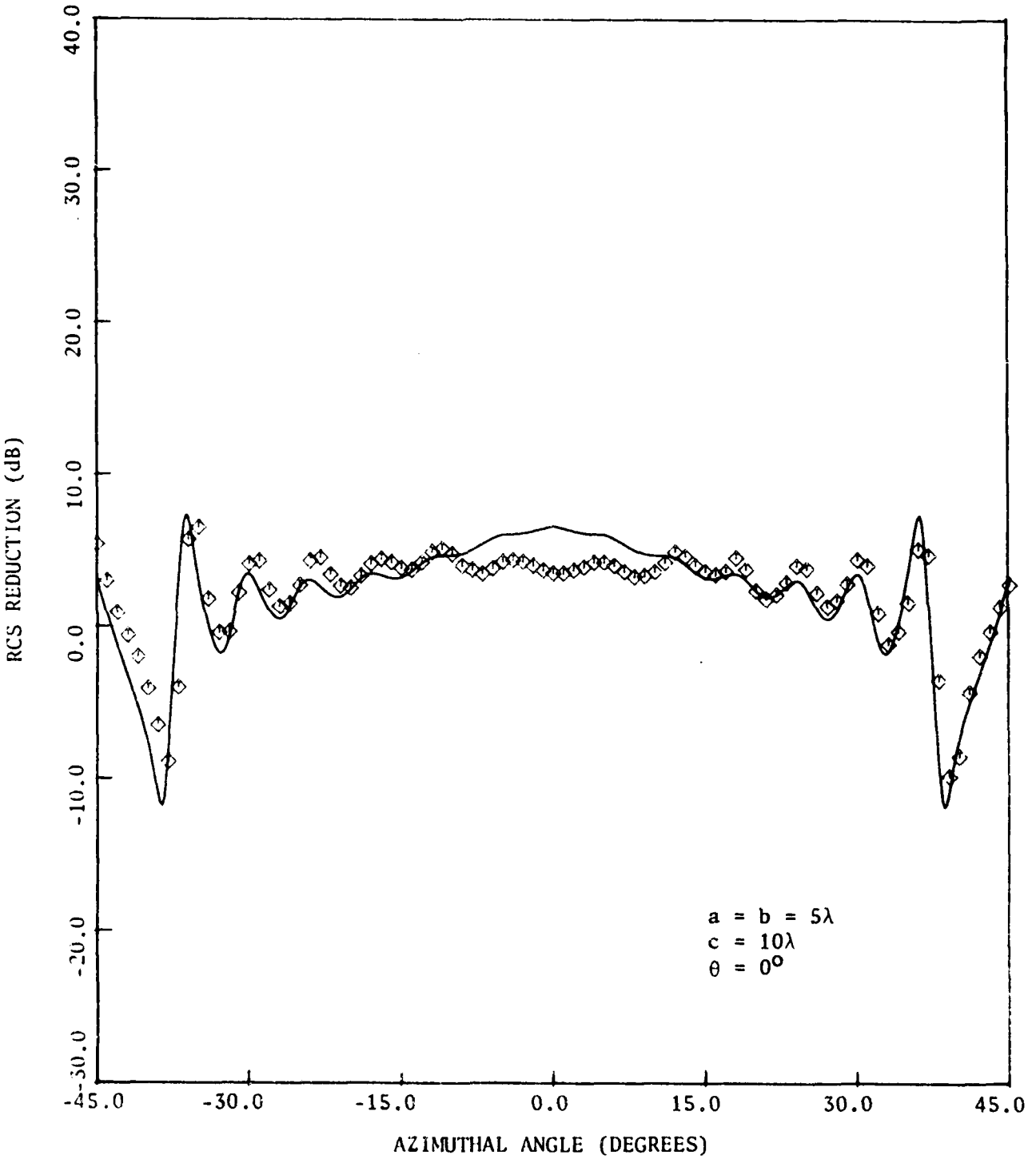

Figure 61. Predicted and measured reduction in RCS for $\delta = 5^{o}$, $a/\lambda = 5.0$ and vertical polarisation

ERL-0325-TR
Figure 62

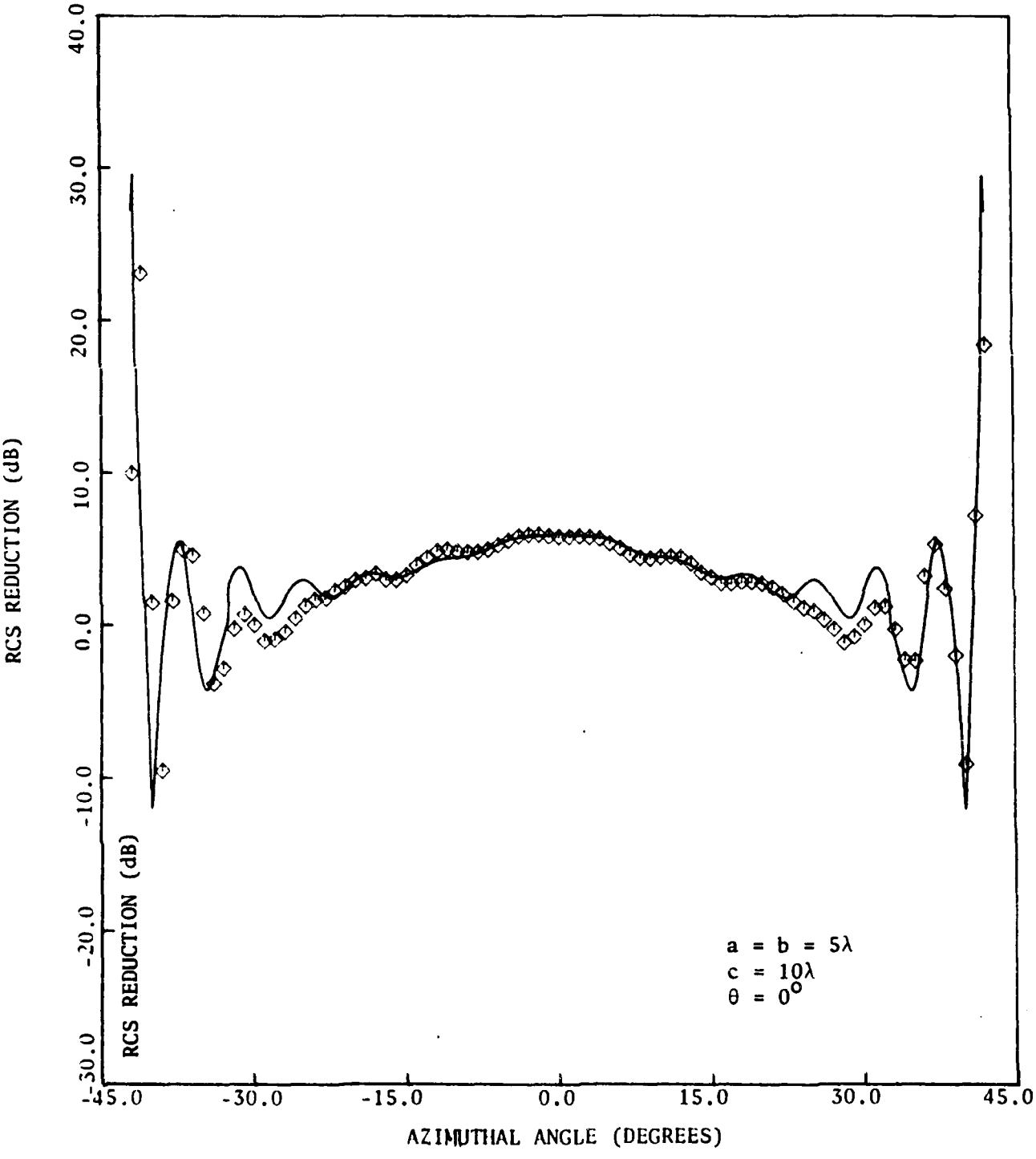

Figure 62. Predicted and measured reduction in RCS for $\delta = -5^{\circ}$, $a/\lambda = 5.0$ and horizontal polarisation

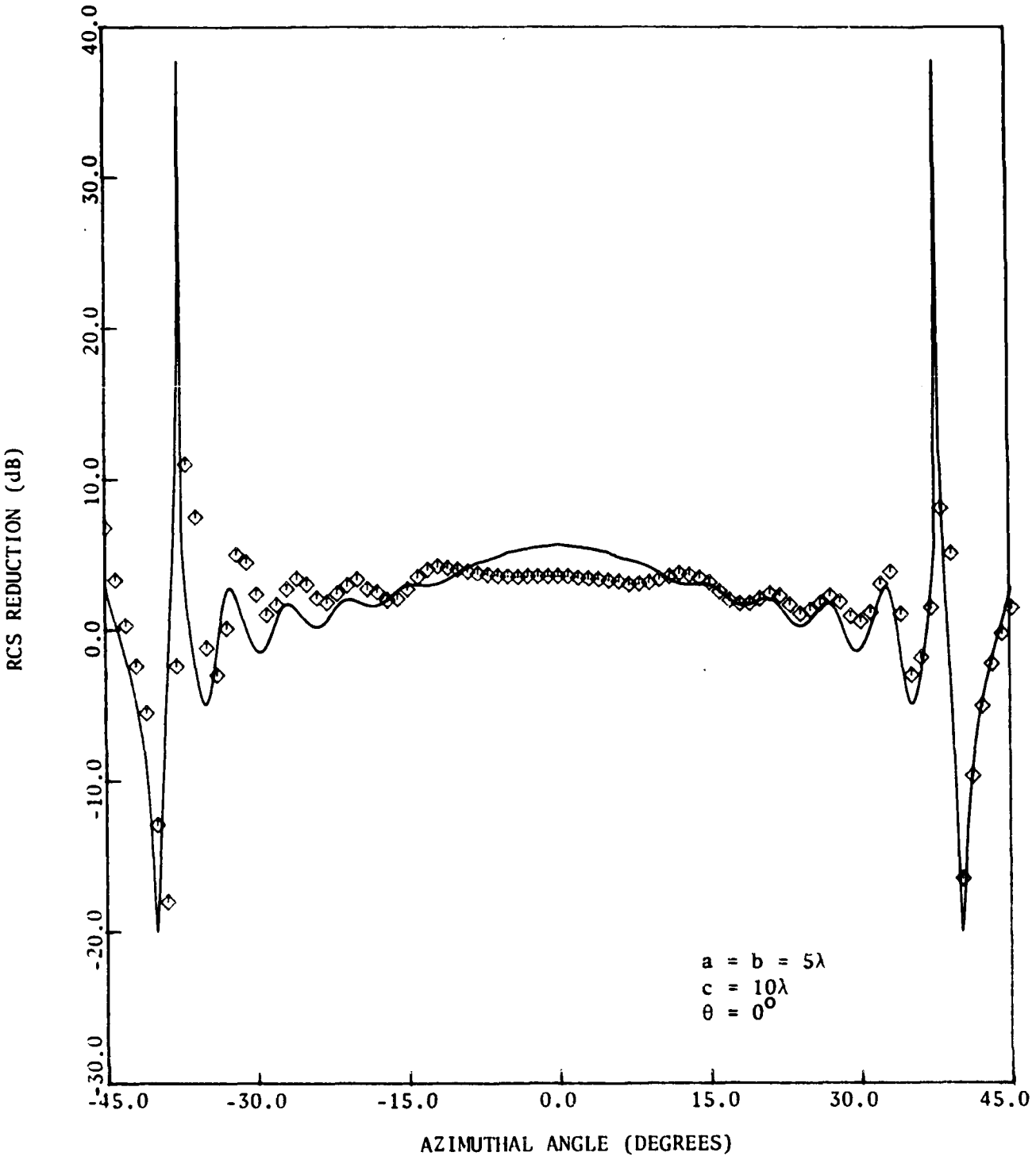

Figure 63. Predicted and measured reduction in RCS for $\delta = 5^{\circ}$, $a/\lambda = 5.0$ and horizontal polarisation

ERL-0325-TR
Figure 64

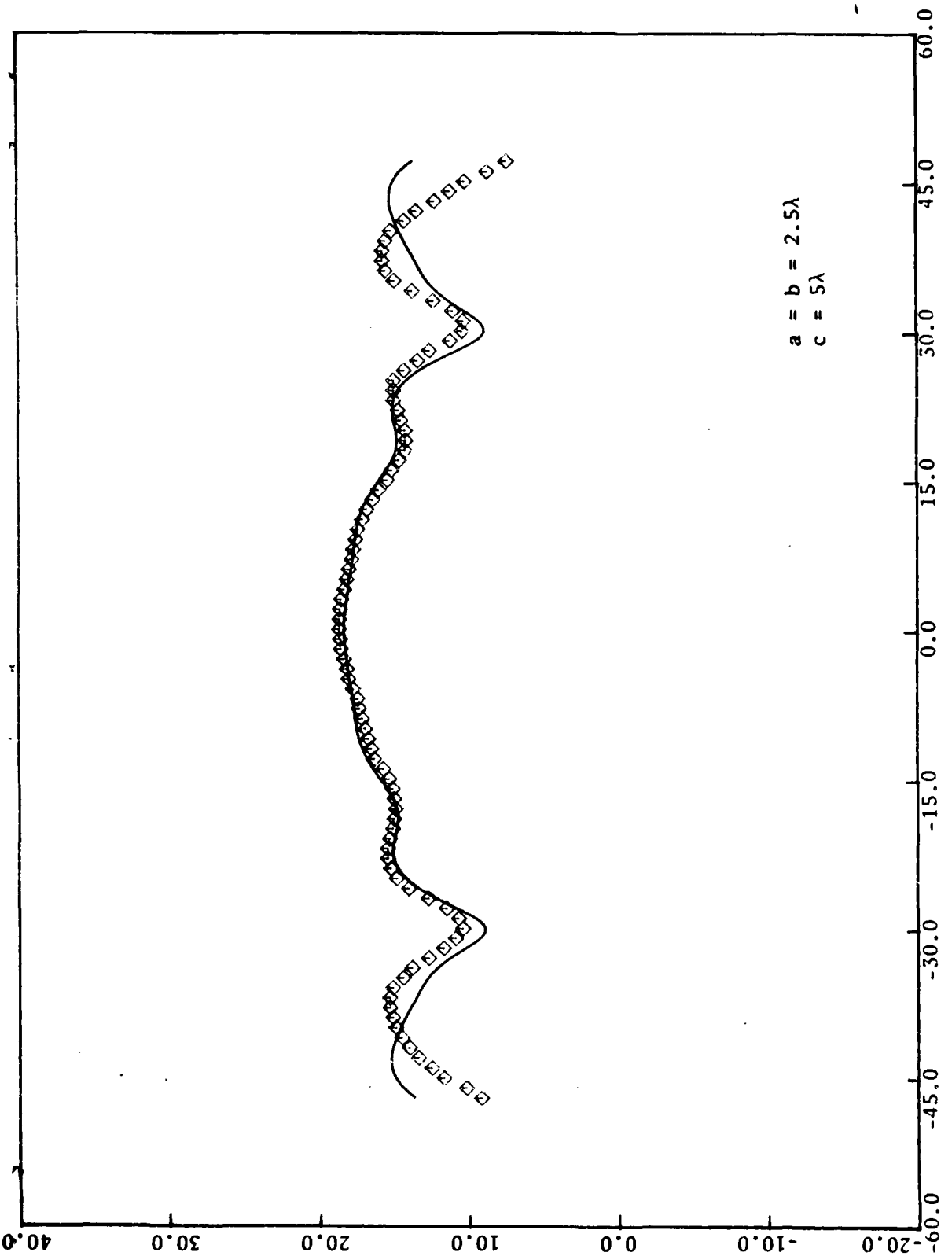

Figure 64. Comparison of theory with experiment for $a/\lambda = 2.5$, $\gamma = 5^{o}$ and $2\gamma = 95^{o}$ (vertical polarisation)

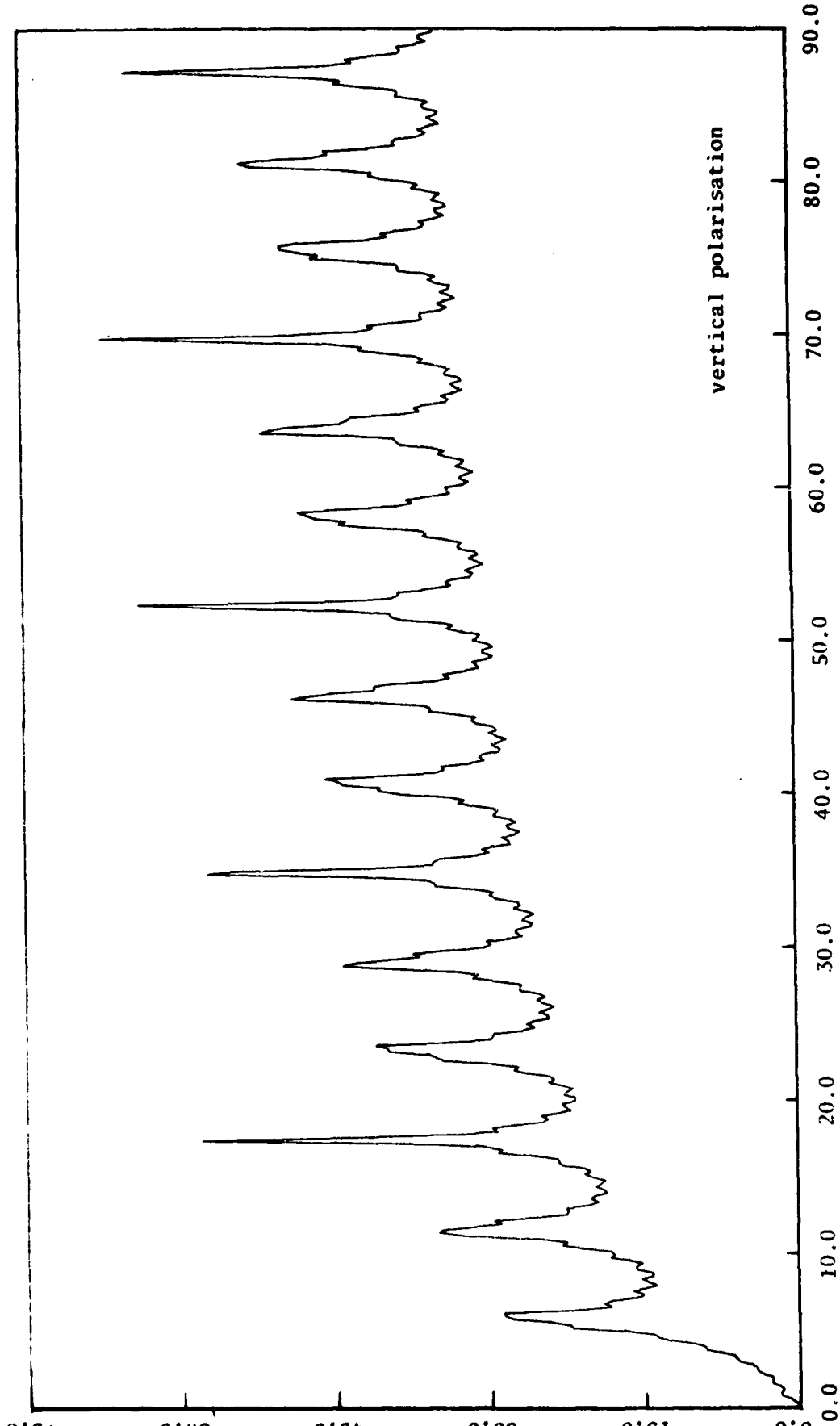

Figure 65. RCS reduction as a function of plate size at $\phi = \Theta = 0^{o}$ for $\delta = 7.5^{o}$

DISTRIBUTION

	Copy No.
EXTERNAL	
In United Kingdom	
Defence Science Representative, London	Cnt Sht Only
British Library, Lending Division	1
Institution of Electrical Engineers	2
Mr P. Varnish, Admiralty Research Establishment, Portsdown	3
In United States of America	
Counsellor, Defence Science, Washington	Cnt Sht Only
Engineering Societies Library	4
Dr E.F. Knott, Georgia Institute of Technology	5
In Australia	
Department of Defence	
Chief Defence Scientist	6
Deputy Chief Defence Scientist	
Controller, External Relations, Projects and Analytical Studies	
Superintendent, Science Programs and Administration	
Air Force Scientific Adviser	7
Navy Scientific Adviser	Cnt Sht Only
Director, Joint Intelligence Organisation	8
Document Exchange Centre Defence Information Services Branch for:	
Microfilming	9
United Kingdom, Defence Research Information Centre (DRIC)	10 - 11
United States, Defense Technical Information Center (DTIC)	12 - 23
Canada, Director, Scientific Information Services	24
New Zealand, Ministry of Defence	25
National Library of Australia	26

DOCUMENT CONTROL DATA SHEET

Security classification of this page: UNCLASSIFIED

1 DOCUMENT NUMBERS	2 SECURITY CLASSIFICATION
AR Number: AR-004-237 AR-004-237	a. Complete Document: Unclassified
Series Number: ERL-0325-TR	b. Title in Isolation: Unclassified
Other Numbers:	c. Summary in Isolation: Unclassified

3 TITLE

THE EFFECT OF VARYING THE INTERNAL ANGLE OF A DIHEDRAL CORNER REFLECTOR

4 PERSONAL AUTHOR(S):	5 DOCUMENT DATE:
W.C. Anderson	May 1985
	6 6.1 TOTAL NUMBER OF PAGES 81
	6.2 NUMBER OF REFERENCES: 4

7 7.1 CORPORATE AUTHOR(S):	8 REFERENCE NUMBERS
Electronics Research Laboratory	a. Task: DST 83/112
7.2 DOCUMENT SERIES AND NUMBER Electronics Research Laboratory 0325-TR	b. Sponsoring Agency:
	9 COST CODE: 429002

10 IMPRINT (Publishing organisation)	11 COMPUTER PROGRAM(S) (Title(s) and language(s))
Defence Research Centre Salisbury	

12 RELEASE LIMITATIONS (of the document):

Approved for Public Release

Security classification of this page: UNCLASSIFIED

Security classification of this page: UNCLASSIFIED

13 ANNOUNCEMENT LIMITATIONS (of the information on these pages):

No Limitation

14 DESCRIPTORS:

a. EJC Thesaurus Terms

Physical optics
Corner reflectors
Electromagnetic scattering
Radar

b. Non-Thesaurus Terms

15 COSATI CODES:

20060

16 SUMMARY OR ABSTRACT:
(if this is security classified, the announcement of this report will be similarly classified)

Small deviations from orthogonality can reduce drastically the back-scattering radar cross section of dihedral corner reflectors. In this paper this effect is studied using the method of physical optics with emphasis on the reductions of RCS achievable for modest departures from orthogonality.

Security classification of this page: UNCLASSIFIED

The official documents produced by the Laboratories of the Defence Research Centre Salisbury are issued in one of five categories: Reports, Technical Reports, Technical Memoranda, Manuals and Specifications. The purpose of the latter two categories is self-evident, with the other three categories being used for the following purposes:

Reports	:	documents prepared for managerial purposes.
Technical Reports	:	records of scientific and technical work of a permanent value intended for other scientists and technologists working in the field.
Technical Memoranda	:	intended primarily for disseminating information within the DSTO. They are usually tentative in nature and reflect the personal views of the author.